Role of the glucose-6-phosphate translocase on bacterial handling in human macrophages

Krithika Balagopal
St Hugh's College
University of Oxford

A thesis submitted for the degree of
Master of Research

06/10/2017

Acknowledgements

Firstly, I would like to express my sincere gratitude to my advisor Prof. Holm Uhlig for the continuous support of my masters study and related research, for his patience, motivation, and immense knowledge. His guidance was of great help to me in my research and writing of this thesis.

I would like to thank Dr. Sumeet Pandey for his guidance, teaching, and stimulating discussions.

I thank my fellow labmates for their timely advice, and their support throughout this year.

I thank Prof. James McCullagh and Elisebete Piers for performing the metabolomics analysis.

I would like to thank Dr. Britta Seigmund for providing me with a patient's sample.

I thank the CCFA grant for partially funding this project.

I thank Ambarish Satheesh, Shreyas Srinivas, Sanjana Sunderesan, Joseph Enguehard, Manasa Bharthwaj, and Dylan Sheerin for their helpful comments and suggestions while preparing my thesis. And finally thank my parents, Balagopal and Aparna, for supporting me completely throughout my year in Oxford.

Abstract

Disruption of the homeostatic balance in the intestine of genetically susceptible individuals can lead to inflammatory bowel disease (IBD), such as Crohn's disease (CD) or ulcerative colitis (UC). Defects in glucose-6-phosphate metabolism due to defects in glucose-6-phosphatase-β or glucose-6-phosphate translocase cause a rare Mendelian form of congenital neutropenia and CD like intestinal inflammation. The aim of this project is to investigate the mechanisms by which defective metabolism in macrophages might cause CD like intestinal inflammation via defective bacterial handling. We used a chemical inhibitor model to study the effect of glucose-6-phosphate-translocase inhibition in macrophages using a cholorogenic acid derivative. Defective glucose-6-phosphate translocase caused a reduction in bactericidal activity by changing the metabolism in macrophages and polarising them to M1 phenotype via the mTOR signalling pathway. Blockade of mTOR using rapamycin reversed the defective bacterial handling in macrophages with defective glucose-6-phosphatase enzyme. This study provides a link between metabolic defect and immune-mediated colitis that is associated with macrophage dysfunction. This might have therapeutic implications for subgroups of patients with intestinal inflammation.

Keywords: G6PT, macrophages, IBD, CD

Contents

List of Figures

List of Tables

0.1 Abbreviation

- ACC: Acetyl CoA carboxylase
- ACO: Aconitase
- Akt: Protein kinase B
- ALDOC: Fructose-bisphosphate
- ATF-6: Activating transcription factor-6
- BPGM: Bisphosphoglycerate Mutase
- CAMs: Classically activated macrophages
- CARKL: Carbohydrate kinase-like protein
- CFU: Colony forming units
- CHOP: C/EBP homologous protein
- CIC: Citrate carrier
- CLRs: C-type lectin receptors
- CPT: Carnitine palmitoyltransferase
- CS: Citrate synthase
- CSF1: Colony stimulating factor 1
- DCA: Di-chloroacetate
- DDIT-3: DNA damage-inducible transcript 3
- 2-DG: 2-Deoxy-glucose
- DHR: Dihydrorodamine
- DLST: Dihydrolipoamide S-Succinyltransferase
- DMEM: Dulbeccos modified eagles medium
- ECAR: Extracellular acidification rate
- ENO1: Enolase 1

- ETC: Electron transport chain
- ER: Endoplasmic reticulum
- FAD: Flavin adenine dinucleotide
- FAO: Fatty acid oxidation
- FAs: Fatty acids
- FASN: Fatty acid synthase
- FCCP: Carbonylcyanide-4 (trifluoromethoxy) phenylhydrazone
- FCS: Fetal calf serum
- FH: Fumarate Hydratase
- FSB: FACS staining buffer
- G6PT: Glucose-6-translocase
- G6P: Glucose-6-phosphate
- G6Pase: Glucose-6-phosphatase
- GABA: γ-aminobutyric acid
- GCK: Glucokinase
- GLUT-1: Glucose transporter type 1
- GM-CSF: Granulocyte-macrophage colony-stimulating factor
- GPI: glucose phosphate isomerase
- GPR: G protein-coupled receptor
- GSD: Glycogen storage disease
- GWAS: Genome-wide association studies
- HIF-1α: Hypoxia-inducible factor 1
- HK1: Hexokinase I
- HSPA5: Heat shock protein family A (member 5)

- IBD: Inflammatory Bowel Disease
- ICL:Isocitrate lyase
- IDH: Iso-citrate dehydrogenase
- IFN-γ: Interferon-γ
- IL-1ra: IL-1 receptor antagonist
- IRE1: Inositol-requiring gene 1
- Irg1: Immuno responsive gene 1
- IRFs: Interferon regulatory factors
- Keap1: Kelch-like ECH-associated protein 1
- α-KG: α-ketoglutarate
- LPS: Lipopolysaccharide
- LRR: Leucine-rich repeat receptors
- MAPKs: The mitogen-activated protein kinases
- MFI: Mean fluorescence intensity
- MMP-9: Matrix metalloproteinase 9
- mTOR: Mammalian target of rapamycin
- NADP: Nicotinamide adenine dinucleotide phosphate
- NF-κ B : Nuclear factor kappa-light-chain-enhancer of activated B cells
- NO: Nitric Oxide
- NOD2: Nucleotide-binding oligomerization domain-containing protein 2
- Nrf2: NF-E2-related factor-2
- OCR: Oxygen consumption rate
- OXPHOS: Oxidative phosphorylation
- PAMPs: Pathogen-associated molecular patterns

- PC: Pyruvate carboxylase
- PCK1: Phosphoenolpyruvate carboxykinase 1
- PDHA1: Pyruvate Dehydrogenase (Lipoamide) Alpha 1
- PDHB: Pyruvate dehydrogenase E1 component subunit beta
- PDK1: Pyruvate dehydrogenase kinase 1
- Pfkb3: Fructose-2,6-biphosphatase 3
- PFKL: 6-phosphofructokinase
- PGC1-α: PPARγ co-activator 1 α
- PGK: Phosphoglycerate kinase
- PGLS: 6-Phosphogluconolactonase
- PGM: Phosphoglucomutase
- PGs: Prostaglandins
- PHD: Prolyl hydroxylase
- PMA: Phorbol-12-myristate-13-acaetate
- PMN: Polymorphonuclear neutrophils
- PPAR-β: Peroxisome proliferator-activated receptor gamma
- PPP: Pentose phosphate pathway
- PRPS: Phosphoribosyl Pyrophosphate Synthetase
- RBKS: Ribokinase
- RIG-I : Retinoic acid-inducible gene 1
- RLRs: (RIG-I)-like receptors
- ROS: Reactive oxygen species
- RPE: Ribulose-5-Phosphate-3-Epimerase
- RPIA: Ribose 5-Phosphate Isomerase A

- RPMI: Roswell Park Memorial Institute 1640 medium
- STAT1: Signal transducer and activation of transcription 1
- SERCAs: Sarcoplasmic/endoplasmic reticulum Ca^{2+} ATPases
- SREBPs: Sterol regulatory element-binding proteins
- SUGLG: Succinate CoA ligase
- TALDO1: Transaldolase 1
- TAMs: Tumour associated macrophages
- TCA: Tricarboxylic cycle
- TGF-β: Transforming growth factor-β
- TKT: Transketolase
- TLRs: Toll like receptors
- TRAF1: Tumour-necrosis factor (TNF) receptor associated factor 2
- UC: Ulcerative colitis
- VEFGA: Vascular Endothelial Growth Factor A
- YY1: Yin and yang 1

Chapter 1

Introduction

Inflammatory bowel disease (IBD) is a disorder with various genetic predispositions, immunological susceptibilities, and environmental triggers [1]. Genome-wide association studies (GWAS) have been conducted for IBD, identifying 215 risk loci [2] [3][4]. Polygenic IBD, in particular CD, is associated with many genetic variants that affect bacterial clearance and autophagy [1] [5]. The strongest risk factor for CD are mutations in nucleotide-binding oligomerisation domain-containing protein 2 (NOD2), which is important for bacterial muramyl peptide sensing [5]. Mechanistic pathways such as epithelial barrier function disruption, impaired phagocytosis, T and B cell defects, hyper-and auto-inflammatory disorders, and impaired immune regulation have been associated with the spectrum of monogenic diseases that lead to IBD-like inflammation[6]. Additionally, a number of rare monogenic disorders can also cause CD, one of which is a deficiency in Glucose-6-phosphate translocase (G6PT) and glucose-6-phosphatase-β (G6Pase-β) [7].

In this chapter, we investigated the role of G6PT in bacterial clearance and in the metabolism of macrophages using a chemical inhibitor model.

1.1 Glycogen storage disease

In the year 1929, Edgar Von Gierke first described a glycogen storage disease (GSD), which was initially named in his honour [8] [9]. It was found that a mutation in the *G6PC* gene on chromosome 17q21, encoding the G6Pase [10] enzyme, is responsible for causing this disease. Glycogen storage disease 1 (GSD-1) is classified into two main forms: GSD 1a, caused by a mutation in the glucose-6-phosphatase α (G6Pase α) which is encoded by *G6PC1* [10] and GSD 1b, caused by a mutation in *SLC37A4* gene which encodes G6PT [11]. The G6PT enzyme localises to the endoplasmic reticulum (ER) and mediates the transport of glucose-6-phosphate (G6P) into the lumen of the ER [12]. G6PT is an anti-porter that facilitates the transport of G6P into the ER in exchange for a phosphate molecule [13]. Inside the ER lumen, G6P acts as the substrate of two enzymes, namely glucose-6-phosphatase (G6Pase-α and G6Pase-β) [10] [11], and hexose-6-phosphate dehydrogenase [12]. A characteristic myeloid dysfunction is unique to patients with G6PT mutation [14]. Unlike G6Pase-α, which is present only in gluconeogenic organs such as the liver, small intestine and kidney [15] [14], G6PT enzyme is present ubiquitously [16] [14]. The myeloid dysfunction in patients with GSD-1b is attributed to either the biological activities of G6PT or due to a second G6pase that exists in myeloid tissues. The G6Pase-β enzyme is encoded by *G6PC3* and exhibits ubiquity similar to that of G6PT [17] [14]. The complex formed by the coupling of G6Pase-β and G6PT aids the hydrolysis of G6P to glucose and inorganic phosphate. Hence, patients with functional mutations in G6Pase-β and G6PT present with a severe congenital neutropenia syndrome [18] [14].

1.2 Clinical manifestation

Another distinct feature of GSD-1b, is the observation of IBD CD-like colitis [7]. Fever, diarrhoea, and perioral and anal ulcers are accompanying symptoms in patients with the G6PT mutation [19][14]. The severity of the primary disease does not correlate with intestinal inflammation [14]. All patients with this mutation have an absolute neutrophil count less than 1000 cell/ml. Although congenital neutropenia is the most obvious phagocyte defect in this disorder, it is not directly linked to IBD. Current treatments for GSD-1b consist of a combination of dietary therapy [20][21] to correct symptoms of G6Pase deficiency, and human granulocyte-macrophage colony-stimulating factor (GM-CSF) therapy [7]. GM-CSF is humoral regulator of hematopoiesis that increases both the proliferation of myeloid precursors and the functional capacity of neutrophils [19][14]. In GSD-1b patients [22], GM-CSF treatment increases neutrophil counts and reduces the frequency of infection and inflammation [7] complications that are not manageable by dietary therapy alone [14]. This provides evidence that neutrophil dysfunction associated with GSD-1b is distinct from the defect in G6P metabolism.

1.3 Competitive inhibitors for G6PT

G6Pase-α is a nonspecific phosphatase and its specificity for the substrate G6PT/G6P complex is achieved by the high specificity of G6PT for G6P [23] [24]. Chlorogenic acid, the ester of caffeic acid and quinic acid (Figure 1.1), is a reversible, competitive inhibitor for G6PT [25][23] [24]. There are many derivatives of cholorogenic acid with the most potent being S3483 [25] and S4048 [26] [24] (Figure 1.1). These inhibitors have been used extensively in mechanistic studies of the metabolic defects in GSD 1 [24][27]. There is also further evidence demonstrating the inhibition of G6PT transport activity in mouse hepatic microsomes [28] [29] and proteoliposomes containing

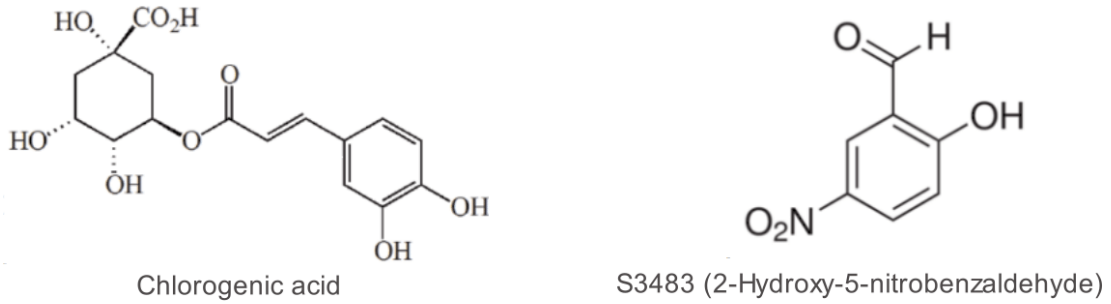

Figure 1.1: **Structure of cholorogenic acid** This figure is adapted from [24]. This is a representation of cholorogenic acid and its derivative S3483

recombinant G6PT by cholorogenic acid [30] [11]. The cholorogenic acid derivative and G6PT inhibitor S3483 was also found to inhibit G6P transport in microsomes isolated from polymorphonuclear neutrophils (PMN) and from differentiated promyelocytic HL-60 cells [31]. Therefore, we used a derivative of cholorogenic acid S3483, to inhibit the G6PT enzyme in monocytes derived macrophages to make our chemical inhibitor model.

1.4 Solute carriers

In our study, we established that G6PT enzyme plays a significant role in bacterial handling in monocyte derived macrophages (MDM). However, Hye-hyun Ahn et al. showed that G6PT modulated autophagy independent of its transporter activity [32]. This is contradicting to our result on bacterial handling by macrophages treated with S3483. Therefore, I explored the literature on the phenotype and the genotype of the *SLC37A4* gene to understand the effect of the transporter activity of the G6PT enzyme. The solute carrier (SLC) gene series consists of over 50 gene families which are predicted to encode membrane-bound transporters [33] [24]. The SLC37 family consists of four characterised sugar-phosphate exchange (SPX) proteins [33] [24] namely, A1, A2, A3, and A4, which are positioned in the ER membrane [33] [24]. *SLC37A1* is

known as SPX1 [34], *SLC37A2* [35] is known as SPX2, *SLC37A3* is known as SPX3 [35], and *SLC37A4* is known as SPX4 [22]. The most studied member of the SLC37 family is *SLC37A4*, also known as G6PT. *SLC37A1*, *SLC37A2*, *SLC37A4* function as phosphate (P_i)-linked G6P antiporters and help in the transportation of cytoplasmic glucose-6-phosphate into the lumen of the ER and translocates inorganic phosphate in the opposite direction [25]. However, *SLC37A3* does not perform any of these activities [36]. G6PT enzyme forms a complex with glucose-6-phosphatase enzymes which is responsible for glucose production through either glycogenolysis or gluconeogenesis [24]. Therefore, this protein plays a central role in homeostatic regulation of blood glucose levels [11] [13].

1.5 Functions of glucose-6-phosphate translocase enzyme

G6PT transports glucose-6-phosphate G6P from the cytosol into the ER. A catalytic subunit, G6Pase-α [15] or -β [16] hydrolyses G6P to glucose and transports it back to the cytosol [24]. Both the G6Pases have their active sites located inside the ER [24] and are functionally dependant on G6PT for their activity [24]. G6PT provides a substrate for the G6Pases by transporting G6P into the ER lumen [12][24]. It also increases G6P transport activity by providing a physical interaction by an allosteric mechanism. [24].

1.6 Glucose-6-phosphatase-β deficiency

The human *G6PC3* gene, comprising of 6 exons on chromosome 17q21 [16], encodes the enzyme G6Pase-β. This gene is expressed ubiquitously, unlike the *G6PC1* gene which is expressed only in gluconeogenic organs. This mutation affects the myeloid

population and patients with this mutation suffers severe congenital neutropenia [16], just like patients with mutation in the SLC37A4 gene. Structurally, G6Pase-α and G6Pase-β are very similar, but they share only 36 % amino acid homology [14]. Till date, 11 mutations have been identified in G6Pase-β protein[14]. These include five missense, three nonsense, and three insertions/deletions [37] [38] [39] [14]. Analysis in the yeast expression system revealed the Arg253His mutant to have negligible or no phosphorylase activity [39] [14]. Apart from this, there have been few studies that have investigated the active site mutants of the G6Pase-β enzyme [14].

1.7 Transmembrane structure of G6PT

The G6PT model was thought to contain either 10 [40] or 12 transmembrane helices[41] based on hydropathy profile analysis [24]. The X-ray crystallography model of *Escherichia coli* glycerol-3-phosphate which belongs to the organo-phosphate: P_i antiporter family suggested that G6PT contains 12 membrane helices (Figure 1.2) [42]. To address the transmembrane structure of G6PT, protease analysis and mutational glycosylation of the G6PT protein was performed [24] [14]. The region of G6PT corresponding to amino acid residues 50-71 was predicted to form a transmembrane segment in a 12-domain model and was shown to be resistant to glycosylation [24] [42]. The 51-residue luminal loop is available for glycolsylation in a 10-domain model [43] [44]. It has been shown that glycosylation of membrane protein is crucial for membrane folding and a disruption in glycolysation can lead to misfolding and degradation of misfolded proteins [45] [24]. T53N and S55N glycoprotein mutants would be misfolded and degraded in the ER [46] if there were 12 helices, but would be expressed without any disruption if the 10 helix model were correct [24]. Analysis of the expression of the T53 and S55N gene showed similar levels of expression bolstering the 10-membrane model theory [24]. There are in total 429 amino acid

residues spanning the transmembrane helices of the G6PT protein [24]. There are 39 missense *SLC37A4* mutations, altering 34 amino acid residues, identified in GSD-1b patients [24]. The signature motif constitutes the amino acids 133-149, of which the residues Q133, A148, and G149 are altered by missense SLC37A4 mutations identified in GSD-1b patients [24] (Figure 1.2).

1.8 Mutations in the *SLC37A4* gene

Patients with a mutation in the *SLC37A4* gene predominantly develop neutropenia. Delineation of missense and codon deletion mutations that result in single amino acid alterations provide valuable information on functionally important residues in a protein [24]. To date, 110 separate mutations have been identified in the *SLC37A4* gene (Table 1.1) in patients with GSD-1b/non GSD-Ia [24] (HGMD database) (Table 1.1). These include 61 missense, 17 nonsense, 19 small deletions (including 2 codon

Mutation Type	Number of mutations
Missense/nonsense	61
Splicing substituent	17
Regulatory Substituents	1
Small deletions	19
Small insertions/duplicates	8
small indels	2
Gross deletions	2
Gross deletions/duplicates	0
Complex rearrangements	0
Repeats variants	0
Total	110

Table 1.1: **Mutation in *SLC37A4*.** There are a total of 110 mutations observed in the *SLC37A4* gene. Table derived from EXAC and HGMD database.

deletion mutations), and 19 splicing mutations that are distributed across the entire coding and exon intron junction regions (Table 1.1). In G6PT, 31 missense and 2 codon deletion mutations have been characterised functionally via site-directed mutagenesis and transient expression assays and were shown to obliterate microsomal

G6P uptake activity [11] [47] [24]. The mutations in the *SLC37A4* gene are grouped into the following three categories: helical (H), nonhelical that includes cytoplasmic (C) and luminal (L) loops, and terminal that includes N- (MIV) and C- (R415X) terminal domains [48] [24] (Figure 1.2).

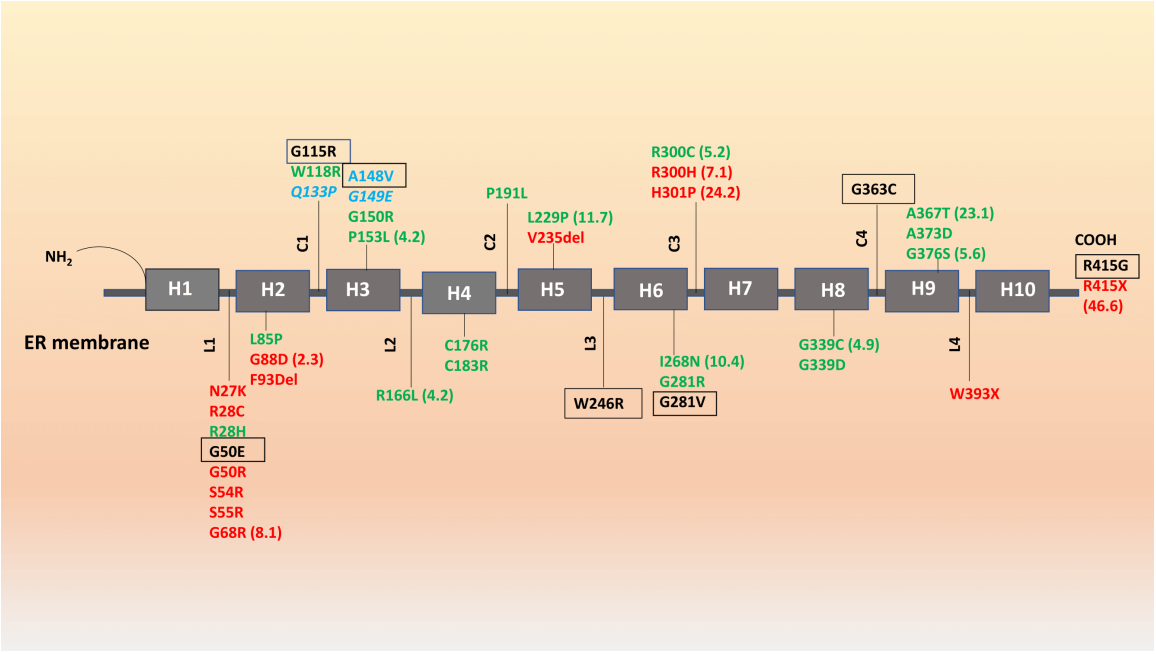

Figure 1.2: **Mutations in *SLC37A4* gene** This figure represents the summary of different mutations that affect G6P uptake activity. The 10-helical transmembrane domains are marked from H1 to H10. The cytoplasmic loops are marked as C1 to C4 and the luminal loops are marked as L1 and L4. Mutations that completely eliminate G6PT activity are represented in red. Mutations that retain residual function are listed with the percentage of wild type activity retained noted in parentheses. The mutations in blue represent the signature motifs mutations in which Q133P and G149E are characterised by proteosomal assays. The boxed mutations are not functionally characterised. Mutations that have been characterised by both cell-based assays and proteoliposomal assays are shown in green. This figure is adapted from [24]

Complete loss in G6P uptake is observed among the 18 helical mutations, 9 missense and 2 codon deletion mutations, while 7 missense mutations retain residual activity [48]. Among the 7 missense mutations characterised in luminal loop-1, 6 are null mutations a finding consistent with this loop being critical for G6P uptake activity [24].

1.9 N and C terminal domains of G6PT

The N-terminal consists of 7 amino acids and plays a crucial role in G6PT activity. The MIV N-terminal mutation lacks the N-terminus, leading to a complete loss in G6PT uptake [30] [24]. However, the R415X mutation lacking C-terminal retains 47% of G6PT activity [49] [24]. The G20D, F93del, C176R, V235del, I278N, G339C and G339D mutations are located in helix 1, 2, 4, 5, 6, 8 and 8, respectively and G50R is located within luminal loop 1. These mutations reduce the uptake of G6P [30] [24]. The C-terminal domain consists of 15 amino acids (from 415-429) in human G6PT [24] enzyme. This domain has been reported for its importance in protein stability [14]. Chen *et al.* reported that the R415X mutant that lacks the entire cytoplasmic tail is degraded more rapidly compared to that of the wild type [49]. The initial three residues (R415X, N416X, I417X) are considered stable when compared to wild type G6PT stability [49]. R415X is less stable compared to N416X, and N416X is less stable compared to the I417X [24]. [24]. This suggests that structural integrity of these helices is crucial for the stability of the G6PT protein [24].

1.10 Analysis of the signature motif in human G6PT

The mammalian G6PT enzyme is a highly conserved, microsomal transmembrane protein consisting of 429 amino acids [41] [22]. The G6PT proteins, including the other organo-phosphate antiporters family such as GlpT, and uhpT, the G6P receptor (uhpC), and the phosphoglycerate transporter (PgtP), share a signature motif (ProSite PDOC00726) which lies between amino acids 133 and 149 in human G6PT [50]. There are only 28 missense mutations identified within the signature motif [24]. A mutation in Q133P at the start of the motif, and G149E at the end of the motif, completely abolish G6P transport activity [30]. This suggests a functional role for the signature motif in G6PT protein.

1.11 Metabolic phenotype of patients with *SLC37A4* mutations

There have been 120 patients identified thus far with a mutation in the *SLC37A4* gene and 90 of these patients have developed GSD-1b (HGMD database). The metabolic phenotype of GSD-1a and GSD-1b is very similar. Patients suffering from these conditions have hypoglycemia after a short fast and exhibit increased levels of G6P in the cytoplasm [14]. This increase in G6P level leads to the synthesis and excessive accumulation of glycogen in the liver and kidney, a process that promotes progressive hepatomegaly and nephromegaly [14]. More than 90 % of the patients with deficiencies in *SLC37A4* have hepatomegaly (Figure 1.3) There was no genotype-phenotype

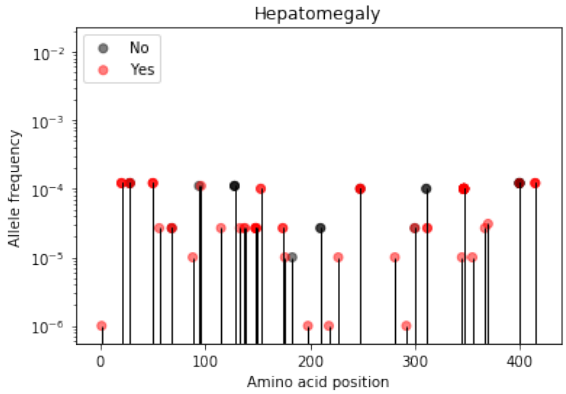

Figure 1.3: **Mutations in *SLC37A4* causing hepatomegaly** This graph is plotted between amino acid and allele frequencies of 100 patients with deficiencies *SLC37A4* gene. The allele frequencies are derived from EXAC database. Each dot represents one patient. Red dots represent patients with hepatomegaly and the black dots represent the patients without hepatomegaly. n=100

correlation observed between mutations in the *SLC37A4* gene and hepatomagaly (Figure 1.3).

Hypercholesterolemia, hypertriglyceridemia, hyperuricemia, and lactic acidemia are other major complications reported in patients with GSD-1b[14] [51]. GSD-1b patients were found to have impaired growth hormone (GH)-insulin-like growth factor (IGF) production[14] [52]. There is an increased incidence of short stature in these

patients due to growth hormone deficiency (GH) [24].

1.12 Myeloid phenotype in *SLC37A4* mutations

Neutropenia, or neutrophil dysfunction, is a major clinical phenotype observed in patients with GSD-1b. As a result, recurrent bacterial infections are common in these patients [14]. A sub-population of patients with neutropenia also are susceptible to inflammatory bowel disease [7]. However, a complete literature analysis of 120 patients [53] [11][54] [55] [22] [19] with *SLC37A4* mutations revealed no correlation between the individual mutation and the presence of neutropenia, bacterial infections, and systemic complications (Figure 1.4) (Figure 1.5)

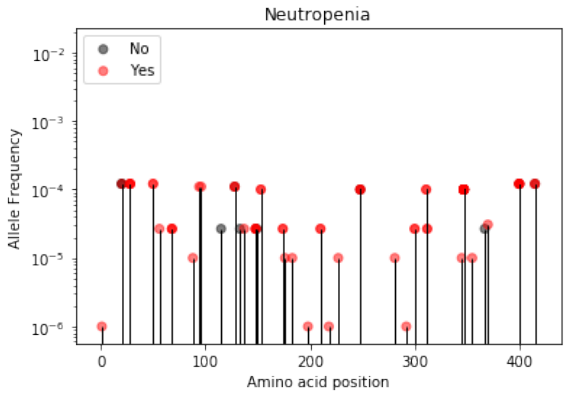

Figure 1.4: **Mutations in *SLC37A4* causing nuetropenia** This graph is plotted between amino acid and allele frequencies of 100 patients with deficiencies *SLC37A4* gene. The allele frequencies are derived from EXAC database. Each dot represents one patient. Red dots represent patients with neutropenia and the black dots represent patients without neutropenia. n=100

A study on two Japanese patients with GSD-1b without neutropenia suggested that neutropenia is not manifested in all GSD-Ib patients [56]. It was reported that it may have been caused due to residual G6PT activity [56]. Chen et al. showed that the mutation R415X was shown to retain 47% of the wild type activity and it has been proposed that the 23.5 % of normal G6PT activity in the compound heterozygote is sufficient to maintain the patients' myeloid function [19] [49]. According

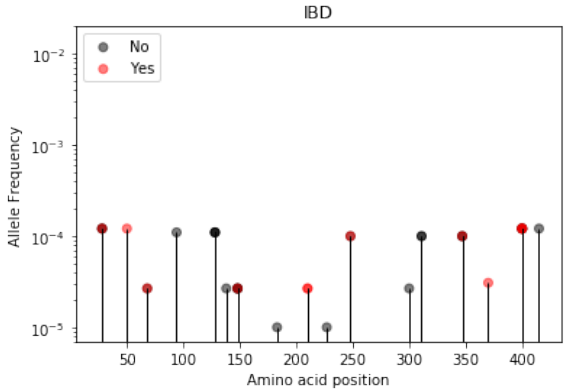

Figure 1.5: **Mutations in *SLC37A4* causing IBD** This graph represents amino acid and allele frequencies of 100 patients with mutations in the *SLC37A4* gene. The allele frequencies are derived from EXAC database.Each dot represents one patient. Red dots represent patients with IBD and the black dots represent the patients without IBD. n=100

to this study, the mutations are divided into leaky mutations retaining some residual activity and mutations completely inactivating the transporter G6PT [49] [19]. The authors concluded that a close relationship exists between the residual activity of the G6PT protein retained by the patients and the susceptibility of GSD-1b patients to neutropenia as well as myeloid dysfunctions [49]. However, this is not consistent with the data currently available in the literature [19].

A study conducted on 14 patients with GSD-1b, 1c, or non-a, detected 13 different mutations in the *SLC37A4* gene [53]. This study provided evidence that the same mutation in the G6PT gene is not necessarily associated with the appearance of a clinically evident neutrophil impairment. One patient with a homozygous mutation (12111212delCT) was diagnosed with neutrophil dysfunction [53] [19]. However, another patient with GSD-1c with the same mutation did not show symptoms of neutrophil impairment [53][19]. A previous report showed that a GSD-1 non-a patient affected by severe neutropenia was found to be homozygous for the Gly-149-Glu mutation [11], whilse another study on a different patient [53], who was also homozygous for Gly-149-Glu mutation, had no evident neutrophil dysfunction. These observations indicate that neutrophil impairment, which has often been assumed to be a distinctive

feature of GSD-1b, cannot be considered so anymore (Figure 1.4).

A recent study of Korean patients with GSD-1b identified a novel variant: 148G>A (Gly50Arg) [57]. This mutation has been shown to completely abolish microsomal G6P uptake activity, and compromise G6PT stability [57] (Figure 1.4). This mutation is classified as a pathogenic variant in accordance with American College of Medical Genetics and Genomics standard guidelines for the interpretation of sequence variants [57]. This provides further evidence that microsomal transport activity is important for bacterial handling.

A complete data analysis of all patients with *SLC37A4* mutation showed 400X to be the most prevalent mutation and was present in 67 (23.6%) of the 284 independent alleles (Figure 2.2, Figure 2.3). All GSD-1b patients with IBD have neutropenia [19], but there is no distinct correlation between these two diseases [19] (Figure 2.4 and 2.5). Granulocyte colony-stimulating factor (G-CSF) is used to restore neutrophil count and improve neutrophil function in GSD-1b patients. All the patients with IBD were on G-CSF treatment whereas 6/10 patients without IBD involvement were also treated with G-CSF [19]. This observation suggests that the severity of neutropenia and neutrophil dysfunction and not the duration of neutropenia are important risk factors for IBD [19].

1.13 Functions of the intestinal macrophages

The intestinal macrophages contribute to gut homoeostasis by eliminating invading pathogens without inducing an inflammatory response of the lymphocytes within the lamina propria [58]. They are positioned under the surface epithelium in the intestinal tissues and are the first immune cells to encounter any foreign material passing the epithelial barrier [58][59]. Intestinal macrophages and dendritic cells (DCs) sense conserved molecular patterns such as pathogen-associated molecular patterns (PAMPs)

on microbes via germ-line encoded pathogen recognition receptors (PRRs) [60] [59] [58]. These PRRs are classified into five families on the basis of shared functional domains [58] [61];

- toll-like receptors (TLRs)
- Nucleotide-binding oligomerization domain (NOD) like receptors (NLRs),
- Leucine-rich repeat (LRR) receptors,
- C-type lectin receptors (CLRs), and
- Retinoic acid-inducible gene 1 (RIG-I)-like receptors (RLRs)

Signalling downstream of each family of PRRs leads to the activation of central immune response pathways such as nuclear factor kappa-light-chain-enhancer of activated B cells (NF-κB), the mitogen-activated protein kinases (MAPKs), and the interferon regulatory factors (IRFs) [62]. Upon activation of PRRs, immune and non-immune cells produce inflammatory cytokines, type I interferons, chemokines, and antimicrobial peptides [62]. As a result, neutrophils are recruited and macrophages are activated, leading to the direct killing and clearance of microbes [58]. Additionally, these inflammatory products induce the maturation of DCs, promoting the induction of adaptive immune responses [62]. This is a carefully synchronised process where microbial sensing and subsequent immune responses are highly regulated [61]. Disregulation of these pathways can lead to both enhanced susceptibility to infections and development of chronic inflammatory diseases such as IBD [61] [58].

1.14 Endoplasmic stress Regulation in macrophages

ER is an organelle that facilitates protein modification, folding, and maturation of transmembrane, secretory, and ER-resident proteins [63]. Disruption of any of these

processes lead to ER stress. Unfolded protein response (UPR) is a signalling pathway that attenuates global protein translation and degradation in response to ER stress [63]. Activating transcription factor-6 (ATF-6) is a gene that encodes a transcription factor that activates target genes for the UPR during ER stress. It has been shown that the ER chaperone binding immunoglobulin protein (Bip/GRP78) binds to ATF6 and dissociates in response to ER stress [64]. Heat shock protein 5 (HSPA5) also known as immunoglobulin (Ig) heavy (H) chain Binding protein (Bip), is encoded by heat shock protein 70 (HSP70). This is located at the lumen of ER and is associated with folding and assembly of proteins in ER [65] [66]. ER stress activates both a mitochondrial-dependent and a mitochondrial-independent apoptotic pathway [67]. DNA damage-inducible transcript 3 (DDIT-3), also known as C/EBP homologous protein (CHOP), is a multi-functional transcription factor that plays a crucial role in various cellular stresses and induces cell cycle arrest and mitochondrial dependent apoptosis in response to ER stress [68] [69]. Mitochondrial independent apoptotic response is signalled by the activation of inositol-requiring gene 1 (IRE1) which recruits tumour-necrosis factor (TNF) receptor associated factor 2 (TRAF2), thus activating procaspase-14 (in mouse) and procaspace-4 (in humans) [67]. The ER undergoes structural and functional reorganisation when monocytes derived macrophages in the presence of macrophage colony stimulating factor (M-CSF). This results in ER stress with an upregulation of UPR [70][63]. In insulin resistant and atherosclerosis mouse models, there was an upregulation of UPR in macrophages at early stages of vascular inflammation [71][63]. Cholesterol uptake in macrophages accelarates the ER stress through peroxisome proliferator-activated receptor-γ (PPAR-γ)-signalling activation [72]. Stimulation of PPAR-γ and -δ also allows the undifferentiated macrophages to acquire the alternatively activated (M2) phenotype[63]. Therefore, ER stress is an important parameter in differentiation and polarisation of macrophages.

1.15 Polarisation of macrophages

Polarisation of macrophages is a process by which macrophages obtain different phenotype. The phenotype of the macrophage relates to the micro-environment they reside in [73]. They can constantly switch their phenotype both *in vivo* and *in vitro* [74] [75]. Analogous to T-helper (Th) distinction, where Th1 cells are associated with the response against bacteria or viruses, and Th2 cells are associated with the response to parasitic infection and tissue remodelling, macrophages can be denoted as M1 and M2 macrophages with similar function to that of Th1 and Th2 phenotype respectively [73]. The polarisation of macrophages is dictated by the activation of stimulus-specific transcription factors (Table 1.2) [73]. This activation is achieved through the effects on inducible gene promoters with specific features (Figure 1.6). M1 macrophages (or classically activated macrophages, CAMs) are pro-inflammatory and have potent microbicidal and tumoricidal activity (Table 1.2), whereas the M2 macrophages (or alternatively activated macrophages, AAMs) are involved in tumour progression and tissue remodelling, including fibrosis (Table 1.2) [76] [77]. Classical

Polarising stimulus	IFN-γ, LPS, IFN-γ+LPS
Phenotype	Proinflammatory
In vitro morphology	Round oval
Products/markers	TNF-α, IL-1β, IL-6, IL-12, IL-23, CXCL10, pSTAT1, MMP9
Phagocytic activity	High
Antigen presentation	High
Arginine metabolism	iNOS: Arginine to NO
Antibacterial capacity	High
Effect on tumours	Tumericidal

Table 1.2: **M-1 phenotype macrophages.** This is table representing the various properties of M1 polarised macrophages. This table is adapted from [78]

macrophage activation requires stimulation with IFN-γ, the standard cytokine generated by Th1 cells, and activation of downstream transcription factors, such as signal transducer and activation of transcription 1 (STAT1), nuclear factor-kappa light chain-enhancer of activated-B cells (NF-κB), and interferon regulatory factor 5 (IRF-

5) [73]. M1 macrophages usually express inflammatory genes such as, TNF-α, IL-1β, and IL-6 (Table 1.2) [73]. The alternate macrophage activation requires Th2 associated cytokines such as IL-4 or IL-13 [79]. M2 macrophage produce cytokines such as IL-10, IL-1 receptor antagonist (IL-1ra), and transforming growth factor-β (TGF-β) [73][76]. These cytokines are closely related to their ability to attenuate inflammation and promote extracellular tissue remodelling [76]. Transcription factors involved in M2 polarisation include STAT3, STAT6, IRF-4, and peroxisome proliferator-activated receptor-γ (PPAR-γ) [76](Table 1.3). Differential metabolism of L-arginine is characteristic of M1 and M2 macrophages. L-arginine is metabolized by inducible nitric oxide (iNOS) to generate nitric oxide (NO) in M1 macrophages (Table 1.1) [77]and by arginase-1 in M2 macrophages to augment the production of polyamines and L-proline, which are essential substrates for collagen synthesis (Table 1.3). [80] [81]. Signalling pathways implicated in M1 and M2 macrophage polarisation is indicated in the figure 1.6. This figure shows the main genes that are characteristic of either the M1 and M2 phenotype macrophages (Figure 1.6).

Polarising stimulus	IL-4, IL-13, Ic, IL-10, GC, TGF-β
Phenotype	Anti-inflammatory
In vitro morphology	Elongated fibroblast like
Products/markers	IL-10, TGF-β, CCL17, CCL22, CD163, CD206, pSTAT3/6
Phagocytic activity	Low
Antigen presentation	Low
Arginine metabolism	Arg1: Arginine to ornithine
Antibacterial capacity	Low
Effect on tumours	Protumerigenic

Table 1.3: **M-2 phenotype macrophages.** This is table representing the various properties of M2 polarised macrophages. This table is adapted from [78]

Therefore there is strong evidence supporting the fact that macrophages phenotypically adapt to the environmental setup, and is strongly associated with radical changes in the transcriptional landscape, although this effect is rather scattered and does not follow a systematic route. Moreover, the molecular determinants driving the

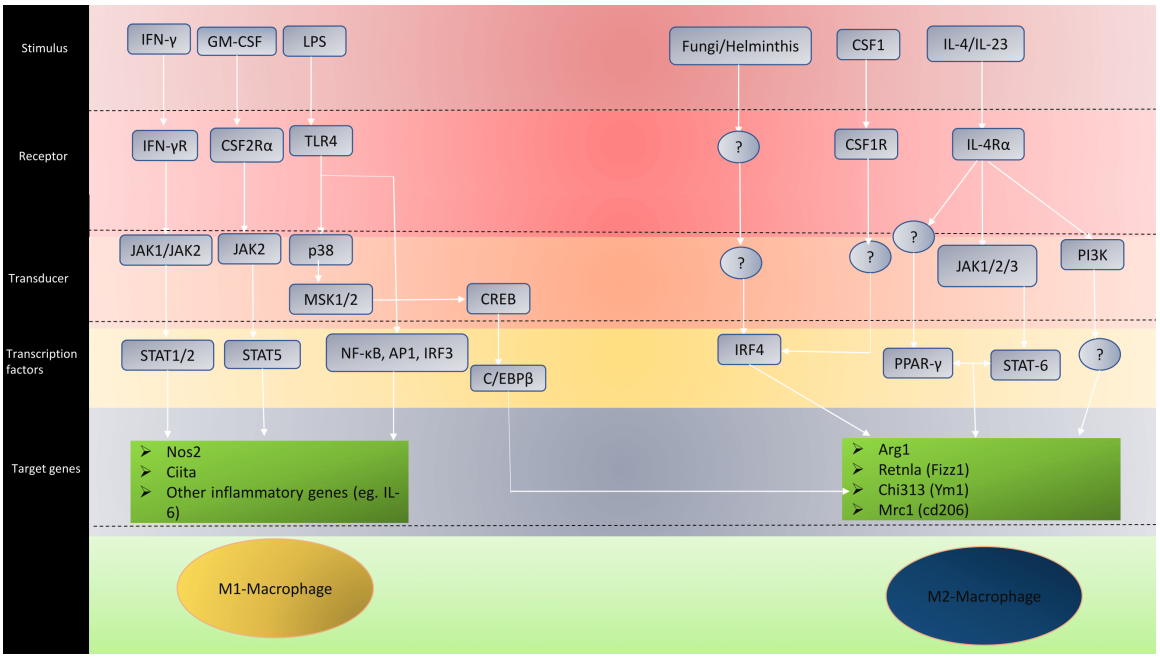

Figure 1.6: **Schematic overview of signal transduction in macrophages** This figure is adapted from [79] The figure illustrates different polarised macrophage populations in specific physiological contexts and gives examples of the transcription factors associated with these phenotypes. Abbreviations: Arginase 1 (Arg1); CCAAT/enhancer-binding protein-β (C/EBPβ); chitinase 3-like 3 (Chi3l3); MHC class II transactivator (Cita); cAMP-responsive element-binding protein (CREB); colony-stimulating factor (CSF); interferon-γ (IFNγ); interleukin (IL); interferon-regulatory factor (IRF); Janus kinase (JAK); lipopolysaccharide (LPS); macrophage mannose receptor 1(Mrc1); mitogen- and stress-activated kinase (MSK);nuclear factor-κB (NF-κB);nitric oxide synthase 2 (Nos2); phosphoinositide 3-kinase (PI3K); peroxisome proliferator-activated receptor-γ (PPARγ); resistin-like-α (Retnla); signal transducer and activator of transcription (STAT); Toll-like receptor 4 (TLR4).

change in macrophage phenotype and their plasticity still remains elusive.

1.16 mTOR, metabolism and polarisation

There are studies that show seemingly contrasting roles of mTOR in individual cells or models [82] [83]. This can be attributed to the species-specific differences between mice and humans highlighting the importance of arginine and NO system [84]. Cytokines play a crucial role and can influence the overall interpretation of the data. It

has been shown that inhibition of mTOR promotes the expression of IL-12 expression and blocks IL-10 expression [84]. This suggests an anti-inflammatory role for mTOR. However, TNF-α and IL-6 are often blocked by mTOR inhibitors such as rapamycin [84]. This suggests a pro-inflammatory role for m-TOR. The complexity of the pathway itself could also account for differential outputs [84]. For example, inhibition of mTORC1 activates the PI3K-Akt pathway through a feedback loop via ribosomal protein S6 kinase 1 (S6K1) [84]. mTORC1 is negatively regulated by the tuberous sclerosis complex comprised of TSC1 and TSC2 [85]. AKt functions upstream of mTORC1 and downstream of mTORC2. Individual Akt isoforms promote distinct macrophage polarisation states, and Akt phosphorylation status changes substrate specificity [86]. $TSC^{-/-}$ macrophages have a marked defect in M2 polarisation in response to IL-4, while the inflammatory response to LPS is enhanced [83]. Aberrant polarisation is due to mTORC1-mediated attenuation of Akt activity, which renders $TSC^{-/-}$ macrophages resistant to the immunomodulatory effects of Akt downstream of IL-4 and LPS signalling. Akt favours the polarisation of macrophages to M2 phenotype [83]. Pharmacological inhibition of Akt leads to induction of M2 macrophages-associated genes [83], but the role of Akt in M1 macrophages is not lucid, with many studies indicating Akt and its upstream regulator PI3K as the negative regulators, and others reporting positive regulation of M1 activation [87]. The mammalian genome encodes 3 Akt proteins, of which Akt1, and Akt2 are thought to be expressed in macrophages [86]. In one study, analysis of genetic models specifically deficient in Akt protein suggests that Akt1 inhibits while Akt2 promotes M1 activation [86] (Table 1.4). The different results obtained by pharmacological inhibition of Akt may be due to inhibition of both the AKt proteins (Akt1 and Akt2) [86]. Activation of mTORC1 drives an anabolic response through hypoxia-inducible factor-1α (HIF-1α), PPARγ, sterol regulatory element-binding proteins (SREBPs) and MYC that induces the synthesis of nucleic acids, proteins and lipids [88]. This enhances glucose import by

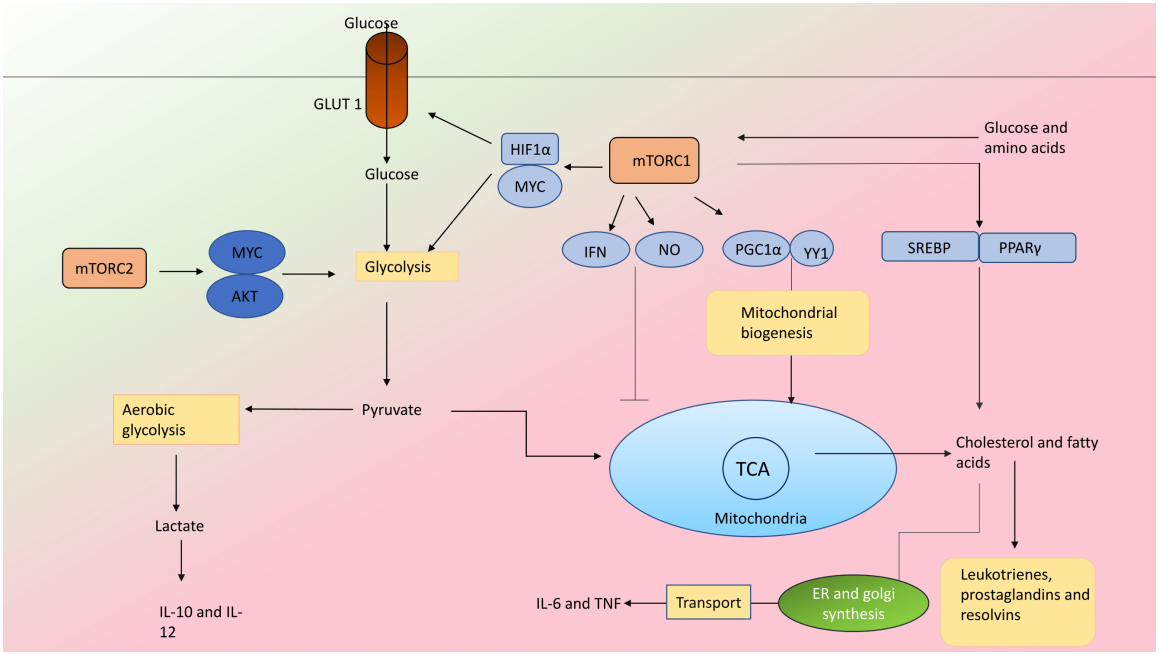

Figure 1.7: **Metabolic control by mTOR in innate immunity** This figure is adapted from [84]. This is a schematic representation of metabolic regulation of mTOR in innate cells. Abbreviations: Mammalian target of rapamycin (mTOR); glucose transporter (GLUT); hypoxia-inducible factor-1α (HIF-1α); peroxisome proliferator-activated receptor-γ (PPARγ); sterol regulatory element-binding proteins (SREBPs); tricarboxylic acid (TCA); PPAR co-activator 1 α (PGC1 α); yin and yang 1 (YY1); nitric oxide (NO); interferon (IFN)

	Macrophage polarization phenotype
TSC-deficient BMDMs	Increased M1 Reduced M2
TSC-deficient DCs	Decreased M; Mixed phenotype
Rictor-deficient DCs and BMDMs (mTORC2 deficiency)	Increased M1
Myeloid specific deficiency in Raptor (mTORC1 deficiency)	Not identified
Akt1-deficient peritoneal macrophages	Increased M1
Akt2-deficient peritoneal macrophages	Reduced M1

Table 1.4: **Macrophages with genetic knockout of mTORC1 and Akt reveal the critical role of polarisation of macrophages. This table is adapted from [86]**

increasing the expression and surface translocation of glucose transporter 1 (GLUT1) and increasing the expression of glycolytic genes (Figure 1.7). Activation of mTORC1 promotes cholesterol and fatty acid synthesis from tricarboxylic acid (TCA) cycle intermediates through a pathway involving sterol regulatory element-binding proteins (SREBPs) and PPARγ, and induces mitochondrial biogenesis through the transcription factors PPAR co-activator 1 α (PGC1 α) and yin and yang 1 (YY1) [89] (Figure 1.7). The mTORC2 also enhances glycolytic metabolism by activating Akt and promoting an inactivating phosphorylation of class IIa histone deacetylases [90]. Lactate, the end product of aerobic glycolysis, can directly re-programme macrophages and reduce the expression of IL-12, while enhancing the production of IL-10 [84]. These outcomes explain the complexity of PI3K-Akt-mTOR pathway.

1.17 Metabolism in macrophages

Macrophages have PRRs on the surface that recognise the PAMPS present in the invaders. As a result, these cells activate intracellular signalling cascades, leading to induction of a pro-inflammatory response [60] [91]. This results in increased gene expression [60]. Interestingly, these cells activated by PRRs undergo profound metabolic changes [60][62]. Early work on metabolism in immune cells were explained with the Warburg effect. In tumour cells, the glycolysis cycle predominates despite the presence of ample oxygen to proceed to oxidative metabolism [91]. Pyruvate, the final product of glycolysis, gets metabolised into lactate instead of feeding into TCA (also known as Kreb's or citric acid cycle) and subsequent oxidative phosphorylation [91]. A similar phenomenon is observed in myeloid cells such as neutrophils and macrophages. Activation of macrophages with various stimuli such as IFN-γ or LPS [92] switches the metabolism from OXPHOS to glycolysis, a phenomenon similar to the Warburg effect [92]. This leads to reduction in TCA cycle activity and enhanced lactate pro-

duction [92]. Furthermore, M1 and M2 macrophages show clear metabolic difference (Figure 1.8).

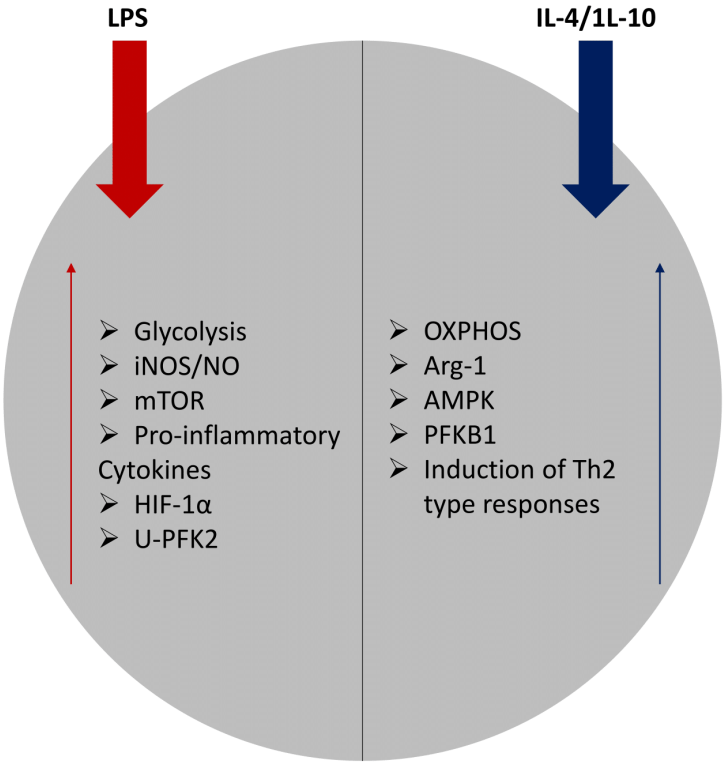

Figure 1.8: **Functions of M1 and M2 macrophages** This figure demonstrates the difference in functions of macrophage with different phenotype. This figure is adapted from [93]

Classically activated M1 macrophages primarily use aerobic glycolysis to generate energy and molecules for biosynthetic processes [94]. This causes an increase in flux through the pentose phosphate pathway (PPP), leading to an increase in NADPH which is an energy substrate for redox homeostasis and the production of reactive oxygen species (ROS) by NADPH oxidases (Figure 1.9) [91]. In macrophages with M1 phenotype, rapid ATP production from the glycolysis process fuels the activation in acute inflammation and anti-bacterial defense[91]. However, ROS are also produced by mitochondria. Although the TCA cycle is mainly fuelled by pyruvate

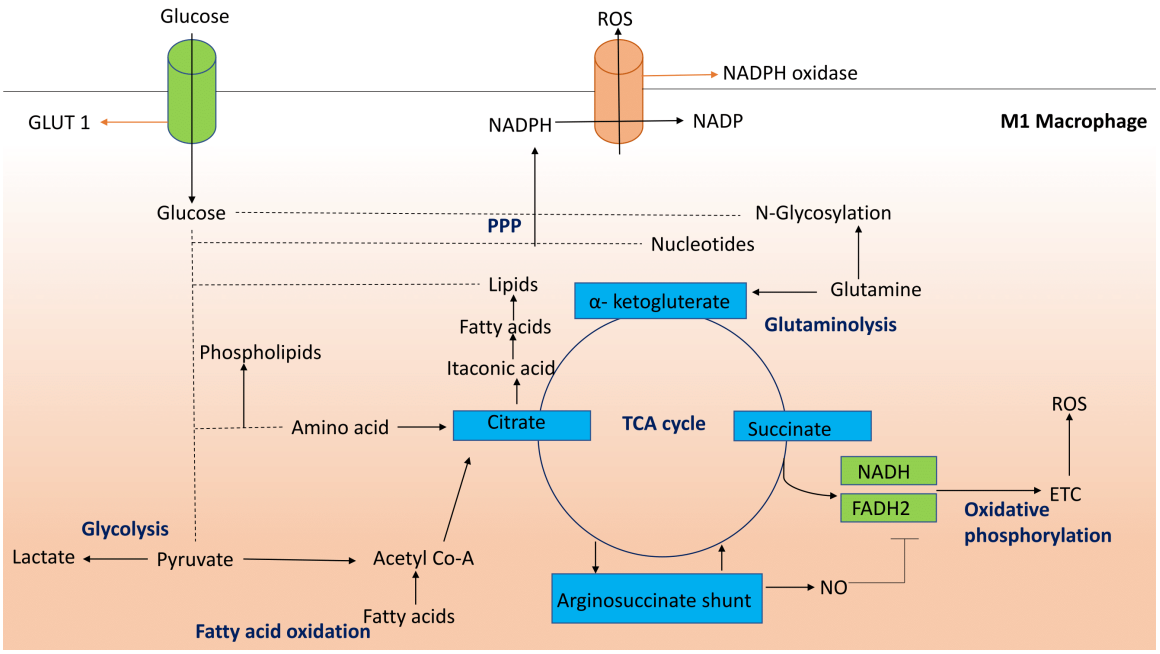

Figure 1.9: **Schematic representation of metabolism in M1 macrophages** Classically activated macrophages favours glycolysis to generate ATP and produces ROS via the PPP pathway. These cells have a broken TCA cycle. The intermediates are removed from mitochondria and moved to cytosol for to fuel the biosynthetic pathways. This figure is adapted from [91]. Abbreviations: tri-carboxylic cycle (TCA); glucose transporters (GLUT); pentose phosphate pathway (PPP); reactive oxygen species (ROS); Nicotinamide adenine dinucleotide phosphate (NADP); Flavin adenine dinucleotide (FADH2); electron transport chain (ETC)

from glycolysis and acetyl-CoA or succinyl-CoA from fatty acid oxidation, TCA intermediates removed from the mitochondria for use in biosynthetic pathways have to be replenished by glutamine in M1 macrophages due to the interruption of the TCA cycle at two positions [93]. The first break in the TCA cycle leads to the accumulation of citrate, a substrate for the synthesis of itaconic acid and fatty acids (including the generation of prostaglandins) [93]. Anabolic synthesis of fatty acids generates NADPH and, subsequently, ROS via NADPH oxidases. The second break leads to the accumulation of succinate, which activates hypoxia-inducible factor-1α (HIF-1α) induced inflammatory gene expression and increases the rate of glycolysis [91]. The argininosuccinate shunt replenishes levels of fumarate and malate, required

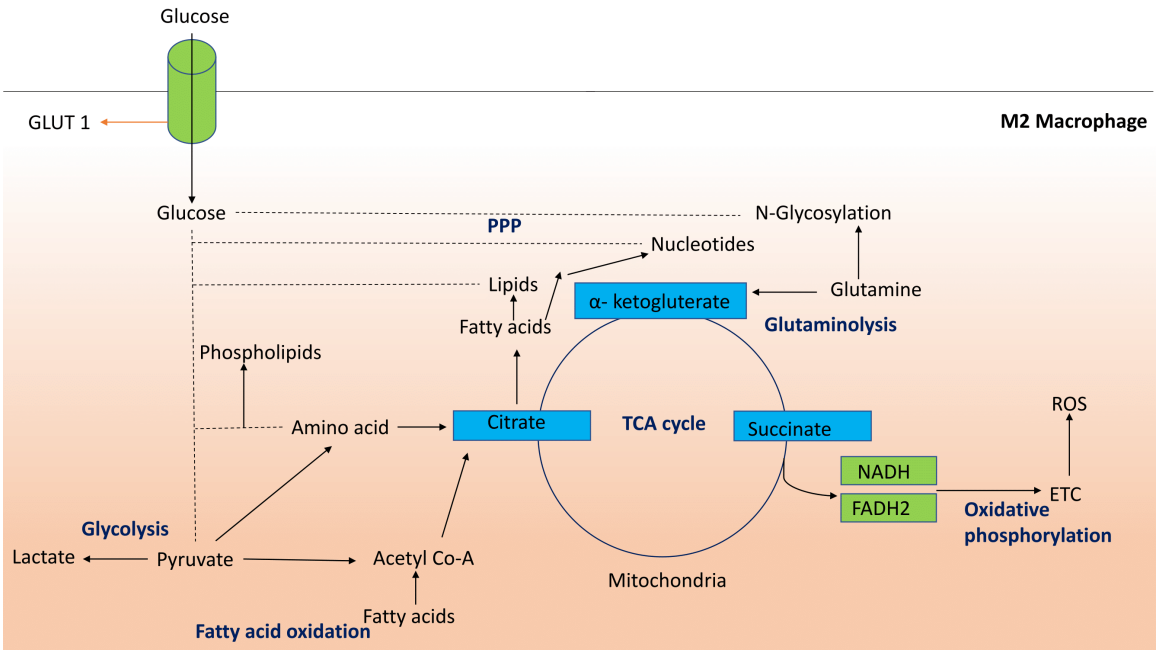

Figure 1.10: **Schematic representation of metabolism in M2 macrophages** Alternatively activated macrophages favours OXPHOS to generate ATP and favours increased fatty acid oxidation. Acetyl-CoA generated by fatty acid oxidation enters the intact TCA cycle for oxidative metabolism. This figure is adapted from [91]. Abbreviations: Electron transport chain (ETC); glucose transporter type 1 (GLUT1); pentose phosphate pathway (PPP); Nicotinamide adenine dinucleotide phosphate (NADP); Flavin adenine dinucleotide (FADH2)

for citrate production, thereby generating nitric oxide (NO), which inhibits succinate dehydrogenase activity (Figure 1.9) [91] [93].

Alternatively activated M2 macrophages are characterised by increased fatty acid oxidation, low glycolysis activity and reduced flux through the PPP [91]. Acetyl-CoA generated by fatty acid oxidation enters the intact TCA cycle for oxidative metabolism [93]. Glutamine is mainly used for the synthesis of amino-sugars and nucleotide sugars but also fuels the TCA cycle [91]. In M2, metabolism favours a complete TCA cycle. In these macrophages, oxidative phosphorylation occurs in the more long-term process of resolution and repair or in anti-parasitic immunity (Figure 1.10) [91]. It is still not fully understood why these differences occur, or indeed how the metabolic rewiring is regulated [93]. The metabolites accumulating in both phenotypes are shown to be ex-

tremely crucial for functions of M1/M2 polarised macrophages, providing compelling evidence to understand the immuno-metabolism in immune cells. Treatment of cancers is thought to be enhanced by drugs that modulate these metabolic pathways [93]. It may be possible that modulation of macrophage differentiation to a regulatory phenotype by the inhibition of metabolic pathways also contributes to cancer treatment, because tumour-associated macrophages exhibit regulatory macrophage phenotype and play critical roles in tumor progression by constituting its microenvironment [95] [96].

1.18 Glycolysis in macrophages

The glycolytic pathway has a profound effect on the differentiation of macrophages to a regulatory phenotype. Macrophages activation in response to TLR agonists causes a marked increase in glucose consumption and lactic acid production [97]. Previous literature shows that inhibition of glycolysis during the differentiation of monocytes to macrophages results in major change in its cytokine pattern [98]. Macrophages are very plastic and they can change their phenotype from an inflammatory to a regulatory phenotype in response to their environment [74] [75]. Macrophages skew towards IL-10 producing phenotype when glycolysis process is inhibited. M2 activation of macrophages is achieved with enhanced mitochondrial respiration. Microarray data of macrophages with impaired glycolytic pathway show down-regulation of genes such as colony stimulating factor 1 (CSF1), pyruvate dehydrogenase kinase 1 (PDK1), and matrix metalloproteinases (MMP-9) and up-regulation of the gene vascular endothelial Growth Factor A (VEFGA) [99] [98]. Glycolysis metabolism affects the differentiation and cellular migration by down-regulating the gene *CSF1*, which encodes M-CSF, and MMP-9 [98]. *PDK1* is a key regulatory enzyme in the glycolysis process. A knockdown of *PDK1* polarises the macrophages to M2 phenotype [99]. Metabo-

lites such as succinate and lactate regulates cytokine production in macrophages [100]. Also, recent studies have described the anti-inflammatory properties of pyruvate or ethyl pyruvate [101]. Ethyl pyruvate is a hyperpermeable analog of pyruvate [101] and these molecules are reported to inhibit the production of pro-inflammatory cytokines (IL-6, TNF, etc.) [99].

1.19 TCA cycle in M1-activated macrophages

Activation of macrophages by IFN-γ and LPS gives rise to a broken TCA cycle at the level of isocitrate dehydrogenase (IDH) and succinate dehydrogenase (SDH), leading to the accumulation of succinate and citrate metabolites (Figure 1.5). The build-up of citrate is the result of transcriptional downregulation of IDH1, the enzyme responsible for the conversion of isocitrate (an isomer of citrate) into α-ketoglutarate [102]. The accumulated citrate serves as a precursor for the synthesis of the macrophage-specific metabolite itaconic acid, which is a major feature of IFN-γ/LPS-polarized macrophages [102].

1.19.1 Role of citrate in M1 macrophages

The LPS activated macrophages lead to an excessive accumulation of citrate [93]. Citrate is only metabolised once in the cytosol in M1 activated macrophages and exit the mitochondria [103]. The mitochondrial citrate carrier (CIC) is responsible for the transport of citrate from the mitochondria to the cytosol [93]. CIC expression was increased in macrophages following LPS stimulation [103], most likely via NFκB as the CIC promoter contains two NFκB binding sites. CIC was required for the induction of ROS, NO and prostaglandins (PGs) in macrophages treated with LPS [103]. This accumulation leads to excessive production of NO, ROS, and PGs [103]. LPS induces the expression of the mitochondrial citrate carrier, and depletion of this

protein by gene silencing decreases the production of NO, ROS, and PGs. Citrate accumulation in M1 macrophages is important for mediators, leading to production of various pro-inflammatory cytokines (Figure 1.9). Citrate is used to synthesise phospholipids which are a source of arachidonic acid that are needed for PGs synthesis [103]. Citrate can also generate NADPH using malic acid enzyme and pyruvate, and this NADPH can be used by iNOS to generate NO [103]. NADPH oxidase uses NADPH to generate ROS.

Furthermore, there is a marked increase in itaconic acid synthesis (Figure 1.9). Itaconic acid is generated through the decarboxylation of aconitate (which is produced from citrate) by the enzyme encoded by immunoresponsive gene 1 (Irg1) [94] [102]. The levels of these are enhanced in both M1 macrophages and macrophages treated with LPS [93]. Itaconic acid has also been shown to inhibit the enzyme isocitrate lyase (ICL), a component of the glyoxylate shunt [104]. This is an essential metabolic pathway required for the survival of bacteria growing on fatty acids (FAs) [102] or acetate as their primary carbon source, such as *Escherichia coli* and *Yersinia pestis*, which is responsible for bubonic plague [103]. Therefore, itaconic acid is a metabolite with unique signalling properties which is elevated in LPS-activated macrophages where it plays an important anti-microbial role.

1.19.2 Role of succinate in M1 macrophages

Inflammatory macrophages show an increased mitochondrial accumulation of succinate [91]. This metabolite expression is also increased in mouse models of obesity and diabetes [105], metabolic disorders associated with inflammation. The increase in succinate levels in LPS-stimulated macrophages is due to the dampened system in reponse to LPS and does not origanate from the TCA cycle [92] [100]. The glutamine metabolism provides the source for the generation of succinate which is followed by α-ketoglutarate (α-KG) [106], and via the γ-aminobutyric acid (GABA) shunt [100].

Succinate is also generated from glyoxylate shunt. This system is conserved in bacteria, fungi, protists, and plants [107] [108]. The first enzyme of this shunt, isocitrate lyase (ICL), converts isocitrate to succinate and glyoxylate [100]. It is unclear whether LPS increases succinate production via the ICL pathway in mammals upon microbial infection. Macrophages highly express immunoresponsive gene 1 (Irg1) during inflammation, which catalyses the generation of itaconic acid from the TCA cycle intermediate cis-aconitate [109]. As mentioned previously, itaconic acid has a strong anti-microbial activity. Interestingly, succinate stabilises HIF-1α, thus promoting the switch to glycolysis leading to inflammation [100][91]. It achieves this by inhibiting the activity of the prolyl hydroxylase (PHD) enzymes, thus destabilising HIF-1α [100]. As a result, HIF-1α can interact with co-activators and induce glycolytic metabolism program and drives inflammation by increasing the production of the cytokine IL-1β [100]. Extracellular succinate signals via the G protein-coupled receptor (GPR) [110]. GPR91 is highly expressed by DCs, and can interact with TLR signaling leading to the induction of the pro-inflammatory cytokines TNF-α by the TLR3 ligand poly(I:C) or the TLR7 ligand imiquimod [111]. Clearly, succinate is an important signalling molecule in innate immune cells, and may also represent a therapeutic target in a variety of pathologies.

1.20 TCA cycle in M2 macrophages

While M1 macrophages obtain their energy from glycolysis, M2 macrophages mainly produce ATP through an oxidative TCA cycle coupled to OXPHOS (Figure 1.6) [94]. In order to fuel an oxidative TCA cycle, IL-4-stimulated macrophages rely on fatty acid oxidation (FAO) (also known as β-oxidation) [112] and glutamine metabolism [102]. Glutamine fuels the TCA cycle through anaplerotic generation of α-ketoglutarate [102]. Furthermore, glutamine contributes to UDP-GlcNAc synthesis

via the hexosamine pathway. UDP-GlcNAc leads to protein glycosylation, including the M2 markers macrophage mannose receptor (MMR) and macrophage galactose binding lectin (Mgl1) [102]. In IL-4/IL-13-stimulated macrophages, the upregulation of FAO and mitochondrial biogenesis is orchestrated by the combined action of STAT6, PPARs, and PGC-1β [113].

1.21 Pentose phosphate shunt in macrophages

The pentose phosphate pathway (PPP) takes place in the cytosol. It helps various process that support cell proliferation and survival. The important protagonist in PPP is the nucleotide production. This happens mainly during cell production [114]. The other important outcome of PPP is NADPH production [115]. NADPH is responsible for various functions in immune cells. For example, it generates ROS during the macrophage respiratory burst [115]. During infection, macrophages and neutrophils are dependent on NADPH functions [114]. They require rapid ROS production to clear the infections and produce antioxidants to prevent excessive tissue damage. This pathway has been found to be elevated in M1 macrophages. It is highly regulated by the enzyme carbohydrate kinase-like protein (CARKL; also known as SHK), which is a sedoheptulose kinase-33 [115]. This enzyme limits the flux through the PPP, and it has been shown to be highly expressed in M2 macrophages [115]. The PPP represents a prime example on how increased carbon-flux can contribute to mount the specific effector functions of LPS-activated macrophages by complementing their appropriate demands through supplying both redox-power and ribose moieties [116]. Inhibition or suppression of CARKL favours the polarisation of macrophages to M1 [115]. In summary, these findings indicate that during macrophage activation the cellular demands are covered by a precisely coordinated interplay of many pathways to sustain such profound polarisation events [115]. The PPP presents a versatile hub to reroute

carbon moieties primary carbohydrate metabolism while independently controlling cellular redox-states [116].

1.22 Fatty acid oxidation in macrophages

The fatty acid synthesis pathway helps cells to generate lipids that are necessary for cellular growth and proliferation from precursors derived from other cell intrinsic metabolic pathways. As mentioned earlier, M2 polarised macrophages rely on FAO [94]. Mitochondria-dependent β-oxidation of long-chain fatty acids requires the carnitine palmitoyltransferase (CPT) system, which consists of one transporter and two mitochondrial membrane enzymes: CPT1 and CPT2 [113] [112]. Its proved to be consistent with the known requirement for CPT2 in FAO, it has been shown that macrophages lacking CPT2 were unable to achieve β-oxidation of fatty acids yet still seemed to fully polarise toward an M2 state after stimulation with IL-4 *in vitro* and *in vivo* [112] [102]. The fatty acid synthesis is also coupled to the mTOR signalling pathway and promotes the fatty acid synthesis pathway [114]. This is done through regulation of main enzymes responsible for *de novo* lipid synthesis, such as SREBP, fatty acid synthase (FASN), and acetyl CoA carboxylase (ACC) [114].

1.23 Aim

- Investigate the role of glucose-6-phosphate translocase (G6PT) on the functions of monocytes derived macrophages. This study was aimed to determine whether the inhibition of G6PT enzyme function has an effect on viability, superoxide production, bacterial handling and differentiation of macrophages.

- Elucidate the metabolic process that influence the performance of macrophages. This study was aimed to understand the immunologic-metabolic interface in

G6PT deficient macrophages and explore the plausible mechanism by which G6PT influences intestinal inflammation.

- Determining polarisation of macrophages (M1/M2) with G6PT enzyme inhibition. This study was aimed to investigate how G6PT enzyme influences the polarisation of the macrophages and how change in the phenotype affects the metabolism.

Chapter 2

Materials and methods

2.0.1 Bacteria

Non-invasive bacteria were used for performing bacterial killing assays which include *Salmonella enterica serovar typhimurium (S. typhimurium)-expressing GFP* (*NCTC*12023).

2.0.2 Cell culture media

For all the cell culture, the following solutions were used; Roswell Park Memorial Institute 1640 medium (RPMI) (Sigma-Aldrich, Gillingham, UK) and Dulbeccos modified eagles medium (DMEM) (Sigma-Aldrich, Gillingham, UK). These media were supplemented with 10 % fetal calf serum (FCS) (Gibco, Life Technologies, Paisley, UK). For cellular washing, as well as in multiple assays, Dulbeccos phosphate buffered saline (PBS) was used (Sigma-Aldrich, Gillingham, UK). For cell dissociation, versene solution (Gibco, Life Technologies, Paisley, UK) was used. Chlorogenic aid derivative S3483 (Sigma-Aldrich, Gillingham, UK) was used as the inhibitor of G6PT. For macrophage differentiation M-CSF (R&D Systems) was used. For bacteria culture, Luria Bertani (LB) broth (Lennox) was used.

2.0.3 Macrophage Differentiation

peripheral blood mononuclear cell (PBMC) were isolated by using standard method of Ficoll gradient (Lymphoprep, Axis-Shield) centrifugation. PBMC were plated in a 10 cm dish with RPMI for a period of 2 hours. Cells were washed twice with PBS) and monocytes were differentiated to monocyte derived macrophages (MDM) over a period of 5 days in RPMI 1640 medium supplemented with 10 % fetal calf serum (FCS), 100 ng/ml M-CSF, and G6PT inhibitor S3483 (30 μM, 50 μM, 70 μM and 100 μM).

2.0.4 Bacterial cultures

Bacterial strain *(S. typhimurium-expressing GFP (NCTC*12023*)* was cultured using LB broth (Lennox) and maintained using agar plates which were autoclaved, in accordance to standard bacterial culture technique. For an overnight incubation, the bacterial colony was cultured using a pipette tip in three ml of LB broth and incubated overnight at 37 °C and 200 rpm.

2.0.5 Viability assay

Live dead stain: MDM (25×10^4) in one mL of RPMI 1640 medium supplemented with 10 % FCS was added to a BD Falcon 12 × 75 mm tube. LIVE/DEAD Red fluorescent fixable dye Cell Stain Kit (Cat. No. L23102) was diluted by adding 50 μl of Dimethyl sulfoxide (DMSO). Red fluorescent dye was used, this distinguishes live cells from dead cells based on cell membrane integrity and access to available amines. The cells were stained with 1 μl of diluted stain and incubated for 30 minutes at 37 °C. Following incubation, the cells were spun at 1700 rpm for 5 minutes. Supernatant was aspirated and re suspended in 250 μl of FSB. Samples acquisition and data analysis was done using the LSR Fortessa flow cytometry system and FlowJo software (Version

10.0.8.r1) respectively.

2.0.6 Bacterial killing assay

Gentamicin protection assay: Bacterial killing ability of MDM was tested in gentamicin protection assay (GPA) using *S. typhimurium*. Drug treatment was done throughout the duration of assay. MDM were infected with *S. typhimurium* at a multiplicity of infection (MOI) of 10 bacteria per macrophage cell for 1 hour. Post infection MDM were washed with PBS and new complete medium supplemented with gentamicin 100 μg/ml was added for additional two hours to kill extracellular bacteria. MDM were washed twice before lysis using 1% Triton X-100 in deionized water. Samples were diluted (1:10 and 1:100) and plated onto square LB agar plates by track method, plate is tilted (around 45 °angle) to allow flow down the agar. Once the plate is dried, they were sealed with Parafilm and were placed in an incubator overnight at 37 °C. Following day, colony forming units (CFU) recovered from the lysed macrophages were counted. The CFU for each inhibitory condition was then normalised as a percentage of the mean CFU for the untreated condition: % CFU= (mean of condition/mean of untreated condition)x100. Each assay was performed in experimental duplicates or triplicates and all the conditions were assayed side by side on the same plate.

2.0.7 Reactive oxygen species assays

Dihydrorodamine FACS: 400 μl MDM (30×10^4) in RPMI 1640 medium supplemented with 10 % fetal calf serum were taken in a BD Falcon $12 \times 75mm$ tube. 100 μl of working dihydrorodamine (DHR) solution (2.5 μg/ml) was added to each 400 μl sample. The staining was performed for a period of 15 minutes at 37 °C. Phorbol-12-myristate-13-acaetate (PMA) (100 μg/ml) stimulation was performed for 15 minutes at 37 °C. Following incubation, the cells were spun at 1700 rpm for 5 minutes at 22

°C. The pellet was resuspended with 250 μl of FACS staining buffer (FSB). Three different conditions, cells only, cells treated with DHR and cells treated with both DHR and PMA were assayed. Samples acquisition and data analysis was done using the LSRFortessa flow cytometry system and FlowJo software (Version 10.0.8.r1) respectively. Data was represented as ΔMFI (Mean fluorescence Intensity) measuring the mean of fluorescence of DHR stain comparing the condition treated or untreated with S3483.

2.0.8 Surface marker expression on MDM

MDM were differentiated in the presence or absence of S3483 for a period of 5 days. MDM (10×10^4) were plated in a 96-well V-bottom plate. The cells were centrifuged at 1700 rpm for 3 mins at 4 °C and washed using FACS staing buffer (FSB) twice. Working solution of antibodies was made by mixing 200 μl of FSB with 5 μl of the following antibodies: CD172 (FITC, eBioscience) , CD11c (PET-R, eBioscience), CD14 (BV650, eBioscience), HLA-DR (BV711, eBioscience) , CD40 (PerCP-Cys5.5, eBioscience) CD64 (BV421, eBioscience) , CD86 (BV605, eBioscience), CD163 (PE, eBioscience) for 20 mins on ice. MDM were stained with 50 μl of the working solution for 20 mins. Following the staining, cells were washed with 200 μl of FSB and centrifuged at 1700 rpm for 3 mins at 4 °C. The supernatant were aspirated and MDM were re-suspended with 200 μl of FSB. Samples acquisition and data analysis was done using the LSRFortessa flow cytometry system and FlowJo software (Version 10.0.8.r1) respectively.

2.0.9 Metabolism Assay

To understand the glycolysis and OXPHOS mechanism, glucose stress and mito stress assay was performed on MDM differentiated in the presence or absence of S3483.

2.0.9.1 Glucose stress assay

Glucose gets converted to pyruvate (referred to as glycolysis), finally getting converted to lactate in cytoplasm or CO_2 and water in mitochondria. The subsequent conversion of glucose to lactate in the cytoplasm results in a net production and extrusion of protons into the extracellular medium leading to acidification of the medium. The agilent seahorse XF instrument directly measures the acidification rate in the extracellular medium (ECAR). In this assay, the cells were incubated with glycolysis stress test medium (free of glucose or pyruvate) primarily and ECAR is measured at this time point. Glucose was injected following this, converting glucose inside the cells to pyruvate producing ATP, NADH, water and protons. This results in increase in ECAR, measuring the glycolysis at basal conditions. The second injection was oligomycin which is an ATP synthase inhibitor. Oligomycin inhibits mitochondrial ATP production thus shifting the energy production to glycolysis, with the subsequent increase in ECAR revealing the cellular maximum glycolytic capacity. The final injection was 2-deoxy-glucose (2-DG), a glucose analog, that inhibits glycolysis through competitive binding to glucose hexokinase. This results in decrease in ECAR confirming that the ECAR produced in the experiment is due to glycolysis (Table 2.1).

Compound(s)	Target	Effect on ECAR
Glucose	Glycolysis	Increase
Oligomycin	Inhibits ATP synthase Complex V	Increase
2-DG	Inhibits Hexokinase	Decrease

Table 2.1: **Effect of glucose stress modulators on glycolysis pathway**

The Aligent Seahorse XF Analyser was switched on the previous night. The MDM ($100 \times 10^4 - 200 \times 10^4$) were plated in triplicates using the Seahorse XF cell culture Microplate in the RPMI medium. The Sensor cartridge in Seahorse Calibrant was hydrated at 37 °C in a non-CO2 incubator. The assay medium was prepared by supplementing Seahorse XF Medium with 1 mM glutamine. The assay medium was

warmed and maintained at 37 °C and the pH was set to 7.4 with 0.1 N NaoH. Stocks of Glucose (100 mM), Oligomycin (100 μM), and 2-DG (500 mM) were prepared. A final concentration of 10 mM of Glucose was injected into Port A, 10 μl of Oligomycin was injected into Port B, and 50 mM of 2-DG was injected into Port C. The microplate with the cell culture that was incubated the previous night was removed from the incubator. The RPMI media was removed from the the microplate and warmed assay medium was added to these cells with the help of a multichannel pippet. The microplate with the assay medium was incubated for 37 °C in a non-CO_2 incubator for 45 minutes prior to the assay. The glycolysis stress kit was run using the XF software. The utility plate with the loaded sensor cartridge was placed on the instrument tray. The assay was run following the calibration. The Seahorse XF Glycolysis Stress Test Report Generator automatically calculated the Seahorse XF Glycolysis Stress Test.The parameters from the Wave data were exported to Excel.

2.0.9.2 Mitostress assay

The Agilent Seahorse XF cell Mitostress kit was used to measure the mitochondrial function. The mitochondrial respiration is measured by directly quantifying the oxygen consumption rate (OCR). The assay measures the basal respiration, spare respitory capacity, and non-mitochondrial respiration. The compounds used in this assay are directly used to target the components of electron transport chain. The workflow of the assay was performed as follows; Oligomycin was injected, which is used to measure ATP production. This was followed by Carbonyl cyanide-4 (trifluoromethoxy) phenylhydrazone (FCCP) injection, which is used to measure the maximal respiration and finally a mixture of rotenone and Antimycin A was added to measure the non-mitochondrial respiration. Oligomycin is used to inhibit ATP synthase (Complex V) leading to a decrease in OCR. FCCP uncouples oxygen consuption from ATP production disrupting the mitochondrial membrane potential and collapses the proton

gradient. This results in uninhibited electron flow through the ETC, leading to an increase in OCR. Rotenone and Antimycin A inhibits complexes I and III respectively. This combination shuts down mitochondrial respiration (Table 1.5).

Compound(s)	Target	Effect on OCR
Oligomycin	Inhibits ATP synthase Complex V	Decrease
FCCP	collapses the proton gradient	Increase
Antimycin A and Rotenone	Inhibits complex I and III	Decrease

Table 2.2: **Effect of mito stress modulators on mitochondrial respiration**

The Aligent Seahorse XFe/XF Analyzer was switched on the previous night. The MDM ($100 \times 10^4 - 200 \times 10^4$) were plated in triplicates using the Seahorse XF cell culture Microplate in the RPMI medium. The Sensor cartridge in Seahorse Calibrant was hydrated at 37 °C in a non-CO_2 incubator. The assay medium was prepared by supplementing Seahorse XF Base Medium by using 1 mM pyruvate, 2 mM glutamine, and 10 mM glucose which was used as a starting point. The medium was Warmed and maintained at 37 °C and the pH was adjusted to 7.4 with 0.1 N NaOH. Stocks of Oligomycin (100 μM), FCCP (100 μM), and mixture of Rotenene and Antimycin A (5o μM) were prepared. A final concentration of 1 μM of oligomycin was injected into Port A, 1 μM of FCCP was injected into Port B, and 0.5 μM of Rotenone and Antimycin was injected into Port C. The microplate with the cell culture that was incubated the previous night was removed from the incubator. The RPMI media was removed from the microplate and warmed assay medium was added to these cells with the help of a multichannel pippet. The microplate with the assay medium was incubated for 37 °C in a non-CO_2 incubator for 45 minutes prior to the assay. The Mito stress kit was run using the XF software. The utility plate with the loaded sensor cartridge was placed on the instrument tray. The assay was run following the calibration. The Seahorse XF Mito Stress Test Report Generator automatically calculated the Seahorse XF Mito Stress Test.The parameters from the Wave data were exported to Excel.

2.0.10 pS6 estimation

MDM (30×10^4) in RPMI 1640 medium supplemented with 10 % FCS were taken in a BD Falcon 12 $\times$ 75 mm tube. The cells were centrifuged at 1700 rpm for 3 minutes at 4 °C. The supernatant was aspirated out and the cells were re suspended in 100 μl of Fix-Perm buffer and were incubated in ice for 20 minutes. Following the incubation, 300 μl of BD perm wash buffer was added to the cells and were spun at 1700 rpm for 3 minutes at 4 °C. The supernatant was aspirated and the cells were stained with pS6 antibody (eBioscience) (1:200 dilution in BD perm wash buffer) for a period of 40 minutes. Following the incubation, 200 μl of BD perm wash buffer and centrifuged at 1700 rpm for 3 minutes at 4 °C. Supernatant was aspirated and the cells were re suspended in 250 μl of FSB. Samples acquisition and data analysis was done using the LSRFortessa flow cytometry system and FlowJo software (Version 10.0.8.r1) respectively. Intracellular Δ pS6 was calculated as the difference between the frequency of MDM unstained and stained with pS6 antibody.

2.0.11 Quantitative Real-Time PCR

Total m-RNA was extracted from MDM ($1 - 2 \times 10^6$) in accordance to the Quiagen kit protocol and 1μg of RNA was reverse transcribed using the High capacity cDNA Reverse Transcription kit (Applied Biosystems), according to the manufacturer's instruction. *ATF-6, DDIT-3, HSPA5, GLUT-1, GLUT-3, NRF-2,* and *HIF-1α* expressions were evaluated using quantitative real-time PCR (q-RT-PCR). PCR amplifications reactions were prepared using Taqman probes (ATF-6, DDIT-3, HSPA5, GLUT-1, GLUT-3, NRF-2, HIF-1α (Applied biosystems). Reactions were performed in triplicates and relative quantification was calculated using ΔCT method. Quantitative PCR was performed using Bio rad software system. The results were expressed relative to the expression of house-keeping gene RPLPO.

2.0.12 PCR array analysis

Total m-RNA was extracted from MDM ($1 - 2 \times 10^6$) in accordance to the Quiagen kit protocol and 0.5μg of total RNA was reverse transcribed using RT^2 first strand kit (Qiagen) for 96-well plate. Quality control analysis was done using the RT^2 RNA QC PCR Array in accordance to the protocol provided in the RT^2 RNA QC PCR Array Handbook using a 6μl aliquot of the diluted cDNA template. RT^2 SYBR green master mix was made which contains hot start DNA Taq Polymerase. PCR components mix was prepared using the RT^2 profiler PCR Array format (Qiagen). A volume of 25μl PCR components mix was added to each well of the RT^2 Profiler PCR Array using an 8-channel pipettor. The plate was carefully sealed using an Optical Adhesive Film. Quantitative PCR was performed using Bio rad software system. The relative quantification was calculated using ΔCT method and results were expressed relative to the expression of house-keeping gene RPLPO.

2.0.13 Metabolomics sample preparation

MDM ($1 - 2 \times 10^6$) from five different healthy controls were differentiated in the presence or absence of S3483 inhibitor in a 10 cm^2 dish under tissue culture conditions in the incubator. The cells were washed twice with 5ml of PBS buffer and the excess media was removed. This was repeated twice. A volume of 100 ml of ice cold 80 percent methanol solution with milli-Q water was prepared and 500 μl of ice cold 80 percent methanol was added to the cells (500 μl per 1-3 $\times 10^6$ cells) helping the cells to detach from the 10 cm^2 dish. The resulting lysate solution was pippeted and the cell debris was transferred into an 1.5ml Eppendorf tube and kept on ice. The mixture was centrifuged at 14,000 rpm for 30 minutes at 4 °C. The supernatent obtained was filtered using a 10kD molecular weight cut-off filter (Amicon ultra 0.5ml centrifugal filters UFC501024) which helps in removing the soluble protein from the metabolite solution. The filters were prepared prior to their use by washing off the glycerol with

milli-Q water and centrifuged for 30 minutes. The samples were normalised with the addition of a volume of MeOH equivalent to the number of cells present (1-3 $\times 10^6$ cells). A volume of 300 μl of the filtered and normalised extract was transferred into a LCGC (Liquid and gas chromatography) certified clear glass $12 \times 32mm$ screw neck total recovery vial, with pre-slit Polytetrafluoroethylene cap. The samples were frozen at -80 °C until the day of analysis. A quality control (QC) of sample was made by mixing equimolar concentration (10-20 μM of each sample) of all samples across all experimental groups. Liquid chromatography/mass spectrometry (LC-MS) was used to analyse the samples. This is powerful analytical technique that combines the resolving power of liquid chromatography with the detection specificity of mass spectrometry. Anion exchange chromatography was used to perform the analysis for the metabolites from glycolysis and other phosphor-sugars, TCA cycle, Pentose phosphate pathway and additional organic acids. Data acquisition and analysis was done in Prof James McCullagh lab from the chemistry department, in accordance to their standardised protocol. The compounds that changed between the two groups significantly (*p<0.05) were plotted as a heatmap associated with major metabolic pathways.

2.0.14 Cytokine assay

MDM were differentiated in the presence or absence of S3483 for a period of 5 days. MDM (10×10^4) were plated in a 96-well V-bottom plate. MDM were stimulated with 200 ng/ml of LPS for 6 hours at 37 °C. The cells were treated with the GolgiPlug immediately after the LPS stimulation. Following the 6 hours incubation, the cells were centrifuged at 1700 rpm for 3 mins at 4 °C and washed using FACS staing buffer (FSB) twice. LIVE/DEAD Red fluorescent fixable dye Cell Stain Kit (Cat. No. L23102) was diluted by adding 50 μl of DMSO. The cells were stained with 1 μl of diluted stain and incubated for 15 minutes at 37 °C. The cells were centrifuged

at 1700 rpm for 3 minutes. Following this, the cells were washed twice with FSB. The supernatant was aspirated out and 400 μl of BD perm wash buffer was added to the cells and centrifuged at 1700 rpm for 3 minutes at 4 °C. Supernatant was aspirated and the cells were re-suspended in 100 μl of fix-Perm on ice for 20 minutes. Following the incubation, 300 μl of BD perm wash buffer was added to the cells and were spun at 1700 rpm for 3 minutes at 4 °C. The supernatant was aspirated and the cells were stained with the following antibody; IL-1α (1:100 in BD perm wash buffer, PE), IL-1β (1:50 in BD perm wash buffer, FITC), IL-4 (1:30 in BD perm wash buffer, APC), IL-6 (1:30 in BD perm wash buffer, AF700), IL-10 (1:30 in BD perm wash buffer, PE-CY7), and TNF-α (1:150 in BD perm wash buffer, BV605) antibody (eBiosciences) for a period of 20 minutes on ice. The cells were centrifuged following the staining for 3 minutes at 1700 rpm and washed twice with FSB. The supernatant was aspirated and the cells were re-suspended in 200 μl of FSB. Samples acquisition and data analysis was done using the LSRFortessa flow cytometry system and FlowJo software (Version 10.0.8.r1) respectively.

2.0.15 Statistical analysis

All statistical analyses were performed using Graphpad Prism software (version 5.0a). For normally distributed data, the mean and standard error of mean is presented, and statistical comparison between groups is assessed using a students t test (one-tailed) and statistical comparison between two groups is assessed using a non-parametric Mann Whitney test.

Chapter 3

Results and discussion

3.1 Results

In order to understand the effect of the enzyme G6PT in macrophages, we used a chemical inhibitor model to mimic the G6PT enzyme defect in macrophages. we used the derivative of cholorogenic acid S3483 [25] to inhibit this enzyme.

3.1.1 Viability of macrophages treated with S3483

Monocytes derived macrophages (MDM) were differentiated in the presence of the inhibitor for 5 days at the following concentrations: 0 μM, 30 μM, 50 μM, 70 μM, and 100 μM. To study the viability of cells, LIVE/DEAD staining was performed. This assay measures the fluorescent reactive dye with cellular proteins (Amines). There was an increase in the amount of dead cells with the increase in concentration of G6PT inhibitor (S3483) (Figure 3.1). Because of the decrease in viable cells to work with at a higher concentration (70 μM and 100 μM), 50 μM was chosen as the ideal working concentration to perform future experiments.

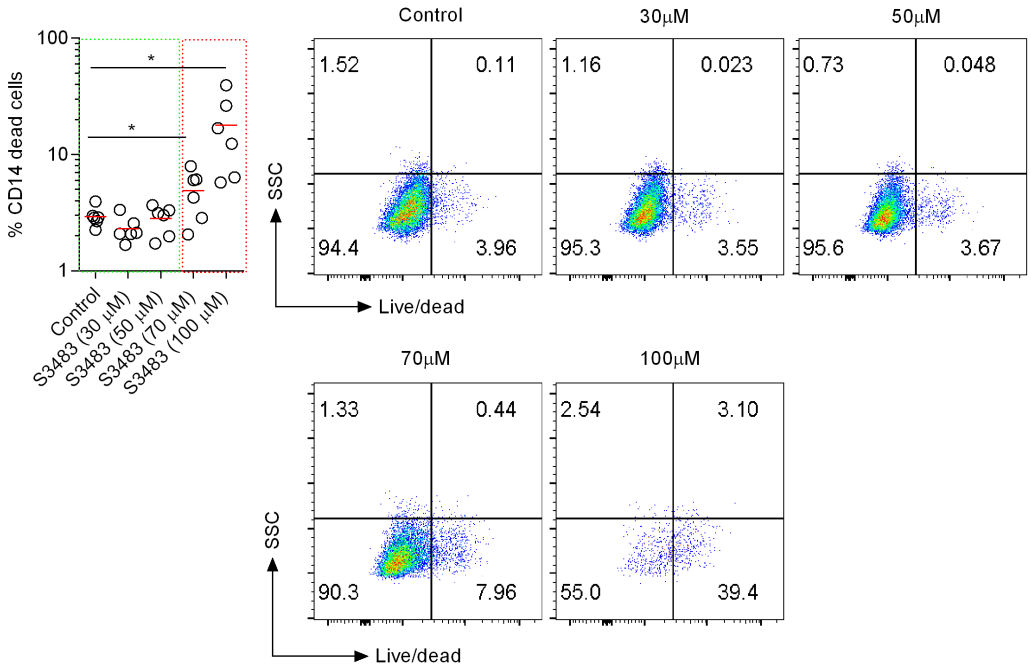

Figure 3.1: **Viability of MDM when treated with S3483.** MDM differentiated in the presence of S3483 at various concentrations (30 μM, 50 μM, 70 μM, and 100 μM). The cells were stained with 1 μl of diluted stain and incubated for 30 minutes at 37 °C. Samples acquisition and data analysis was done using the LSR Fortessa flow cytometry system and FlowJo software (Version 10.0.8.r1) respectively.(n=6, *p<0.05, Mann-Whitney U test).

3.1.2 S3483 impairs bacterial handling in macrophages differentiated in the presence of S3483

The patients with deficiencies in G6PT enzyme have frequent intestinal inflammation and infection. This implicates a possible role for G6PT enzyme in bacterial handling. In order to understand the role of S3483 in macrophage bacterial handling, MDM were treated with S3483 at two different periods of time; MDM were treated or untreated with the inhibitor (50μM) for 24 hours following their differentiation or, MDM were differentiated in the presence of the inhibitor for a period

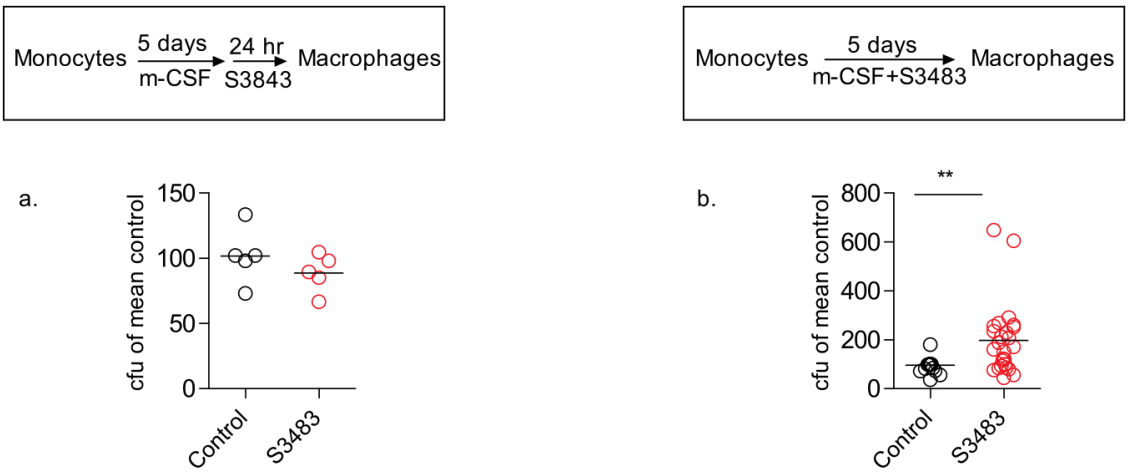

Figure 3.2: **Impaired bacterial handling by MDM when differentiated with S3483 for 5 days** (a) MDM were differentiated in the presence of M-CSF for 5 days. Bacterial killing assay on MDM treated with S3483 (50 μM) for 24 hours after differentiation. MDM treated with S3483 were infected with *Salmonella enterica serovar typhimurium (S. typhimurium)-expressing GFP (NCTC 12023)*. Experiment was performed in duplicates (each dot represents each donor). CFU is plotted as a percentage CFU of mean control.(n=5) (b) MDM were differentiated in the presence of m-CSF and S3483 for 5 days. Bacterial killing ability of MDM differentiated with S3483 (50μM) Experiment was performed in duplicates (each dot represents each donor). CFU is plotted as a percentage CFU of mean control. (n=48, **P<0.005, Mann-Whitney U test).

of 5 days. A gentamicin protection assay (GPA) was performed to assess bacterial killing of intracellular replicating invasive bacteria *S.typhimurium*. Bacterial killing of *S.typhimurium* was analysed in two different conditions of treatment with S3483. No difference was observed in bacterial killing mediated by MDM on treatment with S3483 for 24 hours following differentiation (Figure 3.2). In contrast to this, the MDM differentiated in the presence of S3483 showed a significant increase in the number of bacterial colonies compared to the untreated condition (Figure 3.2) (Figure 3.3). Thus, inhibiting G6PT enzyme affects the macrophages during their differentiation and affects their bacterial handling ability.

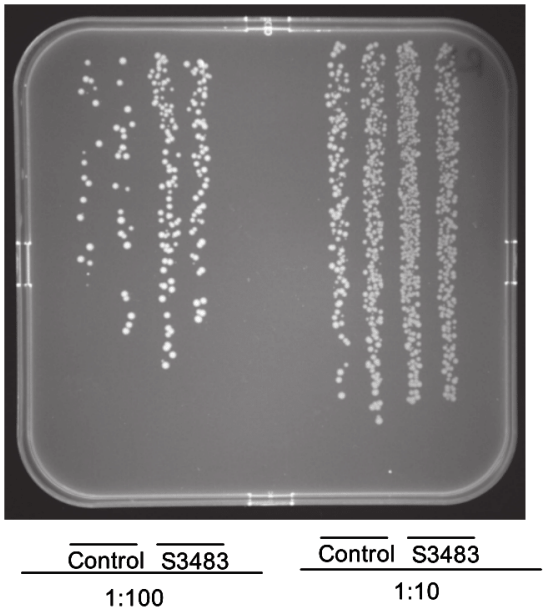

Figure 3.3: **Representative LB agar plate of GPA on MDM treated with S3483** Plate containing the colonies of *S.typhiurium* from MDM differentiated in the presence or absence of S3483.

3.1.3 MDM treated with S3483 is independent of ER stress

G6PT enzyme is located in the lumen of the ER. Inhibiting this enzyme may affect the expression of genes associated with ER. Further to this, impaired bacterial handling by macrophages has also been shown to increase stress associated with ER. Therefore, we hypothesised that the impaired bacterial killing in MDM differentiated in the presence of S3483 causes increase in ER stress. To test this, the monocytes were differentiated into macrophages in the presence of S3483 (50 μM) for 5 days.

The transccription factors ATF-6 (Activating transcription factor-6), DDIT-3 (DNA damage-inducible transcript 3) and HSPA5 (Heat shock protein family A (member 5)) were quantified to detect the ER stress. This experiment demonstrated that there is no difference in ER gene expression in MDM differentiated in the presence of the inhibitor compared to the control (Figure 3.4).

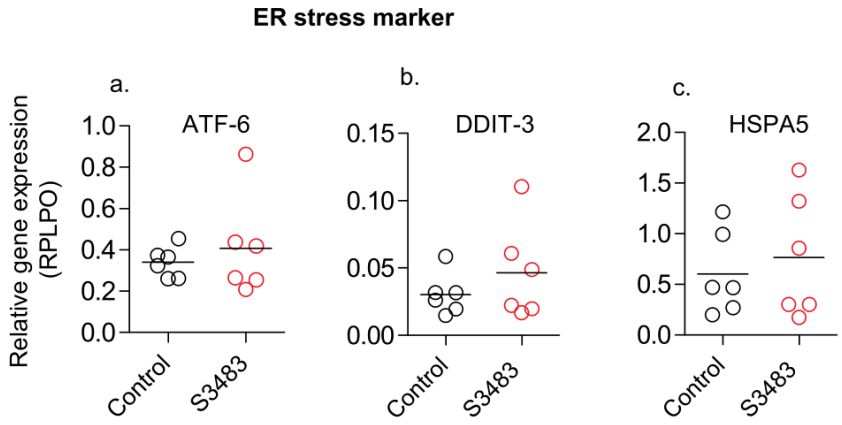

Figure 3.4: **Effect of S3483 on ER stress in MDM with G6PT enzyme.** MDM were differentiated in the presence and absence of S3483 for 5 days. Taqman probe for human (a) ATF-6, (b)DDIT-3, and (c) HSPA5 were used to detect ER stress. Results were expressed relative to the expression of the house-keeping gene RPLPO. Quantitative PCR (qPCR) was performed using a Bio Rad software detection system. Abbreviation: Activating transcription factor-6 (ATF-6), DNA damage-inducible transcript 3 (DDIT-3), and Heat shock protein family A (member 5) (HSPA5)

3.1.4 The effect of S3483 on MDM differentiation is independent of ROS production

ROS derived from superoxide are essential for microbial killing. We hypothesised that impaired bacterial killing by MDM maybe due to reduced superoxide production. In order to investigate this hypothesis, DHR staining was performed on MDM differentiated in the presence or absence of S3483. NADPH oxidase activity was measured through the DHR flow cytometry assay. No difference was observed in the ROS generated from the MDM differentiated in the presence of inhibitor compared to the control when gated on the live cells (Figure 3.5). This experiment suggests that the effect S3483 on bacterial killing is independent of ROS production.

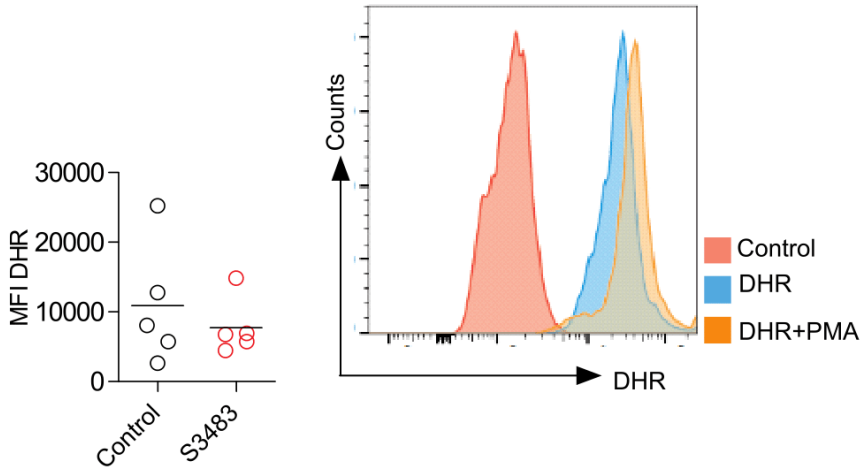

Figure 3.5: **The effect of S3483 on MDM is independent of ROS production.** MDM was differentiated with S3483 for 5 days. MDM was treated with DHR solution (2.5 μg/ml) for 15 minutes and assay was performed under 3 different conditions; control, MDM treated with DHR and MDM treated with both DHR and PMA (n=5). The ΔMFI was calculated as the difference between the cells stimulated or unstimulated with PMA. FACS plot shows MDM stained or unstained with DHR. Sample acquisition and data analysis was done using the LSR Fortessa flow cytometry system and FlowJo software (Version 10.0.8.r1) respectively.Abbreviations: Dihydrorhodamine 123 (DHR), and Phorbol myristate acetate (PMA)

3.1.5 S3483 polarises MDM to M1 phenotype

The previous study demonstrates that treatment with the inhibitor (S3483) during differentiation of monocytes to macrophages for 5 days impairs bacterial handling. This suggested a possible differentiation effect of S3483 on MDM. In order to understand the surface marker expression of MDM with defective G6PT enzyme the following anti-bodies were analysed: CD172, CD163, CD11c, HLA-DR, CD64, CD86, CD14, and CD40. MDM were differentiated in the presence of S3483 for 5 days and surface staining was performed on these cells. Samples acquisition and data analysis was carried out using the LSR Fortessa flow cytometry system and FlowJo software (Version 10.0.8.r1) respectively.

MDM treated with S3483 showed a trend towards the expression of HLA-DR and

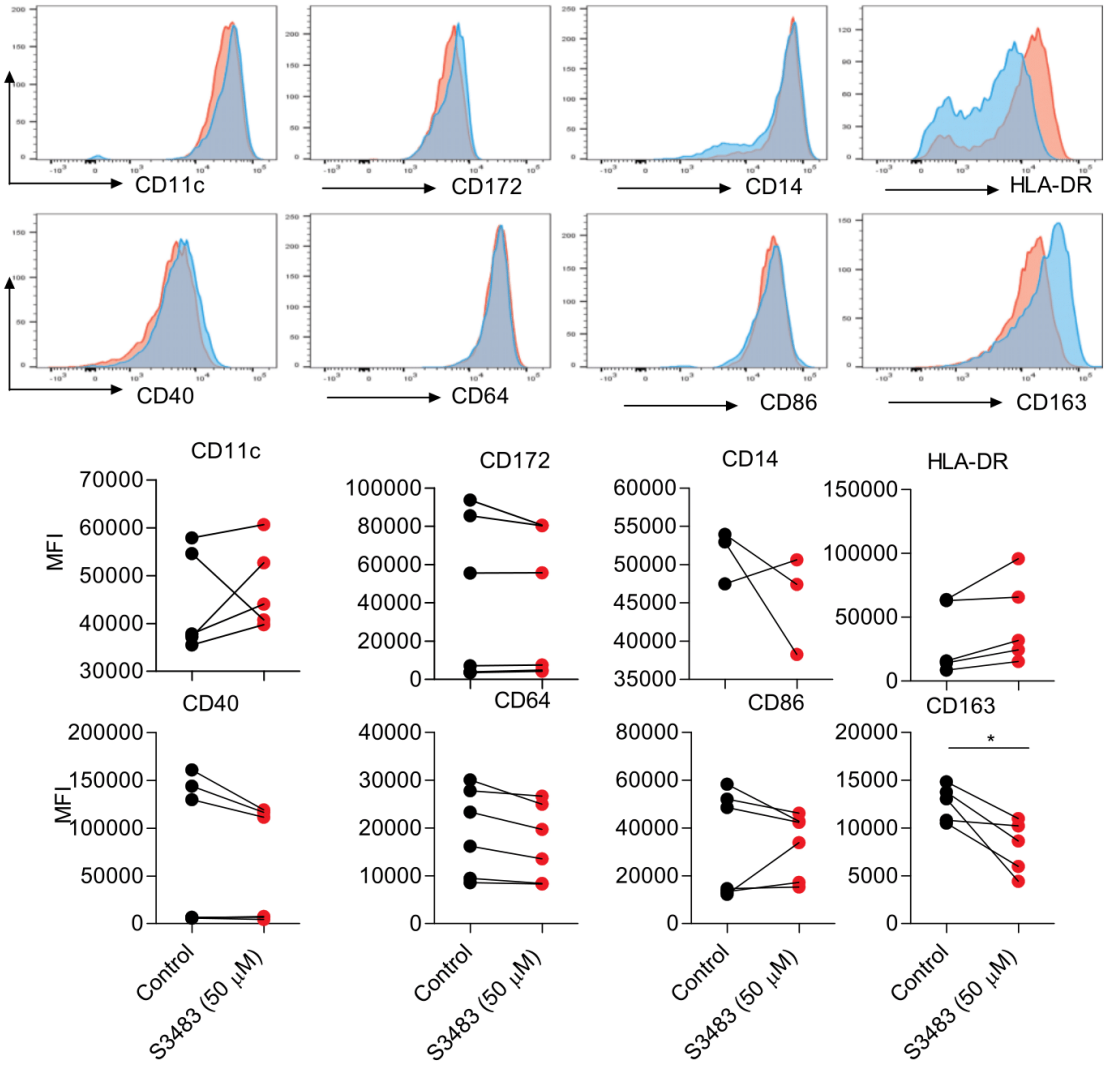

Figure 3.6: **Surface marker expression in MDM treated with S3483** MDM were differentiated in the presence of S3483 for 5 days. Following surface markers were analysed; CD11c, CD172, CD14, HLA-DR, CD40, CD64, CD86, and CD163. Samples acquisition and data analysis was done using the LSRFortessa flow cytometry system and FlowJo software (Version 10.0.8.r1) respectively.The FACS plots represent MDM stained or unstained with the respective antibodies (n=6, *p<0.05, student's t-test (one-tailed))

a significant decrease in CD163 (Figure 3.6). M1-macrophages, the classically activated macrophages can be distinguished from the M2-type by having a high HLA-DR expression [117]. Likewise, M2-macrophages or alternatively activated macrophages have a higher expression of CD163 and CD204 (both scavenger receptors) [118]. This

experiment demonstrated that macrophages gets polarised to M1-phenotype in MDM with defective G6PT enzyme. Further to this, the previous study on bacterial handling defect in MDM treated with S3483 is evident from reduced CD163 surface marker expression (Figure 3.6).

3.1.6 S3483 activates mTOR in MDM

The mTOR (Mammalian target of Rapamycin) mechanism plays a crucial role in the polarisation of macrophages. This pathway also regulates the metabolism and bacterial handling in macrophages. This led to the hypothesis that impaired bacterial handling and polarisation of macrophages with G6PT inhibtion influences the mTOR pathway. Therefore, we aimed to investigate the role to mTOR mechanism in MDM treated with S3483. The protein pS6, an active marker of mTOR pathway was quantified in MDM differentiated in the presence of S3483. The protein pS6 was over-expressed a trend in S3483 treated MDM compared to the untreated condition. This suggests that the activity of enzyme influences the mTOR mechanism (Figure 3.7). Data was represented as MFI (Mean Fluorescence Intensity) measuring the shift in fluorescence intensity of population of MDM stained or unstained with pS6 antibody. To understand how mTOR affects the impaired bacterial handling by MDM treated with S3483, we performed a gentamicin protection assay using mTOR pathway inhibitor, rapamycin. The impaired bacterial handling defect in MDM treated with S3483 was rescued by mTOR inhibitor rapamycin (Figure 3.8). This assay was also performed on patient cells with *G6PC3* functional mutation. Consistent with the chemical model, the bacterial handling defect was also rescued when the MDM from the patient with *G6PC3* mutation were treated with rapamycin (Figure 3.8). Experiment was performed in duplicates in chemical model (each dot represents a donor) and in the patient sample, each dot represents a replicate. CFU for each inhibitory condition was then normalised as a percentage of the mean CFU for the

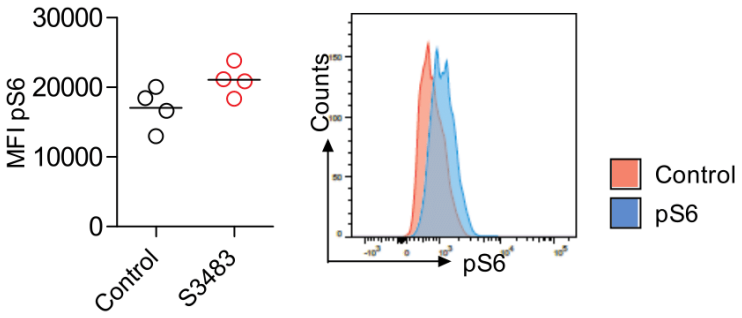

Figure 3.7: **MDM treated S3483 is dependent on mTOR pathway** (a) MDM differentiated in the presence or absence of S3483 for 5 days.The amount of pS6 was quantified in MDM differentiated in the presence or in the absence of S3483. (b) FACS plot of MDM stained or unstained with pS6 antibody. Samples acquisition and data analysis was done using the LSR Fortessa flow cytometry system and FlowJo software (Version 10.0.8.r1) respectively. Data was represented as MFI (Mean Fluorescence Intensity) measuring the shift in fluorescence intensity of population of MDM stained or unstained with pS6 antibody. FACS plot representation of MDM stained or unstained with the antibody pS6. (n=4)

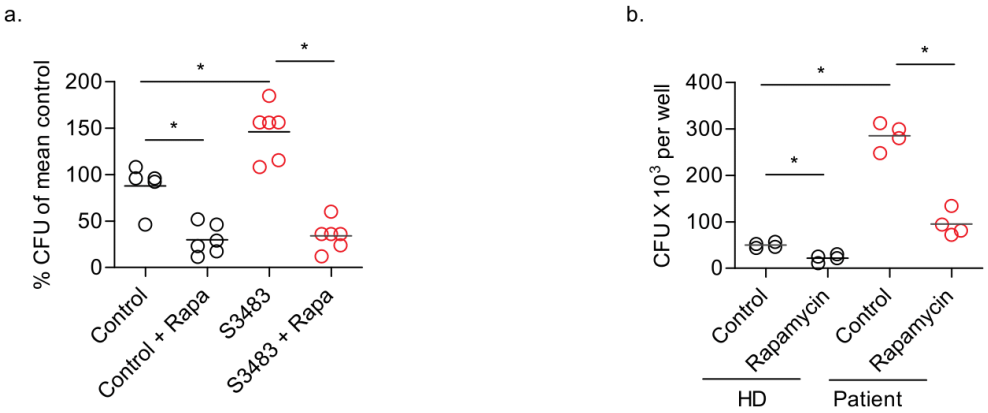

Figure 3.8: **Impaired bacterial killing in MDM treated with S3483 and *G6PC3*$^{-/-}$ patient rescued by rapamycin** (a) MDM treated with S3483 were infected with *(S. typhimurium)-expressing GFP (NCTC 12023)*. Experiment was performed in duplicates (each dot represents a donor). CFU for each inhibitory condition was then normalised as a percentage of the mean CFU for the untreated condition. (n=5, *P<0.05, mann-whitney U test) (b) MDM from patient with *G6PC3*$^{-/-}$ functional mutation were infected with *(S. typhimurium)-expressing GFP (NCTC 12023)*. Experiment was performed in duplicates (each dot represents a replicate). (n=1, *P<0.05, Mann-whitney U-test))

untreated condition.

3.1.7 Cytokines production in MDM treated with S3483

The surface marker expression in MDM treated with S3483 demonstrated that S3483 polarises the macrophages to M1 phenotype. M1 macrophages express pro-inflammatory cytokines, while M2 express anti-inflammatory cytokines. Hence we hypothesised that

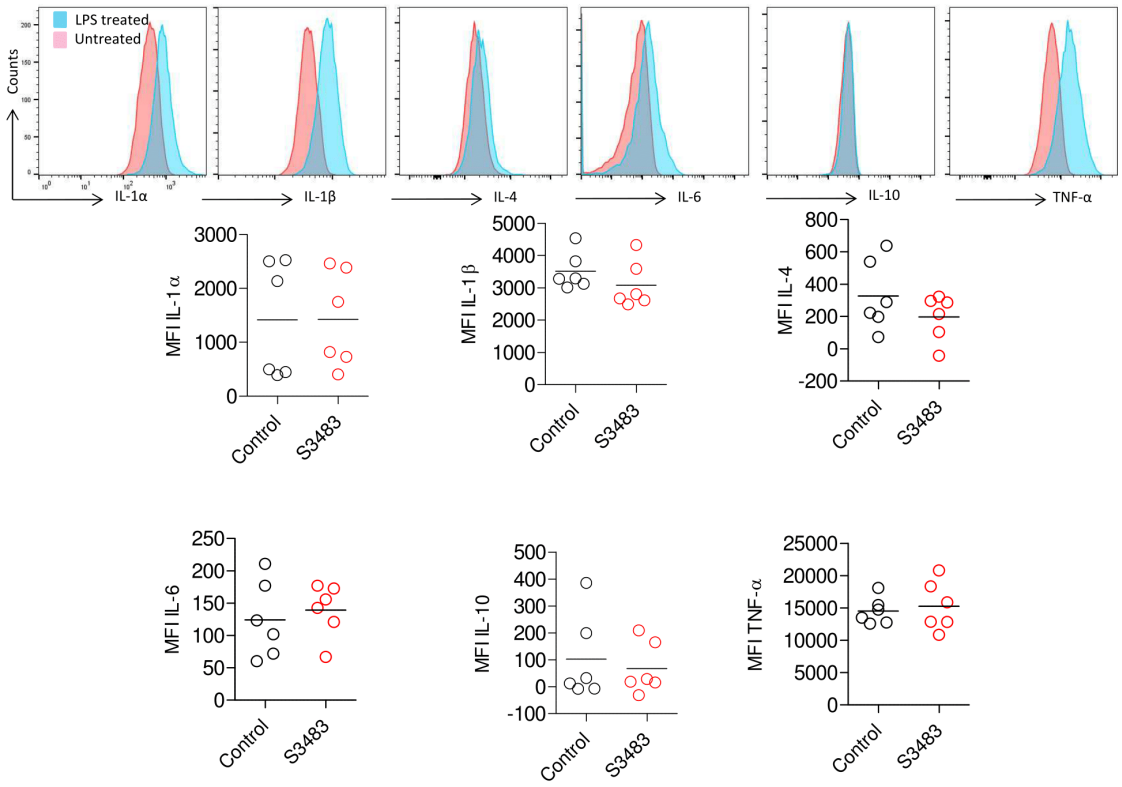

Figure 3.9: **Cytokines production in MDM treated with S3483**. MDM were differentiated in the presence of S3483 for 5 days. The cells were stained with 1 μl of live-dead stain and incubated for 15 minutes at 37 °C. Intracellular staining was performed using the following antibodies; IL-1α, IL-1β, IL-4, IL-6, IL-10, and TNF-α. The ΔMFI was calculated as the difference between the MFI of MDM stimulated and unstimulated with LPS. Samples acquisition and data analysis was done using the LSR Fortessa flow cytometry system and FlowJo software (Version 10.0.8.r1) respectively (n=6). FACS plot representation of MDM stimulated or unstimulated with LPS and stained with respective antibodies.

MDM treated with S3483 will show a higher expression of pro-inflammatory cytokines. We quantified both pro-inflammatory and anti-inflammatory cytokines in MDM differentiated in the presence or absence of S3483 inhibitor for 5 days. Live/Dead

staining was performed prior to intracellular staining to distinguish and gate on the live cells from the dead population. Intracellular staining was performed using the following antibodies; IL-1α, IL-1β, IL-4, IL-6, IL-10, and TNF-α. No variation was observed in the production of IL-1α, IL-6, IL-10, TNF-α. We observed a descending trend in IL-4 production in MDM with G6PT enzyme inhibition (Figure 3.9). However, the expression of these cytokines by the macrophages is dependent various intricate pathways and it cannot necessarily provide lucid information of the polarisation of the macrophages.

3.1.8 Increase in glycolytic rate and decrease in mitochondrial respiration in MDM treated with S3483

Metabolism regulation in macrophages plays a crucial role in determining their phenotype. In order to understand the metabolic changes in MDM treated with S3483, we performed glycolytic stress and mito stress assays on MDM differentiated in the presence or absence of S3483. The glycolytic flux was quantified by measuring the glucose uptake and lactate production. The extracellular measurements were quantified using seahorse extracellular analyser (Seahorse Bioscience). Glycolysis was measured through quantifying the extracellular acidification rate (ECAR) of the surrounding media. This is from the excretion of lactic acid per unit time after its conversion from pyruvate.Glycolysis rate was measured as the difference between ECAR after the addition of Glucose and ECAR after the addition of 2-DG. Glycolysis capacity was measured as ECAR after the addition of oligomycin and ECAR after the addition of 2-DG. Glycolytic reserve was measured as the difference between ECAR after the addition of oligomycin and ECAR after the addition of glucose. Similarly, Mitostress was performed to analyse the oxygen consumption rate. In the assay, modulators of respiration are used to target the components of ETC in the mitochondria. ATP production was measured as the difference between OCR (oxygen consumption rate) after

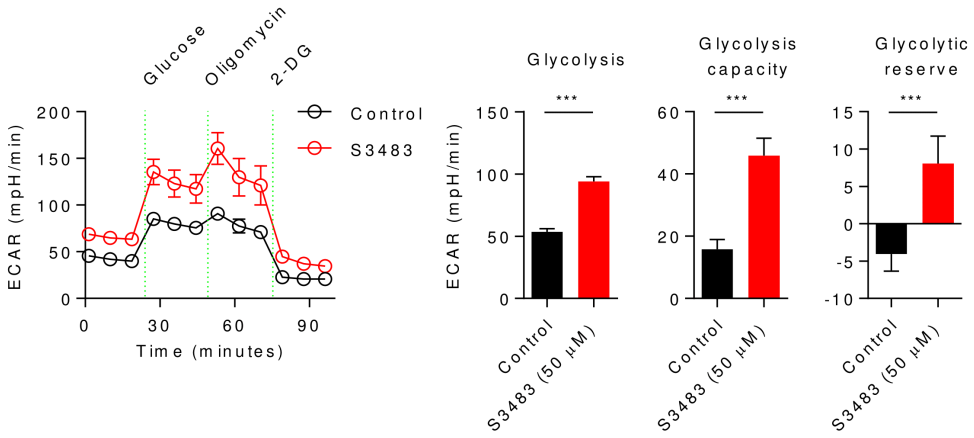

Figure 3.10: **Increase in ECAR in the MDM differentiated in the presence of S3483.** MDM were differentiated in the presence or absence of S3483 for 5 days. Dot plot represents mean of ECAR over 3 different time points after glucose injection. Glycolysis rate was measured as the difference between ECAR after the addition of Glucose and ECAR after the addition of 2-DG. Glycolysis capacity was measured as ECAR after the addition of oligomycin and ECAR after the addition of 2-DG. Glycolytic reserve was measured as the difference between ECAR after the addition of oligomycin and ECAR after the addition of glucose. (n=6, ***P<0.0005, mann-Whitney U test) Abbreviations: Extracellular acidification rate (ECAR), and 2-deoxyglucose (2-DG)

the addition of Oligomycin and OCR after the addition of antimycin and rotenone. Mitochondrial respiration was measured as OCR after the addition of FCCP and OCR after the addition of antimycin and rotenone. Analysis of this assay revealed an increase in ECAR and decrease in OCR in MDM treated with S3483 compared to that of the untreated condition (Figure 3.10) (Figure 3.11). This suggests that S3483 modulates glycolytic flux and mitochondrial respiration in MDM. MDM treated with S3483 derives its energy from glycolysis rather than from oxidative phospharylation (OXPHOS). Increased ECAR and decreased OCR has also been been observed in LPS activated macrophages, which drives an M1-like or classical activation pathway. This results further provides evidence that S3483 polarises MDM to M1 phenotype.

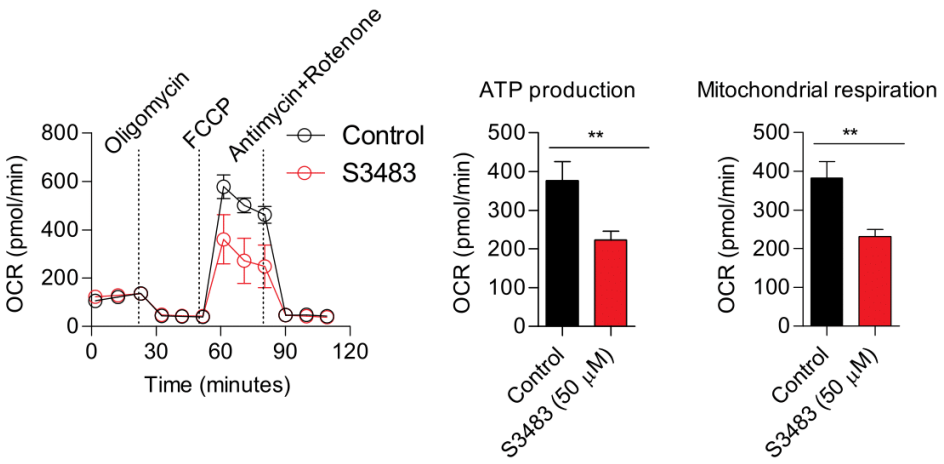

Figure 3.11: **Decrease in OCR in the MDM differentiated in the presence of S3483.** Dot plot represents mean of OCR over 3 different time points after oligomycin injection. ATP production was measured as the difference between OCR after the addition of Oligomycin and OCR after the addition of antimycin and rotenone. Mitochondrial respiration was measured as OCR after the addition of FCCP and OCR after the addition of antimycin and rotenone. (n=6, **P<0.005, mann-whitney U test) Abbreviations: Oxygen consumption rate (OCR), and Carbonylcyanide-4 (trifluoromethoxy) phenylhydrazone (FCCP)

3.1.9 Increase in GLUT 3 expression in MDM treated with S3483

In macrophages, the glucose uptake is through either GLUT 1 or GLUT 3. The previous experiment demonstrated a significant increase in ECAR explaining an increase in glycolytic rate. Increase in glycolysis may contribute to increase in glucose uptake by the overexpression of glucose transporters. This led to the hypothesis that MDM treated with S3483 can lead to an upregulation of glucose transporters. To test this, the monocytes were differentiated into macrophages in the presence of S3483 (50 μM) for 5 days. This experiment showed no variation in the expression of GLUT 1 and a trend suggesting an over-expression in GLUT 3 expression in MDM treated with S3483 compared to the untreated condition (Figure 3.12). Studies also indicate

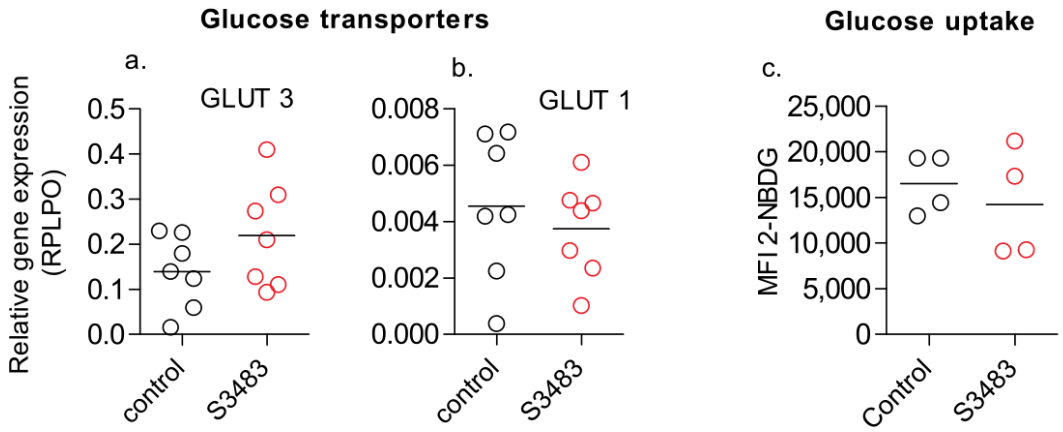

Figure 3.12: **Increase in GLUT 3 expression in MDM with defective G6PT defect.** MDM were differentiated in the presence and absence of S3483 for 5 days. Taqman probe for human (a) *SLCA2*, and (b) *SLCA3* were used to analyse glucose transporters. Results were expressed relative to the expression of the house-keeping gene RPLPO. Quantitative PCR (qPCR) was performed using a Bio Rad software detection system. (c) 2-NBDG was quantifies in MDM with G6PT defect. Samples acquisition and data analysis was done using the LSRFortessa flow cytometry system and FlowJo software (Version 10.0.8.r1) respectively. Data was represented as MFI (Mean Fluorescence Intensity) measuring the shift in fluorescence intensity of population of MDM stained or unstained with 2-NBDG antibody. Abbreviation: Glucose transporter 1 (GLUT 1), Glucose transporter 3 (GLUT 3), and 2-(N-(7-Nitrobenz-2-oxa-1,3-diazol-4-yl)Amino)-2 (2-NBDG)

that LPS stimulated macrophages shows over-expression of GLUT 3 compared to that of GLUT 1 [119]. This experiment also suggests that MDM treated with S3483 behaves similar to LPS activated macrophages. Following this, we further wanted to test if the increase in GLUT 3 leads to increase in uptake of glucose in these cells. The uptake of glucose in MDM was measured by quantifying the uptake of 2-NBDG (2-(N-(7-Nitrobenz-2-oxa-1,3-diazol-4-yl)Amino)-2) in these cells. 2-NBDG is a fluorescent glucose analog that has been used to monitor glucose uptake in live cells (Figure 3.12). However, there was no difference in the glucose uptake in MDM treated with S3483 compared to that of the control (Figure 3.12).

3.1.10 Redox transcription factor expression in MDM treated with S3483

The transcription factor HIF-1 α plays a key role in the regulation of glycolytic capacity and energy metabolism in myeloid cells [120]. The increase in glycolytic rate

Figure 3.13: **Redox transcription factor expression in MDM treated with S3483** MDM were differentiated in the presence and absence of S3483 for 5 days. Taqman probe for human (a) HIF 1α, and (b) NRF2 were used to analyse glucose transporters. Results were expressed relative to the expression of the house-keeping gene RPLPO. Quantitative PCR (qPCR) was performed using a Bio Rad software detection system. Abbreviations: Hypoxia-inducable factor-α (HIF-1α); NF-E2-related factor-2 (Nrf2)

in MDM treated with S3483 may be due to HIF-1α transactivating genes involved in extracellular glucose import (such as GLUT 3).

NF-E2-related factor-2 (Nrf2) is a transcription factor which regulates oxidative/xenobiotic stress response and also has been shown to represses inflammation [121]. Hence, it negatively regulate M1-induced genes by inhibiting pro-inflammatory cytokines gene expression. Therefore, we hypothesised that MDM treated with S3483 causes an upregulation in HIF-1α expression and downregulation in the NRF2 expression. To test the hypothesis on HIF 1α and NRF2 expression, q-PCR was performed. The m-RNA was extracted from MDM from healthy donors differentiated with the

presence or absence of S3483 for a period of 5 days. There was no significant difference observed in the expression of HIF-1α and NRF2. This experiment demonstrated that the regulation of glycolytic capacity and polarisation of macrophages is independent of HIF-1α expression and NRF2 respectively. (Figure 3.13).

3.1.11 Gene profiling of central metabolic pathways in MDM treated with S3483

We have demonstrated in metabolic assay an increase in glycolysis rate and decrease in mitochondrial respiration in MDM treated with S3483. Hence, there is a metabolic reprogramming in MDM when they are differentiated with S3483. In order to understand how the metabolism is regulated, we performed a metabolic gene profiling in MDM treated with S3483. An array of genes associated with glycolysis, TCA, and PPP were analysed using RT^2 profiler pathway signature PCR Arrays in 96 well plate. Data Analysis was performed Using the ΔCT classification algorithm using the protocol provided by the sabioscience web portal PCR array gene analysis. Analysis of the expression of the genes associated with glycolysis showed a trend suggesting an increase in expression of the genes for the enzymes hexokinase I (HK1) and glucokinase (GCK) (Figure 3.14).HK1 and GCK are critical for glucose metabolism and inhibition of these enzymes have been proven to increase OCR and decrease ECAR. This is consistent with the result we observed in MDM treated with S3483.

Analysis of the expression of the genes associated with TCA showed a trend suggesting an increase in expression of genes such as citrate synthase (CS), iso-citrate dehydrogenase (IDH), Succinate CoA ligase (SUCLG1),and malate dehydrogenase (MDH1B) (Figure 3.15). All of these genes are very important in the formation of citrate, α-ketoglutarate, succinate, and malate respectively. Recently it has been shown that in M1 macrophages, there is an accumulation of citrate, succinate, malate, and fumerate associated with a fragmented TCA cycle. Increase in the expression

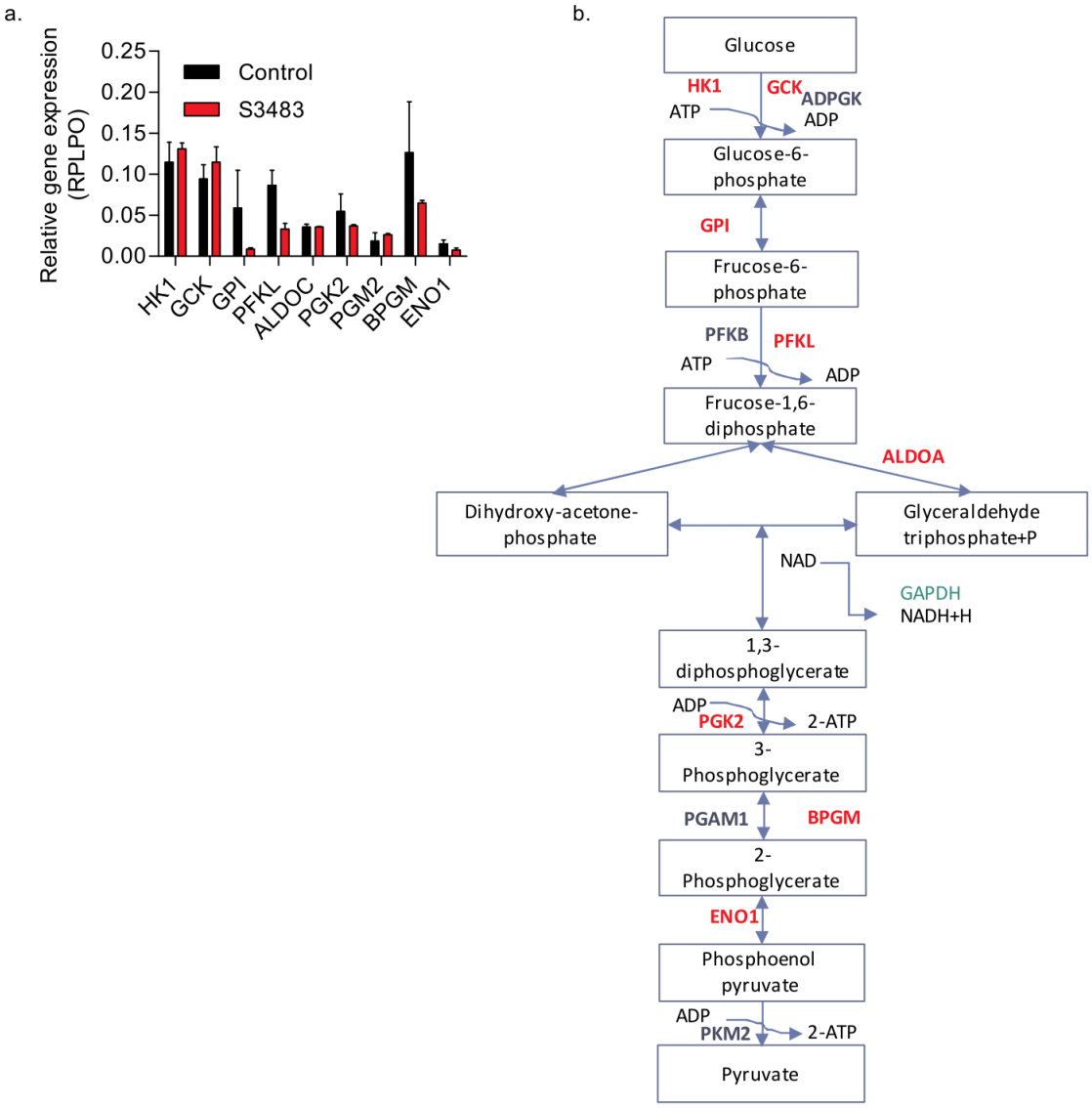

Figure 3.14: **Analysis of genes associated with glycolysis in MDM with defective G6PT enzyme.** (a) Graph representing the Gene expressions associated with the glycolysis pathway.(b) Schematic diagram representing the Glycolysis pathway with essential genes involved. All the letters in red denotes the genes used in the analysis. Abbreviations: Hexokinase (HK); glucokinase (GCK); glucose phosphate isomerase (GPI); 6-phosphofructokinase (PFKL), fructose-bisphosphate (ALDOC); phosphoglycerate kinase (PGK); phosphoglucomutase (PGM); bisphosphoglycerate Mutase (BPGM); enolase 1 (ENO1).

of genes such as CS, IDH1, and SUCLG1 suggests an increase in the expression of the metabolites associated with these genes, therefore explaining a fragmented TCA cycle in MDM treated with S3483.

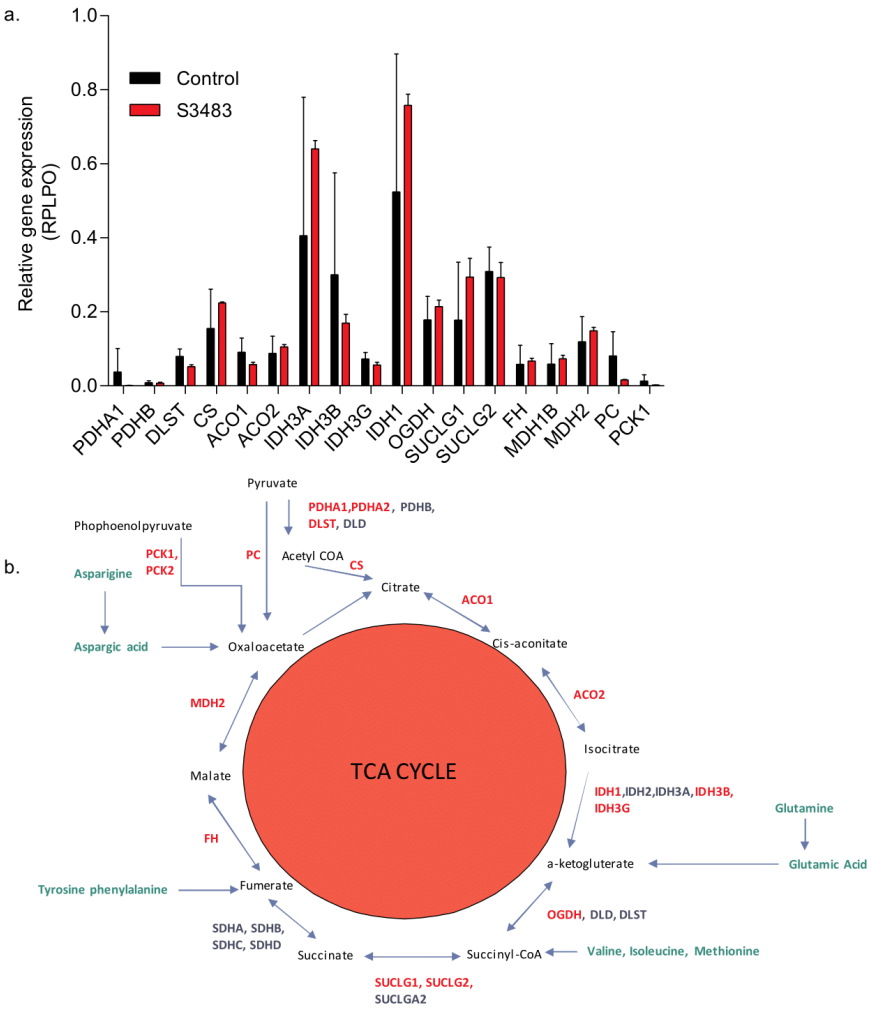

Figure 3.15: **Analysis of genes associated with TCA in MDM with defective G6PT enzyme.** (a) Graph representing the Gene expressions associated with the TCA pathway.(b) Schematic diagram representing the TCA cycle with essential genes involved. All the letters in red denotes the genes used in the analysis. Abbreviations: Pyruvate Dehydrogenase (Lipoamide) Alpha 1 (PDHA1); Pyruvate dehydrogenase E1 component subunit beta (PDHB), dihydrolipoamide S-Succinyltransferase (DLST); citrate synthase (CS); aconitase (ACO); isocitrate Dehydrogenase (IDH); succinate CoA ligase (SUCLG1); fumarate Hydratase (FH); malate dehydrogenase (MDH1B); pyruvate carboxylase (PC); phosphoenolpyruvate carboxykinase 1 (PCK1).

Analysis of expression of genes associated with PPP showed a trend suggesting an increase in the expression of hexose-6-phosphate dehydrogenase/glucose 1-dehydrogenase (H6PD), Phosphoribosyl Pyrophosphate Synthetase 1 (PRPS1), RPIA, transketolase (TKT), and transaldolase (TALDO1) genes. H6PD encodes for the en-

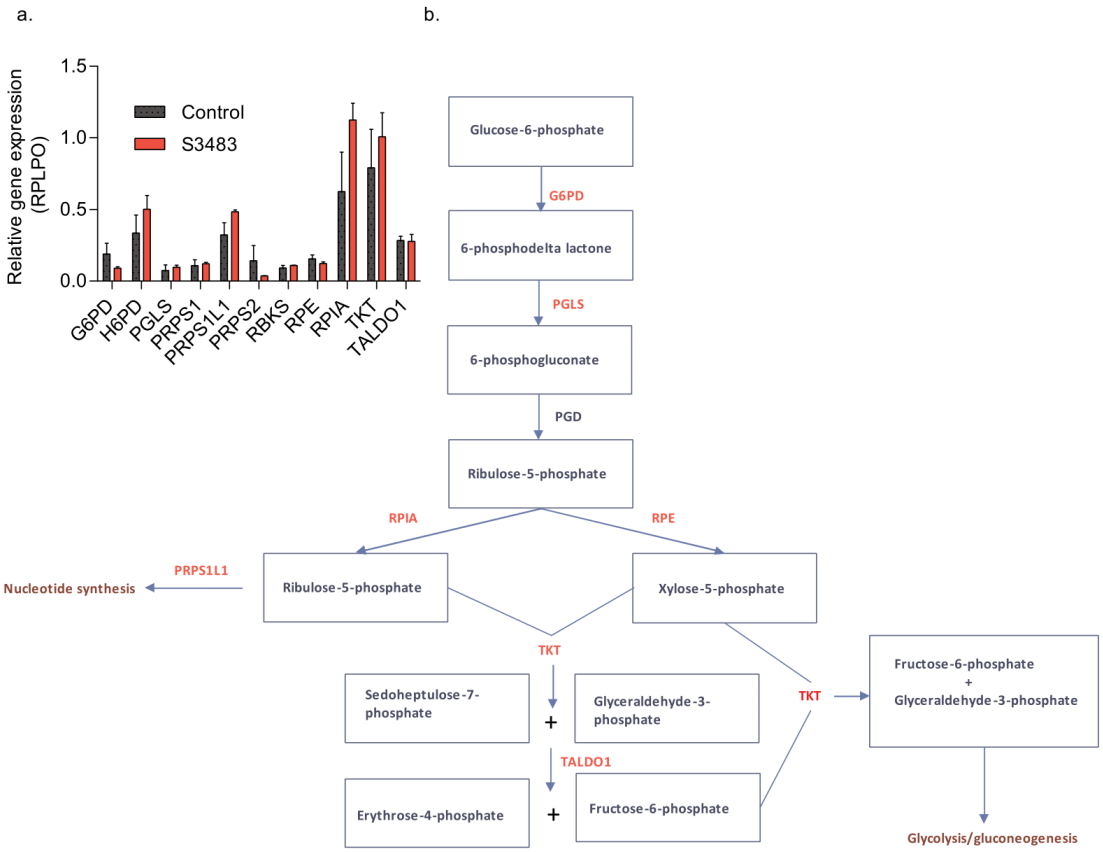

Figure 3.16: **Analysis of genes associated with PPP in MDM with defective G6PT enzyme.** (a)Graph representing the Gene expressions associated with the PPP pathway.(b) Schematic diagram representing the Pentose-phosphate shunt pathway with essential genes involved. All the letters in red denotes the genes used in the analysis. Abbreviations: Glucose-6-phosphate dehydrogenase (G6PD); hexose-6-phosphate dehydrogenase (H6PD); 6-Phosphogluconolactonase (PGLS); phosphoribosyl Pyrophosphate Synthetase (PRPS); ribokinase (RBKS); ribulose-5-Phosphate-3-Epimerase (RPE); ribose 5-Phosphate Isomerase A (RPIA); transketolase (TKT); transaldolase 1 (TALDO1)

zyme glucose-6-phosphate dehydrogenase (G6PD). G6PD, the first and rate-limiting enzyme of the PPP, is a key enzyme in the generation of cytosolic NADPH. Increase in the expression of H6PD may suggest polarising the macrophage to M1 phenotype (Figure 3.16). The PRPS1 gene provides instructions for making an enzyme called phosphoribosyl pyrophosphate synthetase 1, or PRPP synthetase 1. This enzyme helps produce a molecule called phosphoribosyl pyrophosphate (PRPP) and is involved in making purine and pyrimidine nucleotides. This may suggest an increase

in the metabolites associated with purines and pyramidines synthesis in MDM with defective G6PT enzyme.

The gene expression analysis demonstrates that metabolism in MDM with G6PT enzyme inhibition is reprogrammed by genes associated with glycolysis, TCA, and pentose phosphate pathway.

3.1.12 Quantification of metabolites in macrophages treated with S3483

The gene profiling in MDM suggested a trend in the expression of genes associated with glycolysis, TCA, and PPP. The metabolites accumulating are shown to be important for various functions of M1 and M2 macrophages. In order to quantify the metabolites in MDM treated with S3483, metabolomics was performed in collaboration with Prof James McCullagh. Around 3000 compounds were measured related to metabolic signalling pathways. Around 130 of these compounds were identified from the analysis, and the abundances of all the samples were compared between both the experimental groups; control and S3483 treated conditions. The compounds that changed between the two groups were plotted as a heatmap associated with major metabolic pathways.

The metabolomic analysis revealed an increase in expression of metabolites involved in glycolysis; with a significant increase in pyruvate (Figure 3.17). Furthermore, a significant increase in the expression of citrate, malate, and fumerate was observed; which are metabolites pertaining to TCA cycle (Figure 3.17). These metabolites have been shown to accumulate, suggesting a broken TCA cycle in M1 polarised macrophages. This provides evidence that S3483 fragments the TCA cycle in MDM.

In addition, the treatment of MDM with S3483 induce a decrease in the expression of the metabolite sedoheptulose-7-phosphate (S7P) in MDM treated with S3483. CARKL is a sedoheptulose kinase which converts sedoheptulose to S7P. This enzyme

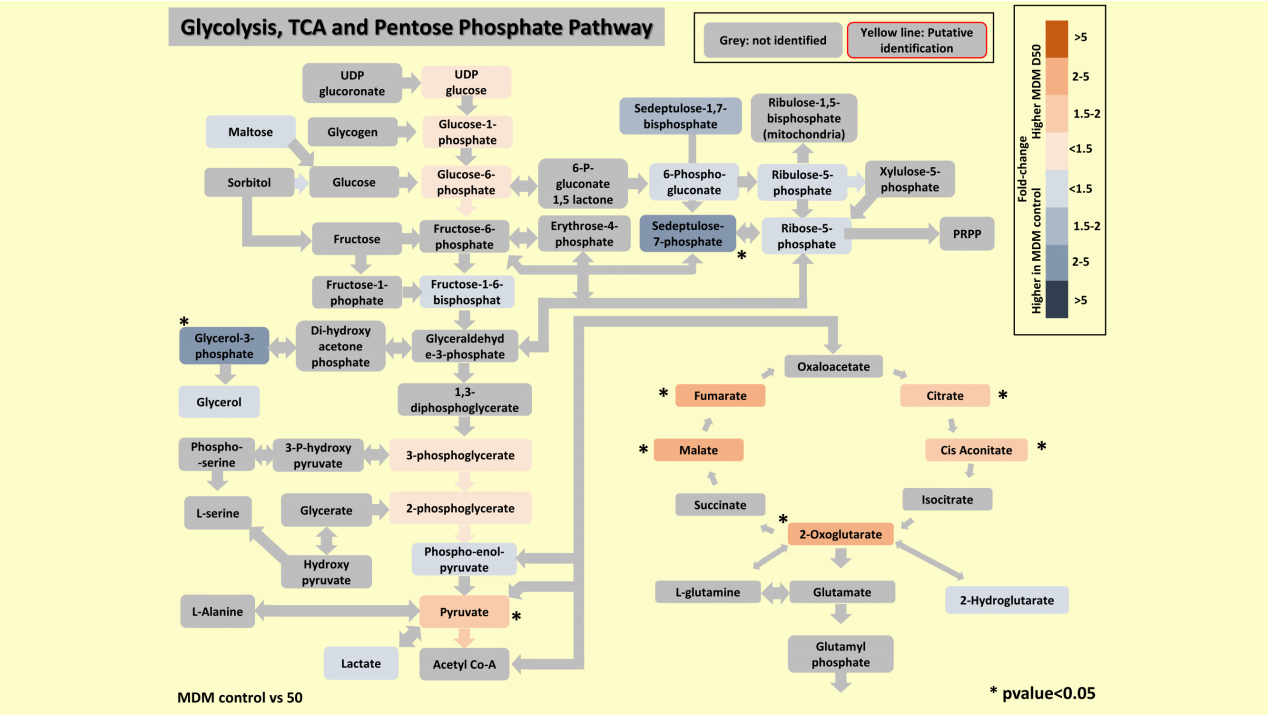

Figure 3.17: **Quantification of metabolites in MDM treated with S3483.** The metabolites were processed using an anion-exchange chromatography. Around 130 of the compounds associated with glycolysis, TCA, and pentose phosphate shunt were identified and the abundances of all the samples were compared between both the experimental groups; control and S3483 conditions (n=5 (individual donors), *p<0.05, student's t-test (one-tailed)) were plotted as a heatmap associated with major metabolic pathways.

is highly expressed in M2-phenotype macrophages. Inhibiting G6PT enzyme affects the metabolism in macrophages (Figure 3.17). It has a profound effect in altering glycolysis and TCA pathway. This may also contribute to the polarisation effect of macrophages to M1 phenotype. In summary, our results highlight the fundamental nature of metabolic reconfiguration in macrophage activation and define unique metabolic demands of distinct activation states.

3.1.13 Quantification of metabolomes associated with purines and pyramidines in MDM treated with S3483

In our gene expression array, the levels of PRPS1L1 showed a trend suggesting an increase in gene expression in MDM treated with S3483 (Figure 3.16). This gene is very important in the synthesis of purine and pyrimidine synthesis. Therefore,

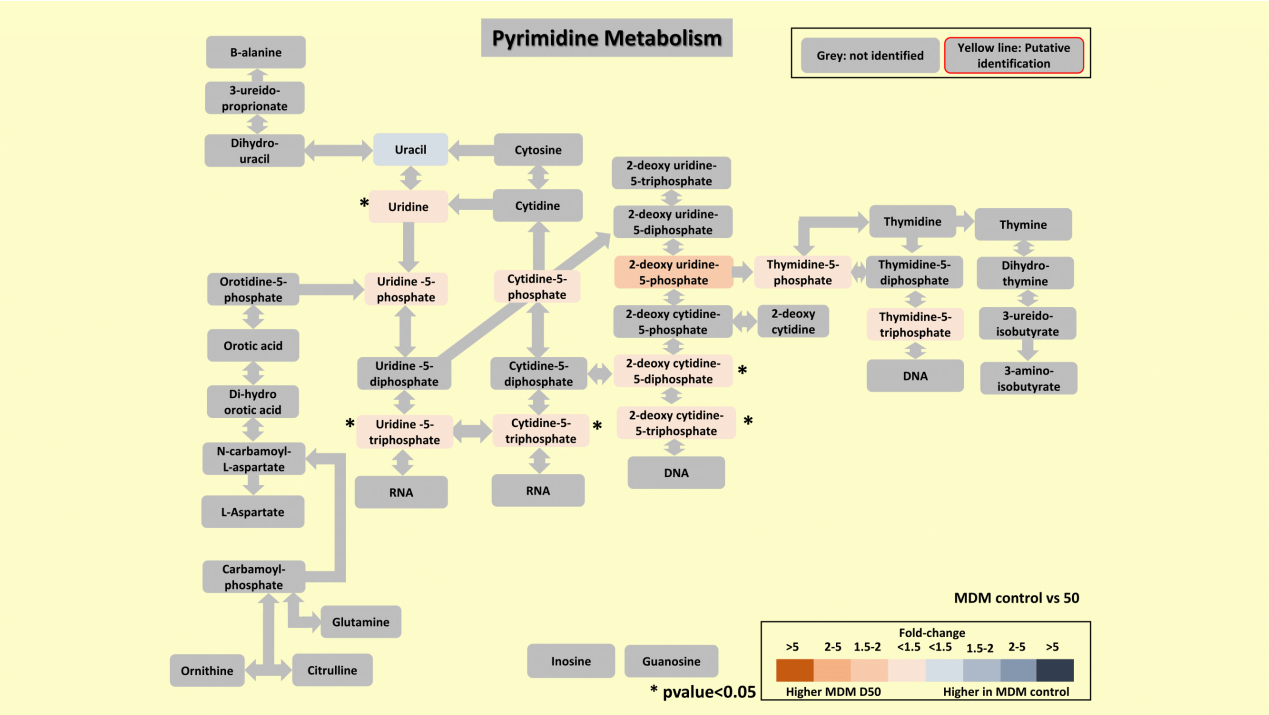

Figure 3.18: **Pyrimidine metabolomes in MDM with defective G6PT enzyme**The metabolites were processed using an anion-exchange chromatography. Compounds associated with pyrimidine were identified and the abundances of all the samples were compared between both the experimental groups; control and S3483 conditions (n=5 (individual donors), *p<0.05, student's t-test (one-tailed)) were plotted as a heatmap associated with major metabolic pathways

we performed a metabolomic analysis to quantify intermediates pertaining to the purine and pyrimidine metabolism in MDM treated with S3483. We observed a significant increase in the expression of uridine-5-triphosphate (UTP) (Figure 3.18). UTP has been shown to modulate inflammatory events in macrophages aiding in the release of in the release of NO, PGE2. We also observed a significant increase

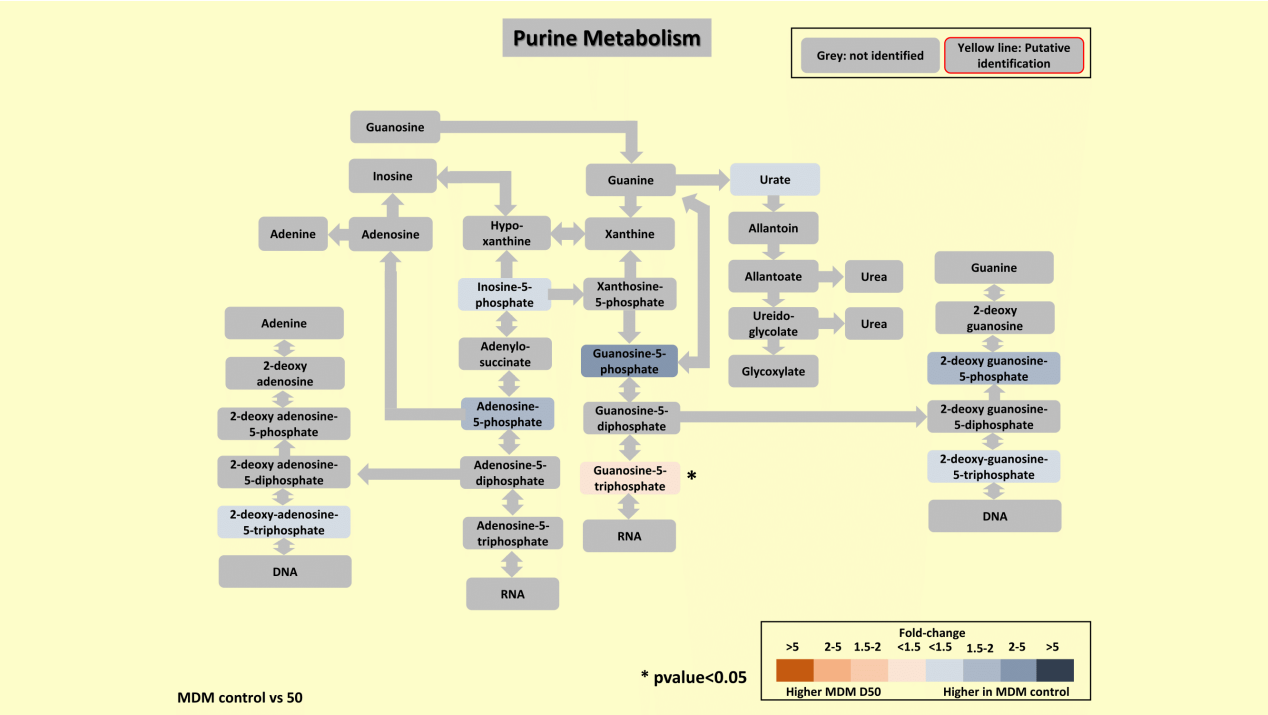

Figure 3.19: **Purine metabolomes in MDM with defective G6PT enzyme**The metabolites were processed using an anion-exchange chromatography. Compounds associated with pyrimidine were identified and the abundances of all the samples were compared between both the experimental groups; control and S3483 conditions (n=5 (individual donors), $p<0.05$, student's t-test (one-tailed)) were plotted as a heatmap associated with major metabolic pathways

in cytidine triphosphate (CTP), 2-deoxy cytidine diphosphate, and 2-deoxy cytidine triphosphate. But, the effect of this metabolite has not been studied extensively in macrophages.

Analysis of metabolites pertaining to purine metabolism revealed an increase in the expression of guanosine triphosphate in MDM treated with S3483 (Figure 3.19). Past literature suggests that GTP upregulation may lead to calcium release in saponin-treated macrophages [122]. But there is no further evidence to understand how GTP modulates the function of macrophages. Therefore, the effect of metabolites in purine metabolism still requires more study and investigation.

3.2 Discussion

In this chapter, we investigated the functional effects of G6PT enzyme in MDM using a chemical inhibitor model. The enzyme was inhibited with a derivative of cholorogenic acid S3483 [28]. G6PT is expressed ubiquitously and a mutation in the gene encoding this enzyme (SLC37A4) has been shown to affect the myeloid population. G6PT and G6Pase-β activities are known to be functionally co-dependent [14] and this complex is responsible for maintaining intracellular glucose homoeostasis in neutrophils [123] and macrophages [124]. Apart from neutropenia, G6PT and G6Pase-β deficient patients present with neutrophil dysfunction, impaired respiratory burst, chemotaxis and calcium immobilisation [124] [123]. The underlying mechanism of this myeloid dysfunction is still not well understood [14].

Investigation of bacterial handling in MDM with G6PT inhibition showed a significant increase in the number of colonies compared to that of the untreated condition (Figure 3.2). This was shown to be a differentiation effect since there was no variation in the number of colonies of bacteria when G6PT was inhibited in macrophages for only 24 hours following 5 days of differentiation. Studies on macrophages and neutrophils from *G6PC3*$^{-/-}$ mice show reduced phagocytic activities [124] and chemotaxis [123]. Previous literature also provides evidence that patients with GSD-Ib have frequent intestinal infection [19], implicating a possible role of G6PT enzyme in bacterial handling.

Macrophages from *G6PC3*$^{-/-}$ mice showed a marked reduction in superoxide production on exposure to PMA, compared to the wild-type macrophages; implying that G6Pase-β expression is important for the respiratory burst activity [124]. This suggests that impaired bacterial killing by macrophages is due to reduced superoxide production. However in our chemical inhibitor model, there was no variation in the amount of ROS generated by the macrophages with G6PT enzyme inhibition. Therefore, the impaired bacterial handling in these cells independent of ROS produc-

tion(Figure 3.5). The diminished ROS production in mice might be specific to the *G6PC3* gene mutation. Alternatively, species-specific differences between mice and humans in the function of G6PT enzyme, might explain this result.

G6Pase-β and G6PT enzymes, located in the lumen of the endoplasmic reticulum, is critical for neutrophil glucose homeostasis and normal neutrophil function in GSD-Ib mice [123]; a defect in either of these enzymes may affect the genes associated with the ER. The neutrophils from the $G6PC3^{-/-}$ mice model showed a significant increase in ER stress compared to the wild type cells [123]. However, there was no variation in ER stress in macrophages from $G6PC3^{-/-}$ [124]. Similar to this result, no variation was observed in the expression of ER stress associated genes (ATF-6, DDIT-3, and HSPA5) in the macrophages with G6PT enzyme inhibition in the chemical inhibitor model (Figure 3.4).

Our previous experiment on bacterial killing by macrophages demonstrated a differentiation effect. The fate of the recruited monocytes and their subsequent differentiation into macrophages, is a key issue because inflammatory monocytes have been shown to cause tissue damage [125]. MDM with G6PT inhibition showed an increase in the expression of HLA-DR and a decrease in the expression of CD163 (Figure 3.6). M1-macrophages, the classically activated macrophages, can be distinguished from the M2-type by having a high HLA-DR expression [117]. Likewise, M2-macrophages, or alternatively activated macrophages, have a higher expression of CD163 and CD204 (both scavenger receptors) [118]. A previous report shows that CD163 functions as a surface receptor for bacteria, including gram negative and gram positive species [126]. Recognition of bacteria by CD163, potently enhanced inflammatory cytokine production in monocytic THP-1 cells and cytokine production by freshly isolated human monocytes [127]. This suggests that there is a possible polarisation of macrophages to M1-phenotype in macrophages with a defective G6PT enzyme.

The mTOR, a central metabolic pathway, plays a key role in polarising the

macrophages to M1 phenotype. TSC is an inhibtitor of mTORC1. $TSC^{-/-}$ macrophages have a marked defect in M2 polarising and they increase the expression of pro-inflammatory cytokines [83]. The TSC-mTOR pathway may alter cytokine secretion to regulate the monocyte-macrophage system [128]. We observed an increase in the expression of protein pS6 (Figure 3.7), a key mTOR marker, in MDM with defective G6PT, which suggests that the activity of the enzyme is influences the mTOR mechanism. Furthermore, the impaired bacterial handling defect was rescued using the mTOR inhibitor, rapamycin, in MDM with G6PT inhibition. In patients with the *G6PC3* mutation, the bacterial handling defect was also rescued when the MDM were treated with rapamycin. This result from the patient samples, validates our findings in the chemical inhibitor model. The mTORC1 inhibits autophagy by phosphorylating UNC-51-like kinase 1 (ULK1) at Ser758 and at multiple sites on ATG14 [129]. After activation, mTORC1 phosphorylates a range of substrates, of which the best characterised are S6K (ribosomal S6 kinase), 4E-BP (eIF4E-binding protein 1) and ULK1 (UNC-51-like kinase 1) [130] [131] [132] [129]. Also, TNF-α and IL-6 are often blocked by mTOR inhibitors such as rapamycin [84] suggesting a pro-inflammatory role for mTOR. Increase in pro-inflammatory cytokines is also observed in MDM with G6PT inhibition. But, it has also been shown that inhibition mTOR promotes the expression of IL-12 expression and blocks IL-10 expression [84]. This suggests a anti-inflammatory role for mTOR. These observations suggest that the PI3K-Akt-mTOR network is not a simple linear pathway that transmits a single signal when activated but integrates diverse intracellular and extracellular cues to regulate a multiple set of basic biological processes within the cell to adapt a given effector response to the environment [84].

In reality, the distinction between the subsets (M1/M2) is not lucid, although it is thought that M1 and M2 macrophages have different metabolic profiles and phenotypes. Nevertheless, it is poorly understood how metabolism contributes to the

control of gene expression during the activation of macrophages. In order to understand the metabolic changes that G6PT inhibition induces on macrophages, we assessed the glycolysis rate and mitochondrial respiration in macrophages with defective G6PT enzyme. This analysis revealed an increase in the glycolytic rate and a decrease in mitochondrial respiration in MDM with G6PT inhibition (Figure 3.10) (Figure 3.11). MDM with G6PT inhibition acquires their energy from the glycolysis process. Metabolic gene profiling of MDM with G6PT inhibition revealed a trend suggesting an increase in the expression of the genes *HK1* and *GCK* (Figure 3.14). *HK1* and *GCK* are vital for glucose metabolism and inhibiting these enzymes has been proven to increase the OCR and decrease the ECAR. Treatment with 2-DG, an inhibitor of HK enzyme, shifts the cellular rates of OCR and lactate production by extracellular acidification to a predominantly oxidative phosphorylation-dependent metabolism [133]. M1-polarised macrophage activation by LPS is dependent on glycolysis [133]. The inhibition of glycolysis by 2-DG significantly decreases the inflammatory response of M1 macrophages [134]. *GCK* mutation has been associated with diabetes mellitus and involved in maintaining blood glucose levels. This mutation inhibits the production of the pro-inflammatory cytokine IL-1β [135] [133]. However, its effect on the metabolic shift in macrophages still requires investigation.

The metabolic gene profiling also showed a trend suggesting an increase in expression of citrate synthase (CS), iso-citrate dehydrogenase (IDH), succinate CoA liage(SUCLG1),and malate dehydrogenase (MDH1B) (Figure 3.15). CS is an important enzyme that converts acetyl CoA and oxaloacetate to citrate. IDH catalyses the third step of the cycle, the oxidative decarboxylation of isocitrate, producing α-ketoglutarate and CO_2 while converting NAD^+ to NADH. SUCLG1 catalyses the formation of succinate. Quantification of the metabolites showed an increase in the expression of proteins involved in glycolysis, with a significant increase in pyruvate. Pyruvate dehydrogenase kinase (also pyruvate dehydrogenase complex kinase, PDC

kinase, or PDK), is a kinase enzyme which acts to inactivate the enzyme pyruvate dehydrogenase by phosphorylating it using ATP [99]. PDK1 is a key regulatory enzyme in the glycolysis process. A knockdown of PDK1 polarised the macrophages to the M2 phenotype [99]. This explains the increase in the glycolytic rate in macrophages with G6PT inhibition. This also provides further evidence that the G6PT enzyme inhibition skews the macrophage to M1 phenotype. Metabolomics analysis also shows a significant increase in the expression of citrate, malate, and fumerate; which are metabolites pertaining to the TCA cycle. In M1 phenotype macrophages, two breaks are observed in the TCA cycle; appearing like a cycle that is completely fragmented [93]. The first break occurs at isocitrate dehydrogenase (IDH) and the other after succinate, with a novel variant of the pathway (termed the aspartate-arginosuccinate shunt) being evident [93]. Citrate in mitochondria gets transported to the cytosol via the citrate transporter. This causes citrate to build-up in the cytosol, which further gets converted to itaconic acid. The citrate built up, will also be withdrawn for fatty acid biosynthesis, which is a characteristic of the M1 phenotype macrophage [93](Figure 3.17). The second break-point in the TCA cycle occurrs after succinate. In the TCA cycle, succinate is converted to fumarate, which is then converted to malate [93]. A moderate increase in succinate was observed in M1 macrophages [109], a large increase in malate was also observed, indicating that the conversion of succinate to fumarate was inefficient [93]. The increase in malate was explained by an enhanced arginosuccinate shunt, which fed into fumarate leading to its build up [93]. The accumulation of citrate, malate, and fumerate in macrophages with G6PT enzyme inhibition confirms a broken citric acid cycle in these cells.

There was also an increase in genes associated with the PPP such as hexose-6-phosphate dehydrogenase/glucose 1-dehydrogenase (H6PD), Phosphoribosyl Pyrophosphate Synthetase 1 (PRPS1), RPIA, transketolase (TKT), and transaldolase (TALDO1) genes. H6PD is a gene that encodes for the enzyme glucose-6-phosphate

dehydrogenase (G6PD). G6PD participates in multiple metabolic pathways, such as reductive biosynthesis, regulation of oxidative stress, and cellular growth. In macrophages, G6PD regulates glucose flux, is elevated in the fat tissue of obese mice, and promotes oxidative stress and pro-inflammatory responses, accompanied by p38 MAPK and NF-κB activation [136]. G6PD, the first and rate-limiting enzyme of the PPP, is a key enzyme in the generation of cytosolic NADPH. Increase in the expression of H6PD may suggest polarising the macrophage to M1 phenotype. It was shown that there is an increase in the expression of genes aiding in the formation of succinate [100]. Interestingly, increased succinate levels may also increase succinylation of metabolic enzymes such as transaldolase (TALDO) [100]. In the metabolomic analysis, there was a significant decrease in the expression of the metabolites, sedoheptulose-7-phosphate (S7P), in MDM with G6PT inhibition. CARKL is a sedoheptulose kinase which converts sedoheptulose to sedoheptulose-7-phosphate. Metabolomics performed after LPS activation revealed S7P, X-5P, R5P, malate, and fumerate levels linked to CARKL expression. An apparent build up of S7P, X5P, R5P, G3P, and G6P/F6P was observed, concomitant with marked reduction in some TCA cycle intermediates and, importantly, NADH but not NAD+ levels [115]. Therefore, an increase in intermediates in the TCA cycle leads to a decrease in S7P, X5P, R5P, G3P, and G6P/F6P. Furthermore, CARKL is identified as a possible repressor of LPS-induced macrophage activation [115] and orchestrates pro- and anti-inflammatory immune responses through metabolic control.

The PRPS1 gene provides instructions for making an enzyme called phosphoribosyl pyrophosphate synthetase 1, or PRPP synthetase 1. This enzyme helps produce a molecule called phosphoribosyl pyrophosphate (PRPP) and is involved in making purine and pyrimidine nucleotides. Quantification of intermediates pertaining to purine and pyrimidine metabolism in MDM treated with S3483 revealed a significant increase in the expression of uridine-5-triphosphate (UTP). UTP can stimulate

arachidonic acid release and the formation of prostaglandin E2 (PGE2). UTP has been shown to modulate inflammatory events in macrophages. Furthermore, simultaneous treatment of the macrophages with lipopolysaccharide (LPS) and UTP results in a synergistic stimulation of NO [137], PGE2 formation and IL-6 production [138]. Therefore, increase in UTP leads to the production of more inflammatory cytokines leading to the M1 phenotype. Increased amounts of these enzymes has been observed in predominant pathways leading to various malignancies in T-cells [139]. Increase in supply of glutamine has been found to be required for the induction of IL-1 by macrophages in response to LPS stimulation [140]. Glutamine can be metabolised via several steps into uridine-5-phosphate (UMP), which in turn can be phosphorylated to uridine-5-diphosphate (UDP) and uridine-5-triphosphate (UTP). Analysis of metabolites pertaining to purine metabolism revealed an increase in the expression of guanosine triphosphate (GTP) in MDM treated with S3483 (Figure 3.19). It is used as a source of energy for protein synthesis and gluconeogenesis [91]. GTP is essential to signal transduction, in particular with G-proteins, in second-messenger mechanisms where it is converted to guanosine diphosphate (GDP) through the action of GTPases [94] [140]. Past literature suggests that GTP up-regulation may lead to calcium release in saponin-treated macrophages [122]. But, there is no further evidence to understand how GTP modulates the function of macrophages.

3.3 Summary

The G6PT enzyme has been shown to be an important protagonist in the bacterial handling of macrophages. Beyond diminished bacterial handling by macrophages with a dysfunctional G6PT enzyme, I was unable to demonstrate the other functional defects associated with inhibition of the enzyme, such as diminished ROS production and ER stress. A complete literature study on 120 patients provides evidence that

mutations which lead to complete loss of activity of the G6PT enzyme can result in severe intestinal inflammation. Several mutations in *SLC37A4*, such as M1V, Gly50Arg, etc., leading to a complete loss in G6PT transport activity, cause severe intestinal inflammation and an increased frequency of infection in patients. We have also shown that inhibiting the transport activity of the G6PT enzyme leads to impaired bacterial handling (figure 3.2) in MDM. Mutations causing loss in G6PT transport activity can cause defective bacterial handling by the macrophages in patients leading to severe infection and inflammation.

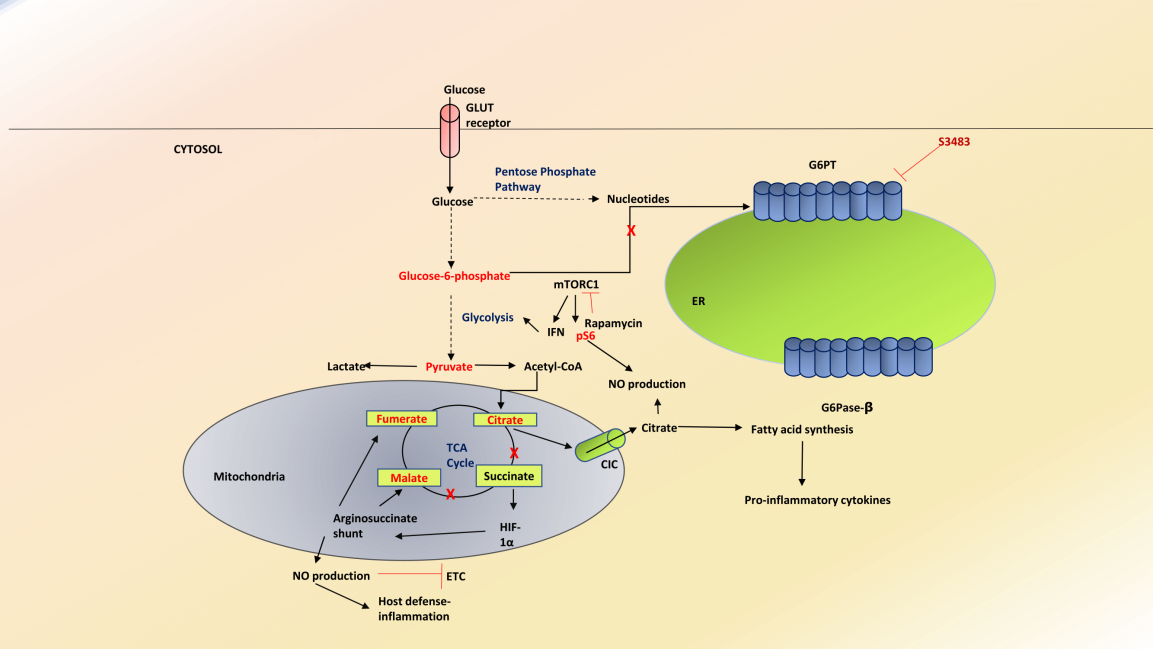

Figure 3.20: **Predicted signalling pathway in MDM treated with S3483** The G6PT enzyme is inhibited by S3483, thus inhibiting the entry of G6P into the ER. Glucose enters the cytosol via the glucose transporter (GLUT) and gets converted into pyruvate by the process of glycolysis. Pyruvate initiates the TCA cycle. This cycle is interrupted in these cells leading to an accumulation of citrate, malate, and fumerate. The rewiring of the TCA cycle leads to the generation of pro-inflammatory cytokines, polarising the macrophages to M1 phenotype. The mTOR signalling pathway also activates the glycolysis pathway, leading to the release of pro-inflammatory cytokines. Inhibiting mTORC1 by rapamycin can reverse the phenotype observed in macrophages with G6PT inhibition

Inhibition of G6PT in MDM leads to accumulation of G6P in the cytosol instead of it being transported into the ER. This increases the glycolytic rate leading to an

accumulation of pyruvate (Figure 3.20). Pyruvate is then transported into the mitochondria in exchange for OH^- and undergoes conversion to acetyl CoA. This in turn is converted to citrate, thus initiating the tri-carboxylic acid (TCA) cycle. Instead of citrate being converted into succinate, it is transported via citrate (CIC) from the mitochondria into the cytosol. Citrate accumulates in the cytosol and initiates fatty acid synthesis, thereby generating pro-inflammatory cytokines. Succinate is generated from α-ketoglutarate (α-KG) rather than from citrate, and this occurs via the γ-aminobutyric acid (GABA) shunt. Similarly, the increased levels of malate and fumerate do not originate from the TCA cycle. The arginosuccinate shunt (pathway linking the urea and TCA cycles) provides the substrate for the synthesis of malate and fumerate (Figure 3.20). MDM with G6PT inhibition acquire energy from glycolysis and have a fragmented TCA cycle (Figure 3.20). The increased expression of pro-inflammatory cytokines suggests polarisation of macrophages to the M1 phenotype. The polarisation and impaired bacterial handling of MDM with G6PT inhibition occurs via the mTOR pathway. The impaired bacterial handling in MDM with G6PT inhibition can be rescued by treatment with the mTORC1 inhibitor, rapamycin (Figure 3.20).

3.4 G6PT chemical inhibition

The chlorogenic acid derivative, SLC37A4, was used to chemically inhibit the G6PT enzyme. This was chosen for use on the basis of the demonstrated specificity of its inhibition, cost, and ease of use. However, there are certain predicaments associated with a chemical inhibitor model. Primarily, despite S3483 being a specific inhibitor of G6PT, it is very toxic to the cells (Figure 1.7). Furthermore, as the killing experiment demonstrates, the duration of inhibition is variable and has a profound impact on bacterial killing in MDM. Therefore, using a chemical inhibitor model limits the

interpretation of our results. In the future, it will be appropriate to test our results with more patient samples and also by constructing a G6PT knockout model using CRISPR/Cas 9 technology.

Chapter 4

Conclusions and future directions

We were able to show that inhibiting G6PT enzyme impairs bacterial handling in macrophages. Inhibiting the transport activity may skew the macrophage polarisation to the M1 phenotype. The G6PT inhibition in MDM may influence the mTOR signalling pathway. These macrophages acquire their primary source of energy from the process of glycolysis. There is an accumulation of metabolites - citrate, malate, and fumerate - in these macrophages, suggesting a broken TCA cycle. Inhibiting the transporting activity in MDM influences purine and pyramidine metabolism by increasing the expression of UTP and GTP metabolites. It is still unclear how the change in metabolism in these macrophages affects their bacterial handling. This study helps to bridge the gap between metabolic and immune mediated diseases, thus providing an alternative treatment option for patients with diabetes, obesity, and cancer. In order to understand the link between the G6PT/Gpase-β variant and bacterial handling, we propose the following experiments:

- Generation of appropriate G6PT/G6pase-β knock-out cells using CRISPR/Cas technology.
- Validation of all experiments using the chemical inhibitor model with macrophages from patients with G6PT and G6pase-β deficiences

- Analysis of the impact of the defective G6PT/G6pase-β enzymes on autophagy
- Investigation of the role of rapamycin as a treatment option for patients with intestinal inflammation and deficiencies in G6pase-β and G6PT enzymes.
- Investigation of the role of small molecule inhibition of metabolic pathway intermediaries may determine key targets for other such interventions in MDM.
- Investigation of the mechanism of T cell metabolism in patients with glucose-6-phosphate metabolism defect to understand and extend our findings in adaptive immunity.

Bibliography

[1] Bernard Khor, Agnès Gardet, and Ramnik J Xavier. Genetics and pathogenesis of inflammatory bowel disease. *Nature*, 474(7351):307, 2011.

[2] Jimmy Z Liu, Suzanne van Sommeren, Hailiang Huang, Siew C Ng, Rudi Alberts, Atsushi Takahashi, Stephan Ripke, James C Lee, Luke Jostins, Tejas Shah, et al. Association analyses identify 38 susceptibility loci for inflammatory bowel disease and highlight shared genetic risk across populations. *Nature genetics*, 47(9):979–986, 2015.

[3] Katrina M de Lange, Loukas Moutsianas, James C Lee, Christopher A Lamb, Yang Luo, Nicholas A Kennedy, Luke Jostins, Daniel L Rice, Javier Gutierrez-Achury, Sun-Gou Ji, et al. Genome-wide association study implicates immune activation of multiple integrin genes in inflammatory bowel disease. *Nature genetics*, 49(2):256, 2017.

[4] Andre Franke, Dermot PB McGovern, Jeffrey C Barrett, Kai Wang, Graham L Radford-Smith, Tariq Ahmad, Charlie W Lees, Tobias Balschun, James Lee, Rebecca Roberts, et al. Genome-wide meta-analysis increases to 71 the number of confirmed crohn's disease susceptibility loci. *Nature genetics*, 42(12):1118–1125, 2010.

[5] Tobias Schwerd, Sumeet Pandey, Huei-Ting Yang, Katrin Bagola, Elisabeth Jameson, Jonathan Jung, Robin H Lachmann, Neil Shah, Smita Y Patel, Claire

Booth, et al. Impaired antibacterial autophagy links granulomatous intestinal inflammation in niemann–pick disease type c1 and xiap deficiency with nod2 variants in crohn9s disease. *Gut*, pages gutjnl–2015, 2016.

[6] Holm H Uhlig. Monogenic diseases associated with intestinal inflammation: implications for the understanding of inflammatory bowel disease. *Gut*, 62(12):1795–1805, 2013.

[7] Thomas F Roe, Daniel W Thomas, Vicente Gilsanz, Hart Isaacs, and James B Atkinson. Inflammatory bowel disease in glycogen storage disease type ib. *The Journal of pediatrics*, 109(1):55–59, 1986.

[8] L Schall. Fälle von glykogenspeicherkrankheit (hepatomegalie glykogenica v. gierke). *Münch Med Wschr*, 79:2078–2080, 3.

[9] Dietrich Matern, Hans Seydewitz, Deeksha Bali, Christine Lang, and Yuan-Tsong Chen. Glycogen storage disease type i: diagnosis and phenotype/genotype correlation. *European journal of pediatrics*, 161:S10–S19, 2002.

[10] Ke-Jian Lei, Leslie L Shelly, Chi-Jiunn Pan, James B Sidbury, and Janice Yang Chou. Mutations in the glucose-6-phosphatase gene that cause glycogen storage disease type 1a. *Science*, 262(5133):580–584, 1993.

[11] Hisayuki Hiraiwa, Chi-Jiunn Pan, Baochuan Lin, Shimon W Moses, and Janice Yang Chou. Inactivation of the glucose 6-phosphate transporter causes glycogen storage disease type 1b. *Journal of Biological Chemistry*, 274(9):5532–5536, 1999.

[12] Emile Van Schaftingen and Isabelle Gerin. The glucose-6-phosphatase system. *Biochemical Journal*, 362(3):513–532, 2002.

[13] Chi-Jiunn Pan, Shih-Yin Chen, Soojung Lee, and Janice Y Chou. Structure–function study of the glucose-6-phosphate transporter, an eukaryotic antiporter deficient in glycogen storage disease type ib. *Molecular genetics and metabolism*, 96(1):32–37, 2009.

[14] Janice Y Chou, Hyun Sik Jun, and Brian C Mansfield. Glycogen storage disease type i and g6pase-β deficiency: etiology and therapy. *Nature Reviews Endocrinology*, 6(12):676–688, 2010.

[15] Chi-Jiunn Pan, Ke-Jian Lei, Hungwen Chen, Jerrold M Ward, and Janice Yang Chou. Ontogeny of the murine glucose-6-phosphatase system. *Archives of biochemistry and biophysics*, 358(1):17–24, 1998.

[16] Marie-Claire Méchin, Borhane Annabi, Jean-Paul Pegorier, and Gérald van de Werve. Ontogeny of the catalytic subunit and putative glucose-6-phosphate transporter proteins of the rat microsomal liver glucose-6-phosphatase system. *Metabolism*, 49(9):1200–1203, 2000.

[17] Jeng-Jer Shieh, Chi-Jiunn Pan, Brian C Mansfield, and Janice Yang Chou. A glucose-6-phosphate hydrolase, widely expressed outside the liver, can explain age-dependent resolution of hypoglycemia in glycogen storage disease type ia. *Journal of Biological Chemistry*, 278(47):47098–47103, 2003.

[18] Yuk Yin Cheung, So Youn Kim, Wai Han Yiu, Chi-Jiunn Pan, Hyun-Sik Jun, Robert A Ruef, Eric J Lee, Heiner Westphal, Brian C Mansfield, and Janice Y Chou. Impaired neutrophil activity and increased susceptibility to bacterial infection in mice lacking glucose-6-phosphatase–β. *The Journal of clinical investigation*, 117(3):784–793, 2007.

[19] Daniela Melis, Rossella Fulceri, Giancarlo Parenti, Paola Marcolongo, Rosanna Gatti, Rossella Parini, Enrica Riva, Roberto Della Casa, Enrico Zammarchi,

Generoso Andria, et al. Genotype/phenotype correlation in glycogen storage disease type 1b: a multicentre study and review of the literature. *European journal of pediatrics*, 164(8):501–508, 2005.

[20] Yuan-Tsong Chen. Glycogen storage diseases. *The metabolic and molecular bases of inherited disease*, 1521, 2005.

[21] J Fernandes, JV Leonard, SW Moses, M Odievre, M Di Rocco, J Schaub, GPA Smit, K Ullrich, and P Durand. Glycogen storage disease: recommendations for treatment. *European journal of pediatrics*, 147(3):226–228, 1988.

[22] Borhane Annabi, Brian C Mansfield, Hisayuki Hiraiwa, Ke-Jian Lei, Tsuneyuki Ubagai, Mihael H Polymeropoulos, Shimon W Moses, Ruti Parvari, Eli Hershkovitz, Hanna Mandel, et al. The gene for glycogen-storage disease type 1b maps to chromosome 11q23. *The American Journal of Human Genetics*, 62(2):400–405, 1998.

[23] William J Arion, Bruce K Wallin, Pamelia W Carlson, and Alex J Lange. The specificity of glucose 6-phosphatase of intact liver microsomes. *Journal of Biological Chemistry*, 247(8):2558–2565, 1972.

[24] Janice Y Chou and Brian C Mansfield. The slc37 family of sugar-phosphate/phosphate exchangers. *Current topics in membranes*, 73:357, 2014.

[25] William J Arion, Wesley K Canfield, Francis C Ramos, Mark L Su, Hans-Joerg Burger, Horst Hemmerle, Gerrit Schubert, Peter Below, and Andreas W Herling. Chlorogenic acid analogue s 3483: a potent competitive inhibitor of the hepatic and renal glucose-6-phosphatase systems. *Archives of biochemistry and biophysics*, 351(2):279–285, 1998.

[26] Andreas W Herling, Hans-Joerg Burger, Gerrit Schubert, Horst Hemmerle, Hans-Ludwig Schaefer, and Werner Kramer. Alterations of carbohydrate and

lipid intermediary metabolism during inhibition of glucose-6-phosphatase in rats. *European journal of pharmacology*, 386(1):75–82, 1999.

[27] Robert HJ Bandsma, Coen H Wiegman, Andreas W Herling, Hans-Joerg Burger, Anke ter Harmsel, Alfred J Meijer, Johannes A Romijn, Dirk-Jan Reijngoud, and Folkert Kuipers. Acute inhibition of glucose-6-phosphate translocator activity leads to increased de novo lipogenesis and development of hepatic steatosis without affecting vldl production in rats. *Diabetes*, 50(11):2591–2597, 2001.

[28] Shigeru Tsuchiya, Michiko Yamabe, Yoshiko Yamaguchi, Yasuko Kobayashi, Tasuke Konno, and Keiya Tada. Establishment and characterization of a human acute monocytic leukemia cell line (thp-1). *International journal of cancer*, 26(2):171–176, 1980.

[29] Ke-Jian Lei, Hungwen Chen, Chi-Jiunn Pan, Jerrold M Ward, Bedrich Mosinger Jr, Eric J Lee, Heiner Westphal, Brian C Mansfield, and Janice Yang Chou. Glucose–6–phosphatase dependent substrate transport in the glycogen storage disease type–1a mouse. *Nature genetics*, 13(2):203–209, 1996.

[30] Li-Yuan Chen, Chi-Jiunn Pan, Jeng-Jer Shieh, and Janice Yang Chou. Structure–function analysis of the glucose-6-phosphate transporter deficient in glycogen storage disease type ib. *Human molecular genetics*, 11(25):3199–3207, 2002.

[31] Rosanna Leuzzi, Gábor Bánhegyi, Tamás Kardon, Paola Marcolongo, Piero-Leopoldo Capecchi, Hans-Joerg Burger, Angelo Benedetti, and Rosella Fulceri. Inhibition of microsomal glucose-6-phosphate transport in human neutrophils results in apoptosis: a potential explanation for neutrophil dysfunction in glycogen storage disease type 1b. *Blood*, 101(6):2381–2387, 2003.

[32] Hye-Hyun Ahn, Yumin Oh, Huikyong Lee, WonJae Lee, Jae-Woong Chang, Ha-Kyung Pyo, Yong-Keun Jung, et al. Identification of glucose-6-phosphate transporter as a key regulator functioning at the autophagy initiation step. *FEBS letters*, 589(16):2100–2109, 2015.

[33] Lei He, Konstandinos Vasiliou, and Daniel W Nebert. Analysis and update of the human solute carrier (slc) gene superfamily. *Human genomics*, 3(2):195, 2009.

[34] Lucia Bartoloni, Marie Wattenhofer, Jun Kudoh, Asher Berry, Kazunori Shibuya, Kazuhiko Kawasaki, Jun Wang, Shuichi Asakawa, Ilana Talior, Batsheva Bonne-Tamir, et al. Cloning and characterization of a putative human glycerol 3-phosphate permease gene (slc37a1 or g3pp) on 21q22. 3: mutation analysis in two candidate phenotypes, dfnb10 and a glycerol kinase deficiency. *Genomics*, 70(2):190–200, 2000.

[35] Lucia Bartoloni and Stylianos E Antonarakis. The human sugar-phosphate/phosphate exchanger family slc37. *Pflügers Archiv*, 447(5):780–783, 2004.

[36] Shih-Yin Chen, Chi-Jiunn Pan, Krishnamachary Nandigama, Brian C Mansfield, Suresh V Ambudkar, and Janice Y Chou. The glucose-6-phosphate transporter is a phosphate-linked antiporter deficient in glycogen storage disease type ib and ic. *The FASEB Journal*, 22(7):2206–2213, 2008.

[37] Kaan Boztug, Giridharan Appaswamy, Angel Ashikov, Alejandro A Schäffer, Ulrich Salzer, Jana Diestelhorst, Manuela Germeshausen, Gudrun Brandes, Jacqueline Lee-Gossler, Fatih Noyan, et al. A syndrome with congenital neutropenia and mutations in g6pc3. *New England Journal of Medicine*, 360(1):32–43, 2009.

[38] Juan I Aróstegui, José Sánchez de Toledo, Mariona Pascal, Carlos García, Jordi Yagüe, and Cristina Díaz de Heredia. A novel g6pc3 homozygous 1-bp deletion as a cause of severe congenital neutropenia. *Blood*, 114(8):1718–1719, 2009.

[39] Jun Xia, Audrey A Bolyard, Elin Rodger, Steve Stein, Andrew A Aprikyan, David C Dale, and Daniel C Link. Prevalence of mutations in elane, gfi1, hax1, sbds, was and g6pc3 in patients with severe congenital neutropenia. *British journal of haematology*, 147(4):535–542, 2009.

[40] K Hofman. Tmbase-a database of membrane spanning protein segments. *Biol. Chem. Hoppe-Seyler*, 374:166, 1993.

[41] Isabelle Gerin, Maria Veiga-da Cunha, Younes Achouri, Jean-François Collet, and Emile Van Schaftingen. Sequence of a putative glucose 6-phosphate translocase, mutated in glycogen storage disease type ib. *FEBS letters*, 419(2-3):235–238, 1997.

[42] Yafei Huang, M Joanne Lemieux, Jinmei Song, Manfred Auer, and Da-Neng Wang. Structure and mechanism of the glycerol-3-phosphate transporter from escherichia coli. *Science*, 301(5633):616–620, 2003.

[43] Carolina Landolt-Marticorena and Reinhart AF Reithmeier. Asparagine-linked oligosaccharides are localized to single extracytosolic segments in multi-span membrane glycoproteins. *Biochemical Journal*, 302(1):253–260, 1994.

[44] IM Nilsson and G Von Heijne. Determination of the distance between the oligosaccharyltransferase active site and the endoplasmic reticulum membrane. *Journal of Biological Chemistry*, 268(8):5798–5801, 1993.

[45] Armando J Parodi. Protein glucosylation and its role in protein folding. *Annual review of biochemistry*, 69(1):69–93, 2000.

[46] Jonas Almqvist, Yafei Huang, Sven Hovmöller, and Da-Neng Wang. Homology modeling of the human microsomal glucose 6-phosphate transporter explains the mutations that cause the glycogen storage disease type ib. *Biochemistry*, 43(29):9289–9297, 2004.

[47] Andreas R Janecke, Martin Lindner, Martin Erdel, Ertan Mayatepek, Dorothea Möslinger, Teodor Podskarbi, Friedrich Fresser, Silvia Stöckler-Ipsiroglu, Georg F Hoffmann, and Gerd Utermann. Mutation analysis in glycogen storage disease type 1 non-a. *Human genetics*, 107(3):285–289, 2000.

[48] Janice Y Chou, Hyun Sik Jun, and Brian C Mansfield. The slc37 family of phosphate-linked sugar phosphate antiporters. *Molecular aspects of medicine*, 34(2):601–611, 2013.

[49] Li-Yuan Chen, Baochuan Lin, Chi-Jiunn Pan, Hisayuki Hiraiwa, and Janice Yang Chou. Structural requirements for the stability and microsomal transport activity of the human glucose 6-phosphate transporter. *Journal of Biological Chemistry*, 275(44):34280–34286, 2000.

[50] Chi-Jiunn Pan, Li-Yuan Chen, Brian C Mansfield, Barbara Salani, Luigi Varesio, and Janice Yang Chou. The signature motif in human glucose-6-phosphate transporter is essential for microsomal transport of glucose-6-phosphate. *Human genetics*, 112(4):430–433, 2003.

[51] J Chou, Dietrich Matern, Brian C Mansfield, and Yuan-Tsong Chen. Type i glycogen storage diseases: disorders of the glucose-6-phosphatase complex. *Current molecular medicine*, 2(2):121–143, 2002.

[52] Daniela Melis, Rosario Pivonello, Giancarlo Parenti, Roberto Della Casa, Mariacarolina Salerno, Francesca Balivo, Pasquale Piccolo, Carolina Di Somma, Annamaria Colao, and Generoso Andria. The growth hormone-insulin-like growth

factor axis in glycogen storage disease type 1: evidence of different growth patterns and insulin-like growth factor levels in patients with glycogen storage disease type 1a and 1b. *The Journal of pediatrics*, 156(4):663–670, 2010.

[53] Lucia Galli, Alfredo Orrico, Paola Marcolongo, Rosella Fulceri, Ann Burchell, Daniela Melis, Rossella Parini, Rosanna Gatti, Ching-Wan Lam, Angelo Benedetti, et al. Mutations in the glucose-6-phosphate transporter (g6pt) gene in patients with glycogen storage diseases type 1b and 1c. *FEBS letters*, 459(2):255–258, 1999.

[54] Maria Veiga-da Cunha, Isabelle Gerin, Yuan-Tsong Chen, Thierry de Barsy, Pascale de Lonlay, Carlo Dionisi-Vici, Christiane D Fenske, Philip J Lee, James V Leonard, Irene Maire, et al. A gene on chromosome 11q23 coding for a putative glucose-6-phosphate translocase is mutated in glycogen-storage disease types ib and ic. *The American Journal of Human Genetics*, 63(4):976–983, 1998.

[55] Maria Veiga-da Cunha, Isabelle Gerin, Yuan-Tsong Chen, Philip J Lee, James V Leonard, Irene Maire, Udo Wendel, Miikka Vikkula, and Emile Van Schaftingen. The putative glucose 6-phosphate translocase gene is mutated in essentially all cases of glycogen storage disease type i non-a. *European Journal of Human Genetics*, 7(6):717–723, 1999.

[56] Shigeo Kure, Dian-Chang Hou, Yasuyuki Suzuki, Atsushi Yamagishi, Masahiro Hiratsuka, Tokiko Fukuda, Hideo Sugie, Naomi Kondo, Yoichi Matsubara, and Kuniaki Narisawa. Glycogen storage disease type ib without neutropenia. *The Journal of pediatrics*, 137(2):253–256, 2000.

[57] Rihwa Choi, Hyung-Doo Park, Jung Min Ko, Jeongho Lee, Dong Hwan Lee, Suk Jin Hong, Chang-Seok Ki, Soo-Youn Lee, Jong-Won Kim, Junghan Song,

et al. Novel slc37a4 mutations in korean patients with glycogen storage disease ib. *Annals of laboratory medicine*, 37(3):261–266, 2017.

[58] Anja A Kühl, Ulrike Erben, Lea I Kredel, and Britta Siegmund. Diversity of intestinal macrophages in inflammatory bowel diseases. *Frontiers in immunology*, 6, 2015.

[59] Charles A Janeway Jr and Ruslan Medzhitov. Innate immune recognition. *Annual review of immunology*, 20(1):197–216, 2002.

[60] Shizuo Akira, Kiyoshi Takeda, and Tsuneyasu Kaisho. Toll-like receptors: critical proteins linking innate and acquired immunity. *Nature immunology*, 2(8):675, 2001.

[61] Taro Kawai and Shizuo Akira. Toll-like receptors and their crosstalk with other innate receptors in infection and immunity. *Immunity*, 34(5):637–650, 2011.

[62] Shizuo Akira, Satoshi Uematsu, and Osamu Takeuchi. Pathogen recognition and innate immunity. *Cell*, 124(4):783–801, 2006.

[63] Jisu Oh, Amy E Riek, Sherry Weng, Marvin Petty, David Kim, Marco Colonna, Marina Cella, and Carlos Bernal-Mizrachi. Endoplasmic reticulum stress controls m2 macrophage differentiation and foam cell formation. *Journal of Biological Chemistry*, 287(15):11629–11641, 2012.

[64] Jingshi Shen, Xi Chen, Linda Hendershot, and Ron Prywes. Er stress regulation of atf6 localization by dissociation of bip/grp78 binding and unmasking of golgi localization signals. *Developmental cell*, 3(1):99–111, 2002.

[65] Joseph P Hendrick and Franz-Ulrich Hartl. Molecular chaperone functions of heat-shock proteins. *Annual review of biochemistry*, 62(1):349–384, 1993.

[66] IG Haas. Bip (grp78), an essential hsp70 resident protein in the endoplasmic reticulum. *Cellular and Molecular Life Sciences*, 50(11):1012–1020, 1994.

[67] Yanjun Ma and Linda M Hendershot. The role of the unfolded protein response in tumour development: friend or foe? *Nature reviews. Cancer*, 4(12):966, 2004.

[68] Hirohito Yamaguchi and Hong-Gang Wang. Chop is involved in endoplasmic reticulum stress-induced apoptosis by enhancing dr5 expression in human carcinoma cells. *Journal of Biological Chemistry*, 279(44):45495–45502, 2004.

[69] Nobumichi Ohoka, Satoshi Yoshii, Takayuki Hattori, Kikuo Onozaki, and Hidetoshi Hayashi. Trb3, a novel er stress-inducible gene, is induced via atf4–chop pathway and is involved in cell death. *The EMBO journal*, 24(6):1243–1255, 2005.

[70] Michael J Berridge. Calcium signalling and cell proliferation. *Bioessays*, 17(6):491–500, 1995.

[71] Ji Zhou, Šárka Lhoták, Brooke A Hilditch, and Richard C Austin. Activation of the unfolded protein response occurs at all stages of atherosclerotic lesion development in apolipoprotein e–deficient mice. *Circulation*, 111(14):1814–1821, 2005.

[72] Jisu Oh, Sherry Weng, Shaili K Felton, Sweety Bhandare, Amy Riek, Boyd Butler, Brandon M Proctor, Marvin Petty, Zhouji Chen, Kenneth B Schechtman, et al. 1, 25 (oh) 2 vitamin d inhibits foam cell formation and suppresses macrophage cholesterol uptake in patients with type 2 diabetes mellitus. *Circulation*, 120(8):687–698, 2009.

[73] Fernando O Martinez and Siamon Gordon. The m1 and m2 paradigm of macrophage activation: time for reassessment. *F1000prime reports*, 6, 2014.

[74] Chao He, Alan J Ryan, Shubha Murthy, and A Brent Carter. Accelerated development of pulmonary fibrosis via cu, zn-superoxide dismutase-induced alternative activation of macrophages. *Journal of Biological Chemistry*, 288(28):20745–20757, 2013.

[75] Cristiana Guiducci, Alain P Vicari, Sabina Sangaletti, Giorgio Trinchieri, and Mario P Colombo. Redirecting in vivo elicited tumor infiltrating macrophages and dendritic cells towards tumor rejection. *Cancer research*, 65(8):3437–3446, 2005.

[76] Tina Lucas, Ari Waisman, Rajeev Ranjan, Jürgen Roes, Thomas Krieg, Werner Müller, Axel Roers, and Sabine A Eming. Differential roles of macrophages in diverse phases of skin repair. *The Journal of Immunology*, 184(7):3964–3977, 2010.

[77] Rinat Zaynagetdinov, Taylor P Sherrill, Vasiliy V Polosukhin, Wei Han, Jamie A Ausborn, Allyson G McLoed, Frank B McMahon, Linda A Gleaves, Amber L Degryse, Georgios T Stathopoulos, et al. A critical role for macrophages in promotion of urethane-induced lung carcinogenesis. *The Journal of Immunology*, 187(11):5703–5711, 2011.

[78] Raymond A Isidro and Caroline B Appleyard. Colonic macrophage polarization in homeostasis, inflammation, and cancer. *American Journal of Physiology-Gastrointestinal and Liver Physiology*, 311(1):G59–G73, 2016.

[79] Toby Lawrence and Gioacchino Natoli. Transcriptional regulation of macrophage polarization: enabling diversity with identity. *Nature reviews. Immunology*, 11(11):750, 2011.

[80] Manuel Modolell, Ines M Corraliza, Franz Link, Germán Soler, and Klaus Eichmann. Reciprocal regulation of the nitric oxide synthase/arginase balance in

mouse bone marrow-derived macrophages by th 1 and th 2 cytokines. *European journal of immunology*, 25(4):1101–1104, 1995.

[81] Markus Munder, Klaus Eichmann, José M Morán, Francisco Centeno, Germán Soler, and Manuel Modolell. Th1/th2-regulated expression of arginase isoforms in murine macrophages and dendritic cells. *The Journal of Immunology*, 163(7):3771–3777, 1999.

[82] Philipp Günzl and Gernot Schabbauer. Recent advances in the genetic analysis of pten and pi3k innate immune properties. *Immunobiology*, 213(9):759–765, 2008.

[83] Vanessa Byles, Anthony J Covarrubias, Issam Ben-Sahra, Dudley W Lamming, David M Sabatini, Brendan D Manning, and Tiffany Horng. The tsc-mtor pathway regulates macrophage polarization. *Nature communications*, 4:2834, 2013.

[84] Thomas Weichhart, Markus Hengstschläger, and Monika Linke. Regulation of innate immune cell function by mtor. *Nature reviews. Immunology*, 15(10):599, 2015.

[85] Andrew R Tee, Diane C Fingar, Brendan D Manning, David J Kwiatkowski, Lewis C Cantley, and John Blenis. Tuberous sclerosis complex-1 and-2 gene products function together to inhibit mammalian target of rapamycin (mtor)-mediated downstream signaling. *Proceedings of the National Academy of Sciences*, 99(21):13571–13576, 2002.

[86] Alicia Arranz, Christina Doxaki, Eleni Vergadi, Yeny Martinez de la Torre, Katerina Vaporidi, Eleni D Lagoudaki, Eleftheria Ieronymaki, Ariadne Androulidaki, Maria Venihaki, Andrew N Margioris, et al. Akt1 and akt2 protein kinases

differentially contribute to macrophage polarization. *Proceedings of the National Academy of Sciences*, 109(24):9517–9522, 2012.

[87] Taro Fukao and Shigeo Koyasu. Pi3k and negative regulation of tlr signaling. *Trends in immunology*, 24(7):358–363, 2003.

[88] Mathieu Laplante and David M Sabatini. mtor signaling in growth control and disease. *Cell*, 149(2):274–293, 2012.

[89] Ken Inoki, Joungmok Kim, and Kun-Liang Guan. Ampk and mtor in cellular energy homeostasis and drug targets. *Annual review of pharmacology and toxicology*, 52:381–400, 2012.

[90] Kenta Masui, Webster K Cavenee, and Paul S Mischel. mtorc2 in the center of cancer metabolic reprogramming. *Trends in Endocrinology & Metabolism*, 25(7):364–373, 2014.

[91] Timo Gaber, Cindy Strehl, and Frank Buttgereit. Metabolic regulation of inflammation. *Nature Reviews Rheumatology*, 13(5):267–279, 2017.

[92] Connie M Krawczyk, Thomas Holowka, Jie Sun, Julianna Blagih, Eyal Amiel, Ralph J DeBerardinis, Justin R Cross, Euihye Jung, Craig B Thompson, Russell G Jones, et al. Toll-like receptor–induced changes in glycolytic metabolism regulate dendritic cell activation. *Blood*, 115(23):4742–4749, 2010.

[93] Luke AJ ONeill. A broken krebs cycle in macrophages. *Immunity*, 42(3):393–394, 2015.

[94] Silvia Galván-Peña and Luke AJ ONeill. Metabolic reprograming in macrophage polarization. *Frontiers in immunology*, 5, 2014.

[95] Roy Noy and Jeffrey W Pollard. Tumor-associated macrophages: from mechanisms to therapy. *Immunity*, 41(1):49–61, 2014.

[96] Neil P Jones and Almut Schulze. Targeting cancer metabolism–aiming at a tumour's sweet-spot. *Drug discovery today*, 17(5):232–241, 2012.

[97] Jonathan Jantsch, Dipshikha Chakravortty, Nadine Turza, Alexander T Prechtel, Björn Buchholz, Roman G Gerlach, Melanie Volke, Joachim Gläsner, Christina Warnecke, Michael S Wiesener, et al. Hypoxia and hypoxia-inducible factor-1α modulate lipopolysaccharide-induced dendritic cell activation and function. *The Journal of Immunology*, 180(7):4697–4705, 2008.

[98] Hiroaki Suzuki, Tadakazu Hisamatsu, Sayako Chiba, Kiyoto Mori, Mina T Kitazume, Katsuyoshi Shimamura, Nobuhiro Nakamoto, Katsuyoshi Matsuoka, Hirotoshi Ebinuma, Makoto Naganuma, et al. Glycolytic pathway affects differentiation of human monocytes to regulatory macrophages. *Immunology letters*, 176:18–27, 2016.

[99] Zheng Tan, Na Xie, Huachun Cui, Douglas R Moellering, Edward Abraham, Victor J Thannickal, and Gang Liu. Pyruvate dehydrogenase kinase 1 participates in macrophage polarization via regulating glucose metabolism. *The Journal of Immunology*, 194(12):6082–6089, 2015.

[100] GM Tannahill, AM Curtis, J Adamik, EM Palsson-McDermott, AF McGettrick, G Goel, C Frezza, NJ Bernard, B Kelly, NH Foley, et al. Succinate is a danger signal that induces il-1β via hif-1α. *Nature*, 496(7444):238, 2013.

[101] Runkuan Yang, Shengtao Zhu, and Tor Inge Tonnessen. Ethyl pyruvate is a novel anti-inflammatory agent to treat multiple inflammatory organ injuries. *Journal of Inflammation*, 13(1):37, 2016.

[102] Abhishek K Jha, Stanley Ching-Cheng Huang, Alexey Sergushichev, Vicky Lampropoulou, Yulia Ivanova, Ekaterina Loginicheva, Karina Chmielewski,

Kelly M Stewart, Juliet Ashall, Bart Everts, et al. Network integration of parallel metabolic and transcriptional data reveals metabolic modules that regulate macrophage polarization. *Immunity*, 42(3):419–430, 2015.

[103] Vittoria Infantino, Paolo Convertini, Liana Cucci, Maria Antonietta Panaro, Maria Antonietta Di Noia, Rosa Calvello, Ferdinando Palmieri, and Vito Iacobazzi. The mitochondrial citrate carrier: a new player in inflammation. *Biochemical Journal*, 438(3):433–436, 2011.

[104] BA McFadden and S Purohit. Itaconate, an isocitrate lyase-directed inhibitor in pseudomonas indigofera. *Journal of bacteriology*, 131(1):136–144, 1977.

[105] Nalini Sadagopan, Wenlin Li, Steven L Roberds, Terry Major, Gregory M Preston, Ying Yu, and Michael A Tones. Circulating succinate is elevated in rodent models of hypertension and metabolic disease. *American journal of hypertension*, 20(11):1209–1215, 2007.

[106] Juan-Carlos Rodríguez-Prados, Paqui G Través, Jimena Cuenca, Daniel Rico, Julián Aragonés, Paloma Martín-Sanz, Marta Cascante, and Lisardo Boscá. Substrate fate in activated macrophages: a comparison between innate, classic, and alternative activation. *The Journal of Immunology*, 185(1):605–614, 2010.

[107] Sharon Hillier and WT Charnetzky. Glyoxylate bypass enzymes in yersinia species and multiple forms of isocitrate lyase in yersinia pestis. *Journal of bacteriology*, 145(1):452–458, 1981.

[108] Fyodor A Kondrashov, Eugene V Koonin, Igor G Morgunov, Tatiana V Finogenova, and Marie N Kondrashova. Evolution of glyoxylate cycle enzymes in metazoa: evidence of multiple horizontal transfer events and pseudogene formation. *Biology direct*, 1(1):31, 2006.

[109] Alessandro Michelucci, Thekla Cordes, Jenny Ghelfi, Arnaud Pailot, Norbert Reiling, Oliver Goldmann, Tina Binz, André Wegner, Aravind Tallam, Antonio Rausell, et al. Immune-responsive gene 1 protein links metabolism to immunity by catalyzing itaconic acid production. *Proceedings of the National Academy of Sciences*, 110(19):7820–7825, 2013.

[110] R Herbert De'Broski, Jun-Qi Yang, Simon P Hogan, Kathryn Groschwitz, Marat Khodoun, Ariel Munitz, Tatyana Orekov, Charles Perkins, Quan Wang, Frank Brombacher, et al. Intestinal epithelial cell secretion of relm-β protects against gastrointestinal worm infection. *Journal of Experimental Medicine*, 206(13):2947–2957, 2009.

[111] Tina Rubic, Günther Lametschwandtner, Sandra Jost, Sonja Hinteregger, Julia Kund, Nicole Carballido-Perrig, Christoph Schwärzler, Tobias Junt, Hans Voshol, Josef G Meingassner, et al. Triggering the succinate receptor gpr91 on dendritic cells enhances immunity. *Nature immunology*, 9(11):1261–1269, 2008.

[112] Divya Vats, Lata Mukundan, Justin I Odegaard, Lina Zhang, Kristi L Smith, Christine R Morel, David R Greaves, Peter J Murray, and Ajay Chawla. Oxidative metabolism and pgc-1β attenuate macrophage-mediated inflammation. *Cell metabolism*, 4(1):13–24, 2006.

[113] Ajay Chawla. Control of macrophage activation and function by ppars. *Circulation research*, 106(10):1559–1569, 2010.

[114] Luke AJ O'Neill, Rigel J Kishton, and Jeff Rathmell. A guide to immunometabolism for immunologists. *Nature Reviews Immunology*, 2016.

[115] Arvand Haschemi, Paul Kosma, Lars Gille, Charles R Evans, Charles F Burant, Philipp Starkl, Bernhard Knapp, Robert Haas, Johannes A Schmid, Christoph

Jandl, et al. The sedoheptulose kinase carkl directs macrophage polarization through control of glucose metabolism. *Cell metabolism*, 15(6):813–826, 2012.

[116] Csörsz Nagy and Arvand Haschemi. Time and demand are two critical dimensions of immunometabolism: the process of macrophage activation and the pentose phosphate pathway. *Frontiers in immunology*, 6, 2015.

[117] Bin-Zhi Qian and Jeffrey W Pollard. Macrophage diversity enhances tumor progression and metastasis. *Cell*, 141(1):39–51, 2010.

[118] Antonio Sica, Paola Larghi, Alessandra Mancino, Luca Rubino, Chiara Porta, Maria Grazia Totaro, Monica Rimoldi, Subhra Kumar Biswas, Paola Allavena, and Alberto Mantovani. Macrophage polarization in tumour progression. In *Seminars in cancer biology*, volume 18, pages 349–355. Elsevier, 2008.

[119] Yuchang Fu, Lidia Maianu, Barry R Melbert, and W Timothy Garvey. Facilitative glucose transporter gene expression in human lymphocytes, monocytes, and macrophages: a role for glut isoforms 1, 3, and 5 in the immune response and foam cell formation. *Blood Cells, Molecules, and Diseases*, 32(1):182–190, 2004.

[120] Thorsten Cramer, Yuji Yamanishi, Björn E Clausen, Irmgard Förster, Rafal Pawlinski, Nigel Mackman, Volker H Haase, Rudolf Jaenisch, Maripat Corr, Victor Nizet, et al. Hif-1α is essential for myeloid cell-mediated inflammation. *Cell*, 112(5):645–657, 2003.

[121] Ken Itoh, Tomoki Chiba, Satoru Takahashi, Tetsuro Ishii, Kazuhiko Igarashi, Yasutake Katoh, Tatsuya Oyake, Norio Hayashi, Kimihiko Satoh, Ichiro Hatayama, et al. An nrf2/small maf heterodimer mediates the induction of phase ii detoxifying enzyme genes through antioxidant response elements. *Biochemical and biophysical research communications*, 236(2):313–322, 1997.

[122] T Hamachi, M Hirata, Y Kimura, T Ikebe, T Ishimatsu, K Yamaguchi, and T Koga. Effect of guanosine triphosphate on the release and uptake of ca2+ in saponin-permeabilized macrophages and the skeletal-muscle sarcoplasmic reticulum. *Biochemical Journal*, 242(1):253–260, 1987.

[123] So Youn Kim, Hyun Sik Jun, Paul A Mead, Brian C Mansfield, and Janice Y Chou. Neutrophil stress and apoptosis underlie myeloid dysfunction in glycogen storage disease type ib. *Blood*, 111(12):5704–5711, 2008.

[124] Hyun Sik Jun, Yuk Yin Cheung, Young Mok Lee, Brian C Mansfield, and Janice Y Chou. Glucose-6-phosphatase-β, implicated in a congenital neutropenia syndrome, is essential for macrophage energy homeostasis and functionality. *Blood*, 119(17):4047–4055, 2012.

[125] Bin-Zhi Qian, Jiufeng Li, Hui Zhang, Takanori Kitamura, Jinghang Zhang, Liam R Campion, Elizabeth A Kaiser, Linda A Snyder, and Jeffrey W Pollard. Ccl2 recruits inflammatory monocytes to facilitate breast tumor metastasis. *nature*, 475(7355):222, 2011.

[126] Karin Schornagel, Rianka PM Vloet, Christine D Dijkstra, Timo K van den Berg, Babs O Fabriek, Robin van Bruggen, Dong Mei Deng, Antoon JM Ligtenberg, and Kamran Nazmi. The macrophage scavenger receptor cd163 functions as an innate. *blood*, 7:167064, 2008.

[127] Babs O Fabriek, Robin van Bruggen, Dong Mei Deng, Antoon JM Ligtenberg, Kamran Nazmi, Karin Schornagel, Rianka PM Vloet, Christine D Dijkstra, and Timo K van den Berg. The macrophage scavenger receptor cd163 functions as an innate immune sensor for bacteria. *Blood*, 113(4):887–892, 2009.

[128] Thomas Weichhart, Giuseppina Costantino, Marko Poglitsch, Margit Rosner, Maximilian Zeyda, Karl M Stuhlmeier, Thomas Kolbe, Thomas M Stulnig,

Walter H Hörl, Markus Hengstschläger, et al. The tsc-mtor signaling pathway regulates the innate inflammatory response. *Immunity*, 29(4):565–577, 2008.

[129] Francesca Nazio, Flavie Strappazzon, Manuela Antonioli, Pamela Bielli, Valentina Cianfanelli, Matteo Bordi, Christine Gretzmeier, Joern Dengjel, Mauro Piacentini, Gian Maria Fimia, et al. mtor inhibits autophagy by controlling ulk1 ubiquitylation, self-association and function through ambra1 and traf6. *Nature cell biology*, 15(4):406, 2013.

[130] Xiaoju Max Ma and John Blenis. Molecular mechanisms of mtor-mediated translational control. *Nature reviews. Molecular cell biology*, 10(5):307, 2009.

[131] Y Mamane, E Petroulakis, O LeBacquer, and N Sonenberg. mtor, translation initiation and cancer. *Oncogene*, 25(48):6416, 2006.

[132] Mathieu Laplante and David M Sabatini. mtor signaling at a glance. *Journal of cell science*, 122(20):3589–3594, 2009.

[133] Róisín M Loftus and David K Finlay. Immunometabolism: cellular metabolism turns immune regulator. *Journal of Biological Chemistry*, 291(1):1–10, 2016.

[134] DN Kellett. 2-deoxyglucose and inflammation. *Journal of Pharmacy and Pharmacology*, 18(3):199–200, 1966.

[135] Hye Young Kim, Hyun Jun Lee, Ya-Jen Chang, Muriel Pichavant, Stephanie A Shore, Katherine A Fitzgerald, Yoichiro Iwakura, Elliot Israel, Kenneth Bolger, John Faul, et al. Interleukin-17-producing innate lymphoid cells and the nlrp3 inflammasome facilitate obesity-associated airway hyperreactivity. *Nature medicine*, 20(1):54–61, 2014.

[136] Mira Ham, Joo-Won Lee, A Hyun Choi, Hagoon Jang, Goun Choi, Jiyoung Park, Chisayo Kozuka, Dorothy D Sears, Hiroaki Masuzaki, and Jae Bum Kim.

Macrophage glucose-6-phosphate dehydrogenase stimulates proinflammatory responses with oxidative stress. *Molecular and cellular biology*, 33(12):2425–2435, 2013.

[137] Bing-Chang Chen, Chun-Fen Chou, and Wan-Wan Lin. Pyrimidinoceptor-mediated potentiation of inducible nitric-oxide synthase induction in j774 macrophages role of intracellular calcium. *Journal of Biological Chemistry*, 273(45):29754–29763, 1998.

[138] BING-CHANG Chen and WW Lin. Potentiation of lipopolysaccharide-induced il-6 release by uridine triphosphate in macrophages: cross-interaction with cyclooxygenase-2-dependent prostaglandin e2 production. *Journal of biomedical science*, 6(6):425–432, 1999.

[139] Arnauld C Verschuur, Albert H Van Gennip, Rene Leen, Rutger Meinsma, PA Voute, and André BP Van Kuilenburg. In vitro inhibition of cytidine triphosphate synthetase activity by cyclopentenyl cytosine in paediatric acute lymphocytic leukaemia. *British journal of haematology*, 110(1):161–169, 2000.

[140] Claire Wallace and David Keast. Glutamine and macrophage function. *Metabolism*, 41(9):1016–1020, 1992.